Studies on Catalytic Hydrothermal Reforming of Biomass and Its Derivatives for the Production of Fuels and Chemicals

イデッシュ, サルール

https://doi.org/10.15017/1398404

出版情報：九州大学, 2013, 博士（工学）, 課程博士
バージョン：

Studies on Catalytic Hydrothermal Reforming of Biomass and its Derivatives for the Production of Fuels and Chemicals

by

Saruul Idesh

Department of Applied Science for Electronics and Materials
Interdisciplinary Graduate School of Engineering Sciences
Kyushu University, Japan

2013

CONTENTS

CHAPTER 1

General Introduction

1.1. Current Status of Energy Mix and Global Energy Outlook

1.1.1. Overview of energy mix and energy outlook

The processes of industrialization and economic development require energy. The world energy demand for energy has been increasing quickly; it raised 2.5 fold from 5,000 million tonnes of oil equivalent (Mtoe) in 1970 to 12,477 Mtoe in 2012. World primary energy consumption will grow up from 12,477 Mtoe in 2012 to 17,517 Mtoe in 2035 [1,2]. Energy resources have been divided into three categories: fossil fuels, renewable resources and nuclear resources. Today, global primary energy consumption from all sources is about 522 EJ and fossil fuels (oil, coal and natural gas) supply over 80% of primary energy consumption [3]. The rapid growth of energy demand in the region, poor in oil and natural gas resources, has caused most crucial problems. Energy demand, particularly fossil fuel demand, is predicted to continue intensifying in the world. The fossil fuels will provide nearly 80% of future energy consumption expansion, the world will stay seriously dependent on fossil fuels even 2035 [2,4]. The world electricity generation is increasing from 22,504 terawatt-hours (TWh) in 2012 to 35,300 TWh in 2035. Nuclear power produces about 11% of world electricity, which accounts for nearly 2% of world energy demand; the number of reactors is increasing slightly but the recent nuclear disaster in Japan has placed nuclear power development in at least temporary neglected. Nowadays renewable energy sources satisfy about 14% of the total global energy consumption [1,5–7].

Future energy expansion is depending on many factors, mainly: economic growth, population growth, energy prices and fuel availability, technologies that improve efficiency and develop new renewable, also environmental and exhaust emissions

regulations and standards.

The current energy landscape is confronted with several strains of developments: supply constraints of conventional primary energy sources at increasing energy demands from emerging economies, climate change, deregulation of energy markets, and new opportunities from innovations in sustainable energy technologies. To meet future energy demands efficiently, energy security and reliability must be improved and alternative energy sources must be investigated aggressively. An effective energy solution should be able to address long-term issues by utilizing alternative and renewable energy sources.

World oil utilization will rise from 83 million barrels per day (Mb/d) in 2010 at an annual rate of 1.2% to 114 Mb/d in 2035. Oil will continue to be the biggest energy source, even if reducing its share of total primary energy consumption from 35% in 2010 to 32% in 2035. Global natural gas consumption will grow up from 3,000 billion cubic meters (Bcm) in 2010 to 5,000 Bcm in 2035 as a result of advancement in natural gas utilization technologies and environmental adaptability of gas. Worldwide coal consumption will climb from 5,000 million tonnes of coal equivalent (Mtce) in 2010 to 7,000 Mtce in 2035 with an annual rate of 1.4% [1,2].

1.1.2. Environmental and food impacts of energy

Global temperatures are generally rising over the past 50 years on average at an unprecedented and exponential rate, alongside with similar rises in greenhouse gas emissions. There is clear evidence of major melting of polar ice caps, glaciers and snow caps; however the 5-year land and ocean average temperature during the 2006–2010 temperature dropped by 0.04 °C relative to the 2001–2005 periods [8], perhaps due to melting of polar caps. The exhaust emissions continue to grow up and concentrations of all long-lived greenhouse gases in the atmosphere had increased to over 390 ppm, or 39% above preindustrial levels, by the end of 2010 [9]. An average global temperature change of more than 2 °C relative to pre-industrialized levels and a mean long-term rate of global temperature change exceeding 0.2 per decade are intolerable parameters of global climate change. It is believed that warming of the climate is likely to lead to extreme weather events becoming more frequent and unpredictable.

Energy and water use are strongly interdependent. Conversion of food to fuel endangers the food and water supply and is likely to raise their price, especially if very large quantities are used. The water and food supply are in crisis, with about 1 in 8 people lacking safe drinking water, 1 in 2 lacking access to it for sanitation and waste, and 1 in 7 being undernourished. The "Living Planet Index" is estimated to have declined since 1970 by about 30% and world seems to be running out of environment much faster than out of resources [10].

1.1.3. Summary of renewable energy resources

Fossil fuels are the world's main energy resource, however the reserves of combustible fuels are restricted, and their large-scale use is associated with environmental deterioration. In the course of the last 25 years, estimations for coal resources have been decreased by 50%, from 10,000 billion tons coal equivalent (Btce) to about 5,000 Btce [11]. On the other hand, visible negative effects of using fossil fuels include ozone layer depletion, acid rain and global climate change, etc. are known. World energy related CO_2 emissions reached to 35 gigatons (Gt) in 2012 compared to 22 Gt in 1990 [6]. Fossil fuels are responsible for an estimated 80% of all CO_2 emissions and 70% of all anthropogenic green house emissions [9,12]. Replacing fossil fuels with renewable energy or other low-carbon technologies can significantly contribute to the reduction of CO_2, NO_x and SO_x emissions. Among non fossil fuels, nuclear energy can cause serious problems for the environment and human health.

Renewable energy is energy that creates from resources which are frequently replenished such as sunlight, wind, rain, tides, waves and geothermal heat. The optimal exploitation of renewable resources minimizes environmental impacts, causes minimum derived wastes, consequently renewable resources are clean sources of energy and sustainable based on current and future economic and social needs. Otherwise, a renewable energy sources can be defined as a simple sustainable resource available over the long term at a reasonable cost that can be used for any task without negative effects [13]. Renewable energy sources include biomass, hydropower, geothermal, solar, wind and marine energies. As mentioned earlier, renewable energy sources provide roughly 14% of energy on global basis. The largest renewable energy contributor is biomass

(11%), with the more than half of the biomass fuel used in traditional cooking and heating applications in developing countries. Hydropower represented 2.4%, whereas other renewable energy sources accounted for 0.6%. Biofuels contributed 3% of global road transport fuel supply, and traditional biomass (17%), modern biomass (8%), solar thermal and geothermal energy (2%) together fuelled 27% of the total world demand for heat in 2010. The contribution of renewable energy to primary energy supply varies substantially by country and region [5,9]. According to the report of the International Energy Agency (IEA) of 2012, electricity generation from renewable sources worldwide in 1990 was 19.5% and grew by an average of 2.7% per year, while the total electricity generation grew by 3% annually, and in 2010, the fraction of electricity produced from renewable sources was 20%. It means in 2010 over 4,206 TWh of power was produced globally using renewable sources of energy. In 2010 the contribution of different renewable energy sources to the overall electricity production was estimated to be 16.3% hydropower, 1.6% wind, 1.6% biomass, 0.32% geothermal, 0.16% solar and 0.01% marine [5,14,15]. The share of renewable energy sources is expected to increase very extensively in the future (30–80% in 2100) [16]. Renewable resources provide various opportunities also can address economic and sustainable development, secure energy supply, climate change mitigation, significantly environmental and health impacts.

Solar energy: Of the several available renewable sources of energy, solar energy is clearly a promising option as it is extensively available. Solar power, especially as it reaches more competitive levels with other energy sources in terms of cost, may serve to sustain the lives of millions of underprivileged people in developing countries. There is vast scope to use available solar energy for thermal applications such as cooking, water and space heating, crop drying, etc. In 2010, the electricity generation of solar PV was 32 TWh and it is expecting to increase 846 TWh in 2035. By the end of 2008, worldwide installed solar thermal capacity was as total 152 GW corresponding to 217 million square meters. Furthermore, solar energy devices can benefit the environment and economy of developing countries [5,17].

Wind energy: Of the renewable energy technologies applied to electricity generation,

wind energy ranks second only to hydroelectric in terms of installed capacity and is experiencing rapid expansion. Wind energy potential studies show that the worldwide wind resources are abundant. Wind power experienced dramatic growth over the last decade. Nowadays, global generation from wind increases dramatically from 342 TWh in 2010 to around 2,680 TWh in 2035, pushing up its share in total electricity generation from 1.6 to 7.3%. Wind energy for electricity production mature, competitive, pollution-free technology widely used in many regions of the world [5,18].

Hydropower energy: Hydropower is the largest single renewable electricity source today, providing 16.3% of world electricity at competitive prices. It dominates the electricity mix in several countries developed and developing. Hydroelectricity presents several advantages over most other sources of electrical power, including a high level of reliability, proven technology, high efficiency, very low operating and maintenance costs, flexibility and large storage capacity. It also helps control water flows and availability. In many others it provides significant amounts of clean, renewable electricity. Hydropower is a fully mature technology in use in 159 countries. It produces about 3,431 TWh of the electricity, in 2010. Global hydropower capacity is projected to increase from 1,067 GW in 2011 to over 1,680 GW in 2035 [5,19].

Geothermal energy: Geothermal energy has long been used to produce electricity in various countries. In recent years, an increase in installed capacity has been observed and this increase is expected to be much greater in a near future. In 2000, geothermal resources have been identified in over 80 countries and there are quantified records of geothermal utilization in 58 countries in the world. Currently, geothermal energy installed power capacity exceeds 11,000 MW, and annual energy produced is near 68 TWh (in 2010). Five countries obtain 10–22% of their electricity from geothermal energy [20]. Total global installed capacity of geothermal heat equaled 15 GW in 2009 with a yearly heat production of 223 PJ. Global geothermal electricity generation increases from 68 TWh to more than 300 TWh and capacity from 15 GW to over 40 GW between 2010 and 2035 [5,14].

Marine energy: There are five different technologies under development, which aim to extract energy from the oceans: tidal power, tidal currents, wave power, temperature

gradients and salinity gradients. None of these technologies is widely deployed as yet, but significant potential exists. Electricity generation from marine energy, which includes tidal and wave power, will increase from less than 1 TWh to almost 60 TWh between 2010 and 2035, with capacity growing from less than 1 GW to 15 GW [5,21].

Bioenergy: The growth in electricity production from solid biomass, biogas and renewable municipal waste and liquid biofuels has been steady since the beginning of the decade. In 2000, over 130 TWh of power was produced from bioenergy. From 2000 to 2010 global electricity generation from bioenergy grew by 6.9% per year. In 2010 power generation from bioenergy has increased 331 TWh, accounting for over 40% of global non-hydro renewable generation. It aimed will reach 1,487 TWh in 2035. Bioenergy is also used for heating and maintaining its share of about two-thirds of total bioenergy demand. Total energy demand for bioenergy will grow up from 526 Mtoe in 2010 to 1,200 Mtoe by 2035 [5].

1.2. Biomass as Bioenergy Resources

1.2.1. Biomass and bioenergy

Biomass is the all organic materials originated from living matter. Living matters absorb solar energy (or via eating plants) and convert it chemical energy. The energy that comes from biomass is called bioenergy. Biomass is the only renewable source that is suitable for producing power, heat and transport fuels but only about 20% of biomass is used on an industrial scale for these productions. Biomass has the potential to provide a cost effective and sustainable supply for energy, at the same time, helping countries in satisfying their greenhouse gas reduction targets. Biomass is largest contributor to the renewable resources, which is accounted for roughly 11% of energy consumption on a global basis, however, most of them used for cooking and heating. In addition, biomass has attracted much attention not only as renewable energy resources; also it can be used as a feedstock to produce valuable chemicals and precious materials [22–24]. Biomass is utilized in several forms through various ways of application.

Biogas: In bioenergy production, the production of biogas (mainly methane (50 to 70%) and CO_2) through anaerobic digestion presents significant advantages over other forms

of bioenergy. It has been evaluated as one of the most energy-efficient and environmentally beneficial technology for bioenergy production [25]. It is possible to use several different raw materials and digestion technologies for the production of biogas. Among the raw materials are organic waste products from households, food industry and agriculture, energy crops, such as crop residues and manure. Nowadays in the animal breeding sector produced large amounts of animal manure and slurries as well as the wet organic waste streams correspond to a constant pollution risk with a potential negative impact on the environment, if not managed properly [26]. Biogas has definite advantages, compared to other renewable energy alternatives. Biogas can be produced when required and combusted onsite to produce heat and/or electricity; can easily be stored, cleaned and upgraded to natural gas quality biomethane for injection into gas grids; or, after compressing or liquefying, distributed to vehicle filling stations for use in dedicated or dual gas-fuelled vehicles, can be distributed through the existing natural gas infrastructure [9].

Biofuels: Biofuel is a clean burning fuel that is renewable and biodegradable. The use of vegetable derivative liquid in internal combustion engines is not a recent innovation. Global biofuels production grew from 16 billion liters in 2000 to more than 100 billion liters in 2010. Today, biofuels provide 2.7% of global road transport fuel on an energy basis, but higher shares are achieved in some countries and regions. The use of biofuel has the potential to reduce emissions from transport industry and from burning fuels. Installed advanced biofuel (e.g. lignocellulosic ethanol, vegetable oils, biomass to liquids and other types) capacity today is about 175 million liters gasoline equivalent (lge)/year [5,14].

Biomass: Most biomass is presently used for traditional small-scale domestic heating and cooking, mostly in developing countries. The progress in biomass for heat over time is difficult to characterize, as it is disguised by extensive use of biomass as a source of heat in the residential sector in developing countries. This “traditional biomass” includes wood, charcoal, crop residues and animal dung and is mostly used for cooking, water heating and space heating. In 2010, 751 Mtoe of traditional biomass, which share of total biomass is 59%, was consumed in the residential sector in developing countries.

A variety of products, such as fuel gases, chemicals, biopolymers, bioliquids and bioproducts can be produced from biomass in various biorefineries. In modern renewable heat, biomass dominates over solar thermal and geothermal heat. The global use of modern biomass, including wood products, such as pellets and briquettes that have been made to burn efficiently, industrial biogas and bioliquids, for producing heat reached 278 Mtoe in 2010 [5,23,24].

1.2.2. Biomass conversion processes

Biomass can be converted to energy by means of biochemical, chemical and thermochemical processes. The anaerobic digestion and microbic fermentation are biological/biochemical processes applied frequently, whereas transesterification, hydrogenation and extraction are chemical processes that utilized typically. As well, there are three major thermochemical processes available for converting biomass to a more useful energy form and for producing valuable chemicals; combustion, gasification and pyrolysis. Biomass gasification has attracted the main attention among the thermochemical technologies, due to its higher efficiencies compared to combustion and fast pyrolysis which is at a rather early stage of development [23,27].

Combustion: Combustion of biomass is widely used commercially on various scales to provide heat and power. The product is heat or steam, which must be used immediately for heat and/or power generation. Overall efficiencies to power range to be rather low at usually 20% for small plants up to 40% for larger and newer plants, with heat transfer losses of 30–90%. Costs are only currently competitive when wastes are used as feed material such as from pulp and paper, and agriculture. Technical problems that caused by emissions and ash handling are still remain. The technology is, however, widely available commercially and frequently utilizing forestry, agricultural and industrial wastes [22,23,28,29].

Gasification: Fuel gas can be produced from biomass by either partial oxidation in steam or pyrolytic gasification. In gasification, when a solid fuel is heated in the absence of an oxidizing agent, it first pyrolyzes to solid char, condensable hydrocarbons or tar, and gases. The gas, liquid and solid products of pyrolysis then react with the

oxidizing agent to produce gases of CO, CO_2, H_2, and lesser quantities of hydrocarbon gases. The yields of gas, liquid and char depend on the rate of heating and the process temperature. Char gasification combines a range of gas-solid and gas-gas reactions, by which carbon in char is oxidized and hydrogen is generated through the water gas shift reaction. Most of the reactions are catalyzed by the alkali metals included in wood ash. The gas composition is depend on many factors such as feed composition, water content, reaction temperature, and the extent of oxidation of the pyrolysis products. The liquid products from the pyrolysis step are not totally converted because of the physical or geometrical restrictions of the reactor. As a result and the occupied chemical reactions, these increase tars contaminant in the final product gas. These tars have a tendency to be refractory and are hard to remove by thermal, catalytic or physical processes, because of the higher temperatures involved in gasification. This feature of tar cracking or removal in gas clean-up is one of the most important technical issues in operation of gasification technologies. The fuel gas quality requirements, for turbines in particular, are very high. Tar is a chief problem and causes the most significant technical difficulty. There are two basic ways of destroying tars: by catalytic cracking using and by thermal cracking [22,28,29].

Pyrolysis: Pyrolysis is thermochemical process occurring in the absence of air. It is also the first step in combustion and gasification processes where it is followed by total or partial oxidation of the primary products. High process temperature and longer residence time tend the biomass conversion to gas, while moderate temperature and short vapor residence time are best for producing liquids. Lower temperature and longer vapor residence times improve the production of charcoal. Fast pyrolysis takes place in few seconds or less. In pyrolysis, chemical reaction kinetics is main subject as well as heat and mass transfer. The critical issue is optimum process temperature to bring the reacting biomass particles and minimize its exposure to the lower temperatures that favor formation of charcoal [23,27,30,31].

1.2.3. Hydrothermal reforming as alternative biomass conversion process

Much of the biomass resources, such as agricultural residuals, aquatic biomass, food processing wastes and municipal sewage is composed of material with higher levels of

moisture, more typically 50 wt % and some even consist of wet biomass or biomass in water slurries at 85 wt % moisture or higher. To efficiently process such resource, a special technology is required and hydrothermal reforming is a concept under development around the world. Among thermochemical methods for energy production from low rank solid fuels such as biomass and brown coal, which contain high amount of oxygen-containing species including water, pyrolysis has been recently focused to produce syngas (H_2/CO) and/or combustible gas, pyrolytic tar, and char, while treatment in a hot pressurized water environment is also alternative effective method to treat those materials for the production of upgraded solid fuel and valuable chemicals. Hydrothermal reforming (HTR) is defined as reactions that convert carbonaceous materials in feedstock to more value added chemicals by rearranging or rebuilding molecules under high temperature and high pressure water condition and is often applied to the process for upgrading low rank resources and by the combination with catalyst termed as "Catalytic hydrothermal reforming" (CHTR). Hydrothermal reforming is a promising method to generate a product gas rich in hydrogen and methane. Feeds with high water content that thus have low calorific value can be used without any pre-drying or upgrading step. At hydrothermal conditions usually the organic compounds react with water to form a fuel gas. Advantages obtained by applying catalytic hydrothermal reforming to treat organics in aqueous feedstock can be summarized as follows: water in the environment can be used as reaction medium and more, has a catalytic activity and a reactant as oxidant; energy efficiency is higher compared to steam gasification process since latent heat to evaporate water is not required; coke formation by thermal effect is suppressed; it is possible to develop an environmentally-friendly reforming system.

Hydrothermal reforming seeks to recover the energy contents of biomass and industrial byproducts or wastes to produce energy as a fuel, alternatively, this process can avoid environmental pollution from biodegradable wastes by utilizing the highly polluting organic wastes for the production useful value added chemicals. The main gain of hydrothermal reforming of biomass is to benefit from the special properties of subcritical water as a solvent, as a catalyst and its presence as a reactant, hence biomass and its derivatives can be directly converted to a desired product, along with high solubility of the intermediates in water medium suppresses of unwanted tar and coke

formation. Successful implement of CHTR system of biomass and biomass derivatives would be applicable in many chemical and power generation processes that exhaust liquids contain organics because properties of the feedstocks used in HTR are relatively harsh as a reaction condition. The estimation of energy efficiency is expected to be desirable as the HTR system because required heat can be recovered by the exhaust hot water and by combustion of a part of product fuel gas. The most significant issue for the industrial application would be a reforming system design because hydrothermal reforming process is operated under high pressure with a flow of viscous and acidic liquids. This process can be expanded the usability of low rank fossil fuels, and impact on the environment in terms of clean fuel resources and treatment of waste streams, is significantly very high.

1.3. Literature Survey

The thermochemical gasification of biomass is likely to be a cost effective process to produce a fuel gas. However, as mentioned above, a large portion of biomass and its wastes is wet biomass, containing up to 95% water and this wet biomass causes high drying costs if classical gas phase gasification process is used. In general, dewatering or drying is the first and essential step in most of biomass utilization process. Similarly, numerous industrial processes produce huge amounts of wastewater that contain organic compounds in small to high concentrations. This causes the loss of combustible organic matter on one hand, and necessitates the wastewater treatment on the other hand. Hydrothermal treatment can be practiced over a range of operating temperatures and pressures. Early works identified supercritical water as an important operating medium with the supercritical condition being the overriding parameter. Later works have shown that subcritical water can also be useful for highly effective gasification when performed with active catalysts. Gasification of organic compounds under hydrothermal (HT) and/or supercritical water (SCW) condition has been paid great attention, because it cannot only gasify the organic compounds in the wastewater in a very short time but also recover some fuel gas. Furthermore, as mentioned earlier, hydrothermal biomass treatment process can advantageously avoid high drying costs. Catalytic hydrothermal gasification of organic compounds has been demonstrated a technology for gasifying

biomass materials to fluid fuel. Recently, this process is also applied to effectively treat organics in wastewater streams to address both environmental cleanup and energy recovery goals [22,31,32].

Several fundamental studies have been performed on the gasification of organic compounds under HT and/or SCW conditions. In the review by Osada et al. [32] three temperature regions for hydrothermal gasification are identified:

1. Region I (500–700 °C supercritical water) biomass decomposes and activated carbon catalyst is used to avoid char formation or alkali catalyst facilitates the water-gas shift reaction.
2. Region II (374–500 °C, supercritical water) biomass hydrolyzes and metal catalysts facilitate gasification.
3. Region III (below 374 °C, subcritical water) biomass hydrolysis is slow and catalysts are required for gas formation. A practical technology is required to convert the cellulose, hemicellulose, lignin, protein, algae and extractive components of a biomass feedstock into a gas rich in hydrogen and methane. As predicted by the early work with cellulose, biomass does not react directly with steam at atmospheric pressure to produce the desired products. Instead, significant amounts of tar and char were formed, and the gas contained higher hydrocarbons in addition to the desired light gases. In hydrothermal conditions conversely, at temperatures above 190 °C a part of lignin and hemicelluloses macromolecules undergo solvolysis after only a few minutes of exposure to hot liquid water. Hydrothermolysis of the remaining lignocellulosic solid occurs at somewhat higher temperatures. The initial products of these solvolysis reactions subsequently undergo a variety of isomerization, dehydration, fragmentation, and condensation reactions that ultimately form gas and tars. At temperatures above 600 °C and pressures in excess of the critical pressure, hydrothermolysis transforms biomass into a combustible gas composed of hydrogen, methane, carbon dioxide and carbon monoxide, together with some tar. Consequently, char formation is suppressed when biomass gasification occurs in liquid water or supercritical water, and tar gasification becomes the chief obstacle to the total hydrothermal reforming of biomass.

Antal MJ [33] and Modell's [34] works are among the first to operate hydrothermal gasification for synthesis gas production from organic wastes by pyrolysis and steam

reforming. Subsequent work by Elliot DC and coworkers [35–38] has studied a use of active catalysts can facilitate the hydrothermal gasification of biomass, even below the critical point of water. Their initial work compared biomass hydrothermal gasification below and above the critical point of water and with or without catalysts. They studied catalytic conversion of *p*-cresol and wet biomass in fixed-bed tubular reactor systems at bench scale and in a scaled up system at 330–360 °C and 17–24 MPa. However, the liquid-hourly-space-velocity (LHSV) value realized by his group was 1–3 h^{-1}, which means that this process was not so effective. Although they continued to investigate a number of biomass feedstock with different types of catalysts and catalyst support materials. As briefly reviewed, a number of trials have been made on HT and SCW gasification. Firstly, many attempts have been made on SCW gasification. In high temperature, in SCW gasification a temperature range of 400–875 °C is usually employed. Minowa's group [39,40] has examined the gasification of cellulose at 400–600 °C using several catalysts. It was found that Na_2CO_3 is suitable to obtain water-soluble components and that Ni catalyst is effective to gasify cellulose. These homogeneous and heterogeneous catalysts are also effective in near- and subcritical water and can be used for biomass gasification, but one problem is that Ni and many of the other metallic catalysts can suffer severe corrosion in sub and supercritical water at temperatures needed to secure high yields of hydrogen. Antal MJ overcame this problem of catalyst by using of charcoal and other carbons as catalysts for the gasification of tars in supercritical water. Xu [41] and Antal's group [42] gasified cornstarch and chemical wastewater using an activated carbon catalyst to produce H_2, CH_4, and CO_2 at 600–715 °C and 22-34.5 MPa and have identified activated carbon as a catalyst for hydrothermal gasification at supercritical water conditions. Moreover, the works by Kruse and coworkers [43–45] provided an assessment of hydrothermal gasification of various biomasses without the use of heterogeneous metal catalysts. Throughout the development of the technology up to today, possibility of biomass gasification in near- and SCW has been shown that complete conversion of biomass into combustible gas is achieved.

Furthermore, there have been done many attempts to produce hydrogen by hydrothermal gasification from a biomass during this decade. Schmieder and coworkers

[46] efficiently gasified wet biomass and organic wastes under hydrothermal conditions to produce a hydrogen rich fuel gas. They found that wet biomass are completely gasified by addition of KOH or K_2CO_3 at 600 °C and 250 bar, forming a H_2 rich gas. Cortright [47] and Davda et al. [48] used low temperature such as 210-225 °C to gasify simple oxygenates for hydrogen production. Furusawa et al. [49] have reported that lignin was gasified in SCW at 673 K and 30-37 MPa to produce hydrogen. Lu [50] and Guo et al. [51] studied the catalyst performance for glucose gasification in supercritical water at 673 K, 24.5 MPa to obtain hydrogen.

In low temperature catalytic gasification, complete gasification of feedstock is still difficult. Since the reaction temperature is low, catalysts play a main role. The catalysts were very effective for promoting biomass gasification, leading to greatly reduced yields of tar and char accompanied by significantly enhanced formation of CO and H_2. Operation at subcritical temperature results in a product gas high in methane and less hydrogen, while operations at supercritical temperatures will produce more hydrogen and less methane. However, development of more effective gasification methods based on highly active catalysts was desired to apply HT and subcritical water gasification practically. An additional significant progress underlying the development of catalytic hydrothermal gasification was the stable formulations of high-surface-area support materials for the catalysts that are useful in hot water systems. In order for catalysis to be an effective adduct for hydrothermal gasification, materials with long-term stability in hot liquid water needed to be identified and utilized in catalyst formulations. Elliot et al. [52–54] have studied development in biomass in a pressurized water-processing environment and have focused on the use of catalysts. Biomass feedstock used in their research included glucose, cellulose, lignin, hemicelluloses, wood flour and different wet biomass, and biomass gasification conducted at 200–450 °C under 13–25 MPa. Elliot's group described results with a number of biomass feedstock, which can be gasified at near- and subcritical temperatures in the presence of a nickel metal or alkali-promoted nickel catalyst. As shown in their research by using a number of commercial catalysts and catalyst support materials, active catalyst and useful supports are identified as nickel metal or alkali-promoted nickel catalyst and carbon, mono-clinic zirconia, titania and α–alumina respectively. In addition they have reported that several studies

have been performed on the catalytic hydroprocessing to upgrade and to produce transportation liquid fuels from thermochemically biomass-derived bio-oils in both batch-bed and continuous-flow bench-scale reactor systems at 180–400 °C under 10–24 MPa. His group has also proposed a wastewater treatment process using this gasification method. Nakagawa et al. [55] have studied a hydrothermal treatment of brown coal for dewatering, upgrading and for wastewater treatment, simultaneously they have found that the reactivity to oxygen at low temperature was reduced. The organic compounds in the wastewater and in organic water were completely gasified at as low as 350 °C under 20 MPa at the LHSV of 50^{-1}, producing combustible gas rich in CH_4 and H_2. Yoshida's group [56] was examined catalytic hydrothermal gasification of some food processing waste biomass slurries at lower temperature (350 °C) with γ-alumina-supported nickel catalyst. Sharma et al. [57–59] gasified organic compounds dissolved in the wastewater and phenol solution into high calorific gases like methane and hydrogen at 360 °C, under 20 MPa at 50 h^{-1} LHSV. Morimoto and coworkers [32,60,61] have proposed the method to combine a hydrothermal extraction and catalytic hydrothermal gasification of organic compounds extracted from brown coal at 350 °C, 18 MPa and produced combustible gas rich in methane and hydrogen. Hammerschmidt and coworkers [62] have studied the catalytic reaction of wet organic matter at near-critical water conditions (330 °C, 25 MPa) to produce a mixture of combustible organics which can be used as liquid biofuel. Hydrothermal treatment of waste biomass, after dewatering, resulted in a biocrude oil of high calorific value. The use of low temperature will also impact the mechanical systems for containing the reaction. Lower temperature operation allows lower capital costs because of lower pressure operation, requiring less containment structure, and less severe attack on the reactor walls, which allows the use of less costly alloys.

From a point of view of catalyst development in HT conditions, earlier were used for CHT homogeneous alkali metal salts and heterogeneous base metal catalysts such as nickel, copper, zinc, cobalt and molybdenum as oxides. Other tests showed that inactive base metals were rhenium, tin, lead, tungsten, chromium. Much work has been reported on the use of heterogeneous catalysts (primarily Ni) to gasify the pyrolytic tars. Nickel was found to be active, but its activity maintenance depends on the support material.

Vogel's group [32] studied different formulations of nickel, which catalyzed hydrothermal gasification above and below the critical point of water. High yields of methane were achieved and nearly tar-free byproduct water, i.e., nearly complete gasification of wood at temperatures from 370 to 420 °C. The Raney-nickel catalyst was clearly more active, and the α-alumina supported catalyst was abandoned [63]. Stable nickel metal catalysts were developed by Elliott et al. [54] by impregnating promoting metals onto the most stable nickel catalyst formulation. The most useful promoter metals were copper, silver, tin impregnated at 1%. Another stable nickel catalyst has been reported by Miura's group [55,58]. The catalyst was formed by ion-exchanging onto a resin and then carbonizing resin. Subsequent development of catalyst was noble metal catalyst. Several tests have demonstrated most active noble catalysts were iridium, ruthenium, rhodium, while silver, platinum, palladium had very low activity for hydrothermal gasification at 350 °C. Elliott and Hart [64] have chosen three model compounds, including guaiacol, furfural, and acetic acid, to study the chemical mechanism of catalytic hydroprocessing of bio-oil to represent those components using Pd and Ru catalysts over a temperature range 150–300 °C. Ruthenium has demonstrated long term stability. Titania was most useful as a support. The carbon supported ruthenium catalyst was active for processing 10% wastewater [38,54,63,65–69]. Oasmaa and coworkers [70] have reported the analytical methods to determine the composition of hydrotreated fast pyrolysis oils. They used Ru/carbon catalyst. The composition of the products was determined by solvent fractionation followed by detailed analysis of the various fractions by GC–MSD, capillary electrophoresis (CE) and NMR (^{1}H NMR, ^{13}C NMR, ^{31}P NMR). Wildschut et al. [71] have concluded that well-reduced Ru is an excellent catalyst in high-pressure aqueous environments, but partially reduced form was not usable under supercritical condition. Other dissimilar results have been reported at higher and lower temperatures. Platinum was a useful catalyst for hydrogen production at low temperature (225–265 °C) [47]. However, in total carbon gasification catalyst activity was as following: Ru>>Pt>Rh~Ni>Pd [48]. Nevertheless, the main problem found in activity maintenance of catalyst, is deactivation by sintering and carbon deposition when using these heterogeneous catalysts for long time [72–75].

1.4. Purpose of the Work and Summary of the Dissertation

Concerns about declining reserves of fossil fuel along with severe environmental deteriorations are leading the world to the exploitation of renewable energy resources. Biomass has a potential to provide a sustainable and cost effective supply for energy as same as well distributed carbon-free renewable sources. Alternatively biomass that only renewable source of organic carbon in the world, is attracting much attention for the production of fuels, valuable chemicals and carbon-based materials. Many biomass feedstocks contain high levels of water and a number of industrial processes produce huge amounts of byproducts containing organic compounds in variable concentrations. In conventional processing, the water is typically thermally separated by vaporization in pyrolysis, by distillation in biochemical processing, by drying in other pretreatment processes. These separation steps lead to huge amounts of energy loss due to latent heat, which can consume much of the energy of feedstock. To efficiently process such resource, a different technology is required and hydrothermal reforming is most promising method among thermochemical methods for the production of upgraded fuels and valuable chemicals.

This study proposes novel processes to convert biomass by catalytic hydrothermal reforming for the production of gaseous/liquid fuels and valuable chemicals, and shows experimental proof of potential of the processes.

The main essence of hydrothermal reforming of biomass is high efficiency of the process, while current chemical energy recovery for gasification of biomass is no higher than 80%. The recovery of chemical energy in feedstock by hydrothermal reforming is theoretically achievable to 100% because required no use of oxygen to supply energy for endothermic reactions to convert biomass to gaseous products. Hydrothermal reforming seeks to recover the energy contents of biomass and industrial wastes to produce energy as fuel, alternatively, this process can avoid environmental pollution from biodegradable wastes by utilizing the highly polluting organic wastes for the production of useful value added chemicals. This process can be expanded the usability of low rank fossil fuels, and impact on the environment in terms of clean fuel resources

and treatment of waste streams, is significantly very high. This dissertation consists of five chapters. The outlines of each chapter are given below.

Chapter 1 clarifies the importance and advantages of utilizing the renewable energy resources, mainly biomass energy, and elucidates biomass conversion technologies for energy and chemicals. The literature survey reviewed studies on hydrothermal gasification and/or reforming process of various biomasses in sub, near- and supercritical condition. The purpose of the present study and summary of the dissertation are also outlined.

Chapter 2 describes details of experimental method and results of CHTR of water-soluble organics of bio-oil from the pyrolysis using a newly developed catalyst aiming at simultaneous production of combustible gas and organics-free clean water. In this work reforming of the feedstock with a total organic carbon concentration (TOC) of 10,000 ppm was performed at the temperature and pressure of 350 °C and 20 MPa over different types of catalysts. NiC catalyst was most active among the examined catalysts with conversion more than 98%. However obtained product liquid from CHTR with NiC had a TOC as high as 160 ppm. To meet environmental strict restriction catalytic activity of NiC was improved by using metal promoter, such as Co, Cu, Fe, Mo, Zn and Pt. The enhanced catalytic activity was found in the NiC impregnated with Pt. Reforming of the feedstock over Pt/NiC successfully reduced TOC of product liquid to 6 ppm. Such a high activity was attributed to that for the reforming of the most refractory compounds, which were components of the feedstock and that formed during hydrothermal process.

Chapter 3 proposes CHTR of vegetable oil without consuming any reagent, such as external hydrogen, for the production of alkanes as a clean and environmentally friendly green fuel. The Jatropha oil, a type of inedible vegetable oil that consisted mostly of triglycerides, was employed as the feedstock. Hydrolysis of triglycerides almost completed within several minutes, but further conversion of the resulting fatty acids did not progress in the absence of catalysts. So commercial and homemade Pt, Pd, and Ni catalysts supported on carbon were applied to the conversion of triglycerides. To clarify the reaction pathway the experiments were conducted at the different conditions (at the range of temperatures of 275–350 °C during reaction time of 0.5–5 h). Alkanes were

produced with the use of catalysts by participation of in situ hydrogen, while the direction of catalysis varied depending on the metallic species of the catalysts. The main products of CHTR over Pt/C were pentadecane and heptadecane, which were formed by decarboxylation of corresponding fatty acids with the total yield of more than 46.3%-C at 350 °C. The product distribution indicated that NiC had the catalysis toward degradation by carbon-carbon cleavage of fatty acids, which yields smaller, lighter alkanes, resulting in selective formation of methane at the yield of 53%-C with higher recovery of energy. As a result two options with these catalysts have been suggested for the production of liquid and gas fuels.

Chapter 4 discusses results of work on CHTR of lignin, which dissolved in alkaline aqueous media, using several kinds of noble catalysts aiming at simultaneous production of fuel gas and phenolic compounds. In this work CHTR over Ru/AC catalysts at 350 °C converted the dissolved lignin to the combustible gas composed of primarily methane, carbon dioxide and hydrogen with cold gas efficiency (CGE) of 86.7-87.9% on HHV basis. A portion of carbon of the lignin was deposited over the catalysts thus gave lower yield of the major product methane than expected from the stoichiometry of full gasification of the lignin. The Ru/AC catalyst maintained its activity through the period of 10 h with the rate of TOC removal over 98%. Alternatively, CHTR with use of Pd/C catalyst produced phenolic compounds from lignin with the yield of 13.1%-C at 275 °C. Simultaneously, Pd/C catalyst was most effective for minimizing heavy material or char, which was formed by cross-link hydrolysis and intermediate products from hydrothermal reforming with each other. It was demonstrated that alkali salts, which were difficult and expensive to recover, in product water could be used by recycling; consequently it increased performance and efficiency of the hydrothermal process.

Chapter 5 summarizes the novel findings described in the preceding chapters and provides a future perspective of catalytic hydrothermal reforming in biomass processing.

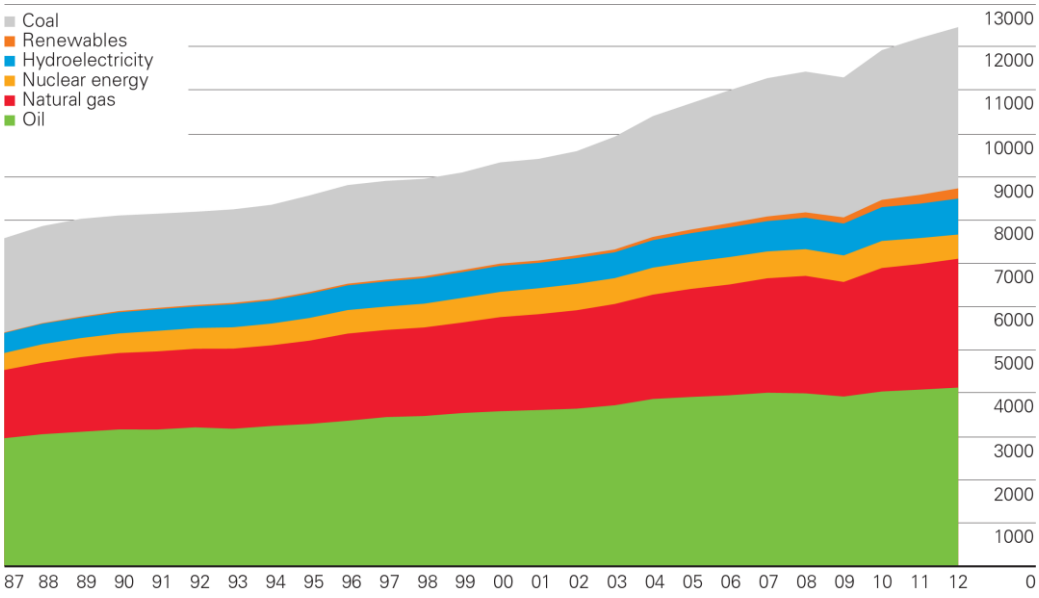

Figure 1.1. World primary energy consumption, Mtoe [1]

1.5. References

1. BP. *BP Statistical review of world energy 2013.* London: BP, June 2013. http://bp.com/statisticalreview. [accessed on 18.06.2013]
2. Matsuo Y, Yanagisawa A, Yamashita Y. *A global energy outlook to 2035 with strategic considerations for Asia and Middle East energy supply and demand interdependencies.* Energy Strategy Reviews, 2013.
3. Zerta M, Schmidt P, Stiller C, Landinger H. *Alternative World Energy Outlook (AWEO) and the role of hydrogen in a changing energy landscape.* International Journal of Hydrogen Energy, 2008. 33(12): p. 3021–3025.
4. Khatib H. *IEA World Energy Outlook 2011—A comment.* Energy Policy, 2012. 48: p. 737–743.
5. OECD/IEA. *WEO2012 Renewable energy outlook.* 2012. http://www.iea.org/. [accessed on 15.05.2013]
6. Khatib H. *IEA World Energy Outlook 2010—A comment.* Energy Policy, 2011. 39(5): p. 2507–2511.
7. Lior N. *Sustainable energy development: The present (2011) situation and possible paths to the future.* Energy, 2012. 43(1): p. 174–191.
8. Smith TM, Reynolds RW, Peterson TC, Lawrimore J. *Improvements to NOAA's historical merged land–ocean surface temperature analysis (1880–2006).* Journal of Climate, 2008. 21(10): p. 2283–2296.
9. IPCC. *Renewable energy sources and climate change mitigation.* Special Report of the Intergovernmental Panel on Climate Change, 2012. http://www.ipcc.ch/pdf/special-reports/ [accessed on 15.05.2013]
10. WWF. *Living Planet report-2012: Biodiversity, biocapacity and better choices.* WWF report, 2012. http://awsassets.panda.org/downloads/. [accessed on 16.06.2013]
11. EWG. *Coal: Resources and future production.* Energy Watch Group: Series, 2007. http://www.energywatchgroup.org/fileadmin/global/. [accessed on 18.05.2013]
12. IPCC. *Climate change 2007: Mitigation of climate change.* Assessment Report

of the Intergovernmental Panel on Climate Change (IPCC), 2007. http://www.ipcc.ch/publications_and_data/. [accessed on 20.05.2013] p. 251–322.

13. Charters WWS. *Developing markets for renewable energy.* Renewable Energy, 2001. 22: p. 217–222.
14. IEA. *Clean energy progress report.* IEA report, June 2011. http://www.iea.org/publications/freepublications/. [accessed on 20.05.2013]
15. Glasnovic Z, Margeta J. *Vision of total renewable electricity scenario.* Renewable and Sustainable Energy Reviews, 2011. 15(4): p. 1873–1884.
16. Fridleifsson IB. *Geothermal energy for the benefit of the peole.* Renewable and Sustainable Energy Reviews, 2001. 5: p. 299–312.
17. Thirugnanasambandam M, Iniyan S, Goic R. *A review of solar thermal technologies.* Renewable and Sustainable Energy Reviews, 2010. 14(1): p. 312–322.
18. Hepbasli A, Ozgener O. *A review on the development of wind energy in Turkey.* Renewable and Sustainable Energy Reviews, 2004. 8(3): p. 257–276.
19. OECD/IEA. *Technology roadmaps: Hydropower.* 2012. http://www.iea.org/. [accessed on 21.05.2013]
20. Chamorro CR, Mondéjar ME, Ramos R, Segovia JJ, Martín MC, Villamañán MA. *World geothermal power production status: Energy, environmental and economic study of high enthalpy technologies.* Energy, 2012. 42(1): p. 10–18.
21. Huckerby J. *OES International vision for ocean energy.* http://www.globalmarinerenewable.com/images/stories/2012Presentations/. [accessed on 22.05.2013]
22. McKendry P. *Energy production from biomass (part 1)- overview of biomass.* Bioresource Technology, 2002. 83(1): p. 37–46.
23. Demirbas A. *Biomass resource facilities and biomass conversion processing for fuels and chemicals.* Energy Conversion and Management, 2001. 42: p. 1357–1378.
24. Heinimö J, Junginger M. *Production and trading of biomass for energy – An overview of the global status.* Biomass and Bioenergy, 2009. 33(9): p.

1310–1320.

25. Weiland P. *Biogas production: current state and perspectives.* Applied Microbiology and Biotechnology, 2010. 85(4): p. 849–860.
26. Holm-Nielsen JB, Al Seadi T, Oleskowicz-Popiel P. *The future of anaerobic digestion and biogas utilization.* Bioresource Technology, 2009. 100(22): p. 5478–5484.
27. Bridgwater AV. *The technical and economic feasibility of biomass gasification for power generation.* Fuel, 1995. 74(5): p. 631–653.
28. Lim JS, Abdul MZ, Wan Alwi SR, Hashim H. *A review on utilization of biomass from rice industry as a source of renewable energy.* Renewable and Sustainable Energy Reviews, 2012. 16(5): p. 3084–3094.
29. Panwar NL, Kothari R, Tyagi VV. *Thermochemical conversion of biomass – Eco friendly energy routes.* Renewable and Sustainable Energy Reviews, 2012. 16(4): p. 1801–1816.
30. Bridgwater AV. *Catalysis in thermal biomass conversion.* Applied Catalysis A: General, 1994. 116: p. 5–47.
31. Maniatis K. *Progress in biomass gasification.* Progress in Thermochemical Biomass Conversion Blackwell Scientific Publications, Oxford, UK, 2001: p. 1–32.
32. Elliott DC. *Catalytic hydrothermal gasification of biomass.* Biofuels, Bioproducts and Biorefining, 2008. 2(3): p. 254–265.
33. Mok WS-L, Antal MJ Jr. *Effects of pressure on biomass pyrolysis. II. Heats of reaction of cellulose pyrolysis.* Thermochimica Acta, 1983. 68: p. 165–186.
34. Mok WS-L, Antal MJ Jr. *Effects of pressure on biomass pyrolysis. I. Cellulose pyrolysis products.* Thermochimica Acta, 1983. 83: p. 155–164.
35. Elliott DC, Sealock LJ Jr. *Low temperature gasification of biomass under pressure*, in *Fundamentals of thermochemical biomass conversion*, Overend RP, Milne TA and Mudge LK, Editors. 1985, Springer Netherlands. p. 937–950.
36. Elliott DC, Butner RS, Sealock LJ Jr. *Low-temperature gasification of high-moisture biomass*, in *Research in thermochemical biomass conversion*, Bridgwater AV and Kuester JL, Editors. 1988, Springer Netherlands. p. 696–710.

37. Elliott DC, Sealock LJ Jr. *Use of aqueous catalytic processing for water-gas shift conversion.* Battelle Memorial Institute, 1991. 5,019,135: p. 14–21.
38. Elliott DC, Sealock LJ Jr, Baker EG. *Chemical processing in high-pressure aqueous environments. 2. Development of catalysts for gasification.* Industrial & Engineering Chemistry Research, 1993. 32(8): p. 1542–1548.
39. Minowa T, Ogi T, Dote Y, Yokoyama D-y. *Methane production from cellulose by catalytic gasification.* Renewable Energy, 1994. 5: p. 813–815.
40. Minowa T, Zhen F, Ogi T. *Cellulose decomposition in hot-compressed water with alkali or nickel catalyst.* The Journal of Supercritical Fluids, 1998. 13: p. 253–259.
41. Xu X, Matsumura Y, Stenberg J, Antal MJ Jr. *Carbon-catalyzed gasification of organic feedstocks in supercritical water.* Industrial & Engineering Chemistry Research, 1996. 35: p. 2522–2530.
42. Antal MJ Jr, Allen SG, Schulman D, Xu X. *Biomass gasification in supercritical water.* Industrial & Engineering Chemistry Research, 2000. 39: p. 4040–4053.
43. Buhler W, Dinjus E, Ederer HJ, Kruse A, Mas C. *Ionic reactions and pyrolysis of glycerol as competing reaction pathways in near- and supercritical water.* The Journal of Supercritical Fluids, 2002. 22: p. 37–53.
44. Kruse A, Gawlik A. *Biomass conversion in water at 330–410 °C and 30–50 MPa.* Industrial & Engineering Chemistry Research, 2003. 42(2): p. 267–279.
45. Kruse A, Dinjus E. *Hot compressed water as reaction medium and reactant.* The Journal of Supercritical Fluids, 2007. 41(3): p. 361–379.
46. Schmieder H, Abeln J, Boukis N, Dinjus E, Kruse A, Kluth M, Petrich G, Sadri E, Schacht M. *Hydrothermal gasification of biomass and organic wastes.* The Journal of Supercritical Fluids, 2000. 17: p. 145–153.
47. Cortright RD, Davda RR, Dumesic JA. *Hydrogen from catalytic reforming of biomass derived hydrocarbons in liquid water.* Nature, 2002. 418: p. 964–967.
48. Davda RR, Shabaker JW, Huber GW, Cortright RD, Dumesic JA. *Aqueous-phase reforming of ethylene glycol on silica-supported metal catalysts.* Applied Catalysis B: Environmental, 2003. 43(1): p. 13–26.
49. Furusawa T, Sato T, Sugito H, Miura Y, Ishiyama Y, Sato M, Itoh N, Suzuki N.

Hydrogen production from the gasification of lignin with nickel catalysts in supercritical water. International Journal of Hydrogen Energy, 2007. 32(6): p. 699–704.

50. Lu Y, Li S, Guo L, Zhang X. *Hydrogen production by biomass gasification in supercritical water over Ni/γAl_2O_3 and Ni/CeO_2-γAl_2O_3 catalysts.* International Journal of Hydrogen Energy, 2010. 35(13): p. 7161–7168.
51. Guo Y, Wang SZ, Xu DH, Gong YM, Ma HH, Tang XY. *Review of catalytic supercritical water gasification for hydrogen production from biomass.* Renewable and Sustainable Energy Reviews, 2010. 14(1): p. 334–343.
52. Elliott DC, Peterson K, Muzatko D, Alderson E, Hart T, Neuenschwander G. *Effects of trace contaminants on catalytic processing of biomass-derived feedstocks*, in *Proceedings of the twenty-fifth symposium on Biotechnology for Fuels and Chemicals.* Held May 4–7, 2003, in Breckenridge, CO, M. Finkelstein, et al., Editors. 2004. Humana Press. p. 807–825.
53. Elliott DC, Neuenschwander G, Hart T, Butner R, Zacher A, Engelhard M, Young J, McCready D. *Chemical processing in high-pressure aqueous environments. 7. Process development for catalytic gasification of wet biomass feedstocks.* Industrial & Engineering Chemistry Research, 2004. 43: p. 1999–2004.
54. Elliott DC, Hart T, Neuenschwander G. *Chemical processing in high-pressure aqueous environments. 8. Improved catalysts for hydrothermal gasification.* Industrial & Engineering Chemistry Research, 2006. 45: p. 3776–3781.
55. Nakagawa H, Namba A, Böhlmann M, Miura K. *Hydrothermal dewatering of brown coal and catalytic hydrothermal gasification of the organic compounds dissolving in the water using a novel Ni/carbon catalyst.* Fuel, 2004. 83(6): p. 719–725.
56. Yoshida T, Oshima Y, Matsumura Y. *Gasification of biomass model compounds and real biomass in supercritical water.* Biomass and Bioenergy, 2004. 26(1): p. 71–78.
57. Sharma A, Nakagawa H, Miura K. *A novel nickel/carbon catalyst for CH_4 and H_2 production from organic compounds dissolved in wastewater by catalytic*

hydrothermal gasification. Fuel, 2006. 85(2): p. 179–184.

58. Sharma A, Nakagawa H, Miura K. *Uniform dispersion of Ni nano particles in a carbon based catalyst for increasing catalytic activity for CH_4 and H_2 production by hydrothermal gasification.* Fuel, 2006. 85(17–18): p. 2396–2401.
59. Sharma A, Saito I, Nakagawa H, Miura K. *Effect of carbonization temperature on the nickel crystallite size of a Ni/C catalyst for catalytic hydrothermal gasification of organic compounds.* Fuel, 2007. 86(7–8): p. 915–920.
60. Elliott DC. *Historical developments in hydroprocessing bio-oils.* Energy & Fuels, 2007. 21: p. 1792–1815.
61. Morimoto M, Nakagawa H, Miura K. *Hydrothermal extraction and hydrothermal gasification process for brown coal conversion.* Fuel, 2008. 87(4–5): p. 546–551.
62. Hammerschmidt A, Boukis N, Hauer E, Galla U, Dinjus E, Hitzmann B, Larsen T, Nygaard SD. *Catalytic conversion of waste biomass by hydrothermal treatment.* Fuel, 2011. 90(2): p. 555–562.
63. Waldner MH, Krumeich F, Vogel F. *Synthetic natural gas by hydrothermal gasification of biomass.* The Journal of Supercritical Fluids, 2007. 43(1): p. 91–105.
64. Elliott DC, Hart TR. *Catalytic hydroprocessing of chemical models for bio-oil.* Energy & Fuels, 2009. 23: p. 631–637.
65. Sato T, Osada M, Watanabe M, Shirai M, Arai K. *Gasification of alkylphenols with supported noble metal catalysts.* Industrial & Engineering Chemistry Research, 2003. 42: p. 4277–4282.
66. Osada M, Sato O, Watanabe M, Adschiri T, Arai K. *Low-temperature catalytic gasification of lignin and cellulose with a ruthenium catalyst in supercritical water.* Energy & Fuels, 2004. 18: p. 327–333.
67. Osada M, Sato O, Arai K, Shirai M. *Stability of supported ruthenium catalysts for lignin gasification in supercritical water.* Energy & Fuels, 2006. 20: p. 2337–2343.
68. Osada M, Hiyoshi N, Sato O, Arai K, Shirai M. *Subcritical water regeneration of supported ruthenium catalyst poisoned by sulfur.* Energy & Fuels, 2008. 22: p.

845–849.

69. Dreher M, Johnson B, Peterson A, Nachtegaal M, Wambach J, Vogel F. *Catalysis in supercritical water: Pathway of the methanation reaction and sulfur poisoning over a Ru/C catalyst during the reforming of biomolecules.* Journal of Catalysis, 2013. 301: p. 38–45.

70. Oasmaa A, Kuoppala E, Ardiyanti A, Venderbosch RH, Heeres HJ. *Characterization of hydrotreated fast pyrolysis liquids.* Energy & Fuels, 2010. 24(9): p. 5264–5272.

71. Wildschut J, Melián-Cabrera I, Heeres HJ. *Catalyst studies on the hydrotreatment of fast pyrolysis oil.* Applied Catalysis B: Environmental, 2010. 99(1–2): p. 298–306.

72. Lee I, Ihm S. *Catalytic gasification of glucose over Ni/Activated charcoal in supercritical water.* Industrial & Engineering Chemistry Research, 2009. 48: p. 1435–1442.

73. Escobar A, Pereira M, Pimenta R, Lau L, Cerqueira H. *Interaction between Ni and V with USHY and rare earth HY zeolite during hydrothermal deactivation.* Applied Catalysis A: General, 2005. 286(2): p. 196–201.

74. Li H, Zhao Y, Gao C, Wang Y, Sun Z, Liang X. *Study on deactivation of Ni/Al_2O_3 catalyst for liquid phase hydrogenation of crude 1,4-butanediol aqueous solution.* Chemical Engineering Journal, 2012. 181–182: p. 501–507.

75. Waldner M, Vogel F. *Renewable production of methane from woody biomass by catalytic hydrothermal gasification.* Industrial & Engineering Chemistry Research, 2005. 44: p. 4543–4551.

CHAPTER 2

CATALYTIC HYDROTHERMAL REFORMING OF WATER-SOLUBLES FROM THE PYROLYSIS OF BIOMASS

2.1. Introduction

Energy shortage and severe environmental concerns have attracted great attention on the exploitation of lignocellulosic biomass as a clean and renewable energy resource [1]. Pyrolysis is a cost effective way to convert biomass into degraded products, and the distribution of the products, i.e., gas, liquid, and char, is variable over a wide range. Fast pyrolysis, operated at moderate pyrolysis temperature (~500 ºC), high heating rate (10^3–10^5 ºC s^{-1}), short vapor residence time (< 2 s), and with rapid quenching of volatiles, effectively converts biomass into the liquid termed bio-oil at yield as high as 70–80% [2,3]. In fast pyrolysis, biomass decomposes to generate mostly vapors and aerosols and some charcoal. After cooling and condensation, a dark brown mobile liquid is formed which has a heating value about half that of conventional fuel oil. The main product, bio-oil, is obtained in yields of up to 75 wt % on dry feed basis, together with byproduct char and gas which are used within the process. The crude pyrolysis liquid is dark brown and approximates to biomass in elemental composition. It is composed of a very complex mixture of oxygenated hydrocarbons with an appreciable proportion of water from both the original moisture and reaction product. Considerable research and development have been made toward utilization of the bio-oil as a fuel alternative to petroleum derived fuels. It is, however, still required methods to upgrade the bio-oil

with respect to heating value, moisture content, stability, and corrosiveness [3]. Slow pyrolysis produces more char, termed bio-char, than the fast pyrolysis. The bio-char has a potential of not only a renewable solid fuel but also a soil amender with a function of carbon sequestration [4]. The slow pyrolysis produces bio-oil at yield comparable with the bio-char, but the bio-oil is often a byproduct. Bio-oil from the slow pyrolysis is generally separated into two phases, i.e., oil and water phases. Hydrothermal treatment of biomass as a way of upgrading produces effluent water, composition of which is more or less similar to that of the water phase of the bio-oil [5].

A possible utilization of biomass derived liquids is extraction of flavoring and resin by adding water into the liquid causing an oil phase separated from the water phase. The resultant aqueous phase still consists of complex mixture of aldehydes, acids, ketones, furans, phenols, and saccharides, and its further application is limited [6]. Conventional catalytic steam reforming is a possible option of converting the water-soluble organics into gas, but is inevitably associated with problems of carbon deposition onto the catalyst and reactor material, and energy penalty arisen from enormous latent heat of water and the organics [7,8]. It is expected in future that green and cost-effective techniques will be required to process a variety of aqueous liquids from biomass utilization processes in the industrial scale.

Catalytic hydrothermal reforming (CHTR) has advantages over the gas phase steam reforming to produce fuel gas or syngas: (i) high reaction rate due to an elevated reactivity of water, (ii) production of concentrated gas, (iii) formation of less coke leading to a stable operation and a long life of catalyst, and (iv) no need of heat supply to evaporate water [9,10]. Although there are drawbacks coming from a high cost of reactor material and difficulty of scaling-up, it is deemed that the CHTR is an effective process to directly produce fuel gas from organics dissolved in water, in particular, those with relatively low concentration. Since the pioneering research by Elliott and Baker [11], many attempts have been made in the CHTR to produce hydrogen or methane from specific model compounds. Elliott and co-workers [12] investigated CHTR of phenol as a model compound of wastewater over several types of catalysts. They confirmed the catalytic activities for only nickel, ruthenium, and rhodium. It was also found that support materials such as monoclinic zirconia, rutile titania, and carbon were stable under hydrothermal conditions. The CHTR has thus been examined for a

wide range of organics and evidenced to be effective. Valle et al. [13] directly subjected crude bio-oil to hydrothermal transformation into hydrocarbons over acidic catalysts. However, there has been no report on CHTR of either bio-oil or bio-oil derived water-soluble organics.

Among the catalysts so far applied to the CHTR, Ni/carbon catalysts developed by Miura and co-workers [14–17] showed an outstanding catalytic activity. The catalysts included up to 47 wt % of highly dispersed Ni particles with a diameter of around 4 nm on a porous carbon support. These Ni/C catalysts were applied to CHTR of phenol [15,16], and extracts from brown coal [14,17]. Despite relatively severe reaction conditions with LHSV = 50 h^{-1} and total organic carbon concentration (TOC) = 2,000–20,000 ppm (mg-C g^{-1}), more than 95% of organics were converted into gas over 25 h. However, there has been no report on detailed information of composition of refractory species that survived the CHTR.

From a point of view of wastewater treatment, removal of organics from water by CHTR is required to be complete or nearly complete. Previous reports suggest difficulty to treat biomass-derived liquids that are multi-component mixtures with a single metal catalyst, the activity of which largely depends on organic species to be converted [18,19]. It, in other words, is better to have the catalyst contain two or more active metals to totally remove the organics. In this work, CHTR of biomass-derived water-solubles was studied, aiming to develop catalysts that enable to convert the solubles into syngas rich in CH_4 and/or H_2 simultaneously with production of organic-free water. Based on the knowledge of the Ni/Carbon catalysts [14–16], attempts have been made to develop carbon-supported mono-metallic and bi-metallic catalysts that enable complete or nearly complete reforming of the organics dissolved in water.

2.2. Experimental

2.2.1. Materials

Preparation of Feedstock, Water-solubles from the Pyrolysis of Biomass. An aqueous solution of biomass-derived water-solubles was prepared through the pyrolysis of chipped Japanese cedar using a lab-scale horizontal screw-conveyer pyrolyzer with

an inner diameter of 50 mm and effective length of 150 mm. The chips were rectangular in shape with an average size of 10 x 10 x 2 mm and composed of 50.9 wt % C, 6.3 wt % H, 0.2 wt % N, 42.3 wt % O and < 0.2 wt % ash. 160 g of the dried biomass was continuously fed into the pyrolyzer at a rate of 3.3 g min^{-1}, and heated up to 550 ºC at an average heating rate of 350 ºC min^{-1} in a flow of N_2. Condensable matter of the volatiles from the pyrolysis was collected in a series of an aerosol filter (170 ºC) and three cold traps (0, –40 and –70 ºC) located downstream of the reactor. The product distribution is given in Table 2.1.

Condensables collected in the 0 ºC cold trap was used for preparing the feedstock. The solution, separated in three-phases (i.e., lighter oil phase, water phase, and heavier oil phase), was mixed with 100 mL of deionized water, and the resulting emulsified solution was filtered through a membrane filter with a pore size of 0.45 μm. Three repeated water-addition/filtration cycles produced a single-phase aqueous solution containing water-solubles with a TOC of about 20,000 ppm (mg-C g^{-1}). The amount of carbon included in the solution accounted for 11.8% of the feedstock biomass. The solution was stored at 5 ºC protected from light. The TOC concentration of the solution was adjusted to 10,000 ppm by diluting with water before every run of CHTR.

Catalyst Preparation and Characterizations. Three different types of catalysts were prepared; Ni/Carbon (NiC), bi-metallic Me (Mo, Co, Fe, Cu, and Zn)-Ni/carbon (Me-NiC), and NiC impregnated with Pt (Pt/NiC). NiC was prepared through the carbonization of a Ni^{2+}-exchanged polymer resin. This method was reported in detail elsewhere [14–17]. 60 g of a methacrylic acid type ion exchange resin (Mitsubishi Chemical, WK-11) as received, which was spherical in shape with an average diameter of 0.5 mm, was suspended in 300 mL of an aqueous solution of $Ni(NO_3)_2 \cdot 6H_2O$ (0.67 mol L^{-1}). The pH of the solution had been adjusted at 8.8 by adding an aqueous solution of ammonia. The suspension was stirred for 24 h at room temperature. The resultant resin was washed with distilled water, and vacuum dried at 70 °C for 2 h. The dried resin was heated at a rate of 10 °C min^{-1} up to 500 °C and further heated at this peak temperature for 1 h in a steady flow of N_2 at 5 L min^{-1}. Me-NiC was prepared through co-ion exchanging of Me (Mo, Co, Fe, Cu, or Zn) with Ni and subsequent carbonization in the same way as above. The molar ratio of Me to Ni in the solution for ion exchange

was fixed at 1:4 with a total concentration of 0.2 mol L^{-1}. Pt/NiC catalyst was prepared by impregnating Pt into the NiC in a rotating evaporator for water evaporation at 60 °C and 20 kPa using $H_2PtCl_6 \cdot 6H_2O$ as a metallic precursor salt. This solution was completed with distilled water up to 10 mL solution per g of NiC to obtain 1 and 5 wt % of the final catalysts, Pt/NiC (1 wt %) and Pt/NiC (5 wt %), respectively. These catalysts were dried under vacuum overnight, and finally activated by reduction under H_2 (50 mL min^{-1}) for 3 h at 350 °C.

Specific surface areas of the catalysts were measured by N_2 adsorption at 77 K with a Quantachrome Autosorb-1 and analyzed by the Brunauer–Emmett–Teller (BET) method. Prior to the N_2 adsorption, the sample was outgassed at 200 °C for 2 h under high vacuum. X-ray powder diffraction patterns (XRDs) were measured by an X-ray diffractometer (Rigaku, SmartLab) equipped with a Cu Kα radiation source at a voltage and current of 45 kV and 200 mA, respectively. Transmission electron microscope (TEM) observation was conducted with a JEOL, JEM-2100F with an accelerating voltage of 200 keV. Energy dispersive X-ray spectrometry (EDS) mapping was performed with a JEOL, JED-2300T analyzer. For the TEM observation, the sample was crashed, ground, and dispersed in ethanol under ultrasonic agitation. A drop of this suspension was then transferred to a carbon-coated Cu mesh grid and dried at room temperature. Thermogravimetric analysis (TGA) was conducted using a Brucker TG-DTA 2000S to estimate the content of metals in the catalyst by combustion of the carbon support. The content was calculated with assuming that the weight change was caused by the loss of carbon and the oxidation of Ni to NiO.

2.2.2. Catalytic Hydrothermal Reforming (CHTR)

Figure 2.1 shows the experimental setup used for the CHTR. 0.6–0.7 g of catalyst was charged in a reactor assembled from Swagelok fittings with an inner volume of 0.67 mL. After the preliminary reduction in H_2 flowing at a rate of 50 mL min^{-1} at 350 °C and atmospheric pressure for 3 h, the catalyst was cooled down to room temperature in a flow of N_2. Then water was supplied to the flow channel from a HPLC pump (Shimadzu, LC-10A*i*) with 20 MPa pressure that was maintained by using a backpressure regulator, while the reactor temperature was raised to 350 °C at the rate of

10 °C min^{-1}. When the temperature reached 350 °C, the flow water was replaced by that of feedstock solution to start CHTR. The solution was continuously supplied to the catalyst bed at a rate of 0.5 mL min^{-1} for a typical reaction period of 40 min. The flow rate corresponded to LHSV (liquid hourly space velocity) of 45 h^{-1}. A thermocouple was inserted into the reactor so that its tip had contact with the bottom surface of the sintered SUS-made filter supporting the catalyst bed. The thermocouple was employed to regulate the bed temperature. The temperature distribution over the bed was within a range of 20 °C. The effluent stream passing through the backpressure regulator was led to a glass pot, where the product liquid or liquid/solid mixture was collected. The gaseous product was purged with 50 mL min^{-1} of N_2 out of the glass bottle, and then led to a gasbag. Aqueous solutions containing acetone, acetol, or acetic acid at TOC of 500 ppm was used as feedstocks in examination of catalytic activity toward these specific compounds.

2.2.3. Product Analysis

TOCs of the feedstock solution and liquid products were determined with a TOC analyzer (Shimadzu, TOC-5000A). Conversion of water-soluble organics in the solution was normally calculated based on TOC of the feedstock and product liquids. The gaseous products were analyzed by gas chromatography using general TCD and FID GCs (Shimadzu, GC-8A and GC-14B). Compositions of the feedstock and product liquids were measured by gas chromatography-mass spectrometry (GC–MS) with a Perkin-Elmer Clarus 600C that was equipped with a capillary column: TC-1701 (14% cyanopropylphenyl-86% dimethylsiloxane, 60 m, 0.25 mm i.d., 0.25 μm d.f.). A temperature profile with the following sequence was employed: holding at 40 °C for 5 min, rising up to 250 °C at 4 °C min^{-1}, and holding at 250 °C for 20 min. The injector temperature was set to 345 °C. Quantification of compounds was performed in a selected mass mode. Major peaks were assigned relying on the National Institute of Standards and Technology (NIST) MS library.

2.3. Results and Discussion

2.3.1. Water-solubles of the Bio-oil from the Biomass Pyrolysis

Figure 2.2 gives GC–MS chromatograms of the feedstock just after preparation and dilution of TOC to 10,000 ppm and that after storage for three months at TOC of 20,000 ppm. Both of these two solutions consisted of about 70 detectable compounds that involved aldehydes, alcohols, acids, ketones, furans, phenols, and sugars. Acetic acid and acetol were found in the fresh solution at highest TOCs, 2,263 and 1,970 ppm, respectively, as for general bio-oils [4]. Such high concentration of acetic acid seemed to be responsible for pH of the solution as low as 2.7. Other major compounds quantified were acetone, furfural, and phenol, with TOC of 103, 55, 155 ppm, respectively. Although most of chemical reactions causing aging of the bio-oil in the storage are not well understood, it is generally believed that aldehydes, phenols, and sugars react to form water-insolubles, while acids are not involved in such reactions [20]. It is seen in Figure 2.2 that relative peak intensities for aldehydes decreased after the storage. Conversion of the aldehydes probably caused increases of acetic acid and acetol concentrations to 2,355 and 2,173 ppm, respectively. The aging of the solution was obvious because brownish flakes were formed in the storage. The composition of water-solubles changed to some extent due to the aging, but not significantly. Based on the rate and extent of the aging of the present feedstock solution, all of the CHTR runs were carried out within two weeks since the feedstock preparation.

2.3.2. Catalytic Hydrothermal Reforming of Water-solubles over NiC and Me-NiC.

First various types of catalysts were examined for the catalyst activity for reforming. The results of this examination are shown in the Table 2.2. Among them NiC was selected due to its best activity for the further assessment to achieve the aim of this study. CHTR of water-solubles using Me-NiC was carried out, and the catalytic performance was compared with that of NiC, expecting improvement of NiC's activity by the coexisting metal. Kudo et al. [21] prepared a Cu/ZnO/C catalyst through simultaneous ion exchanging of Cu^{2+} and Zn^{2+} on the same resin as used in this study. They found that the presence of ZnO in the carbon matrix changed the morphology of

Cu particles, reducing of their size from 40 nm to less than 10 nm and improving the size uniformity. Steam reforming of methanol and dimethyl ether demonstrated that the catalytic activity was dramatically enhanced by such morphological changes as well as the synergic catalysis of Cu with ZnO. When used no catalyst, the conversion of water-solubles on TOC basis was less than 10% (Figure 2.3). The use of NiC or Me-NiC, on the other hand, removed more than 80% of the initial TOC. However, none of the Me-NiC had catalytic activity higher than that of NiC judging from the TOC of the product liquid. This result indicates that secondary metals, i.e., Mo, Co, Fe, Cu, and Zn, neither had higher catalytic activity than Ni, nor improved the morphology of Ni particles. In other words, Ni particles in NiC were already dispersed to a significant degree without morphological modification to show very high catalytic activity. The conversion of water-solubles was 98.4% for NiC, which increased pH of the product liquid from 2.7 to 5.4. However, the product liquid still had TOC of 161 ppm, which is higher than that can be ready to be disposed to the environment. For further improvement of the catalytic activity of NiC, it is desirable to add another type of metal with keeping the structure of NiC. In the following sections, effect of the Pt impregnation into NiC is shown and discussed.

2.3.3. Catalyst characterization

Results of the analyses of the NiC and Pt/NiC are summarized in Table 2.3. The NiC prepared in this study had properties slightly different from those reported by Miura and co-workers [15], having higher specific surface area (228 > 178 m^2 g^{-1}) and lower Ni content (42.6 < 47 wt %). Such differences were probably arisen from those in the preparation conditions; use of nickel nitrate as a Ni precursor instead of the sulfate, and employment of a higher flow rate of N_2 at 5 L min^{-1} during the carbonization of the resin for avoiding deposition of volatiles onto the pyrolyzing resin. On the other hand, it was confirmed that the catalyst in this study also had a highly dispersed Ni nanoparticles with a diameter less than 4 nm as shown in Figure 2.4 (a). Other beneficial characteristics of NiC are hard spherical form and metallic (not oxidized) Ni at as-prepared state, i.e., no need for molding and reduction before use.

Catalysts impregnated with Pt had surface area greater than that of NiC. This was probably due to the destruction and consumption of carbon support in the highly acidic chloroplatinic acid solution in the impregnation and subsequent heating process. N_2 adsorption and desorption isotherms shown in Figure 2.5 indicate that the change was caused largely by the increase in the macropore and not by the micropore that is more responsible for the degree of the surface area. In fact, the impregnation did not make much difference in the surface area compared to the change in the pore volume. This result ensures that the effect of Pt impregnation on the catalytic activity can be discussed only from the viewpoint of Pt without considering the difference in the structure of the carbon support. It was difficult in TEM observation to distinguish Pt from Ni particles, while EDS mapping clearly detected presence of Pt particles in the catalyst matrix as shown in Figure 2.4 (b). In contrast to the very uniform distribution of Ni particles on/in the carbon support, Pt particles were interspersed in the size of 6–8 nm. As is found in the image, coarse particles with a size even larger than 30 nm were also observed. Crystal growth of Pt inside the carbon matrix might be another reason for the increase in surface area and pore volume by the Pt impregnation. The measurement limitation of EDS mapping was upper than 3-4 nm. Hence it was not possible to reveal small particles of Pt less than limitation. However the experimental results on the improvement of catalytic activity by impregnating of Pt were indicating that there was a presence of active small particles of Pt. Because it was obvious from CHTR results that the impregnating of Pt into NiC catalyst was promoted the catalytic activity. There are two possible ways for enhancement of catalytic activity of NiC by Pt. One is the metal particles of Pt are located mostly on the surface on the Ni particles and Pt can contribute active hydrogen to promote resistance to the oxidation of Ni. It would be easy for active hydrogen to be transferred from Pt to Ni because of close contact between Pt and Ni nano-sized particles. However, it was difficult to confirm it by TEM and EDS mapping measurement. The other mechanism is the oxidized Ni species reduced to Ni again by the attendance of Pt. Consequently Pt played an important role to promote the catalytic activity of NiC and maintain its activity. Weight change curves during heating the catalyst in air are shown in Figure 2.6. The weight increase at around 200–300 ºC was caused by oxygen chemisorption onto the catalyst, while the decrease at 300–500 ºC was due to the combustion of carbon. The oscillation of the curves for NiC and Pt/NiC

(1 wt %) at 300–350 ºC represents a mechanical function of furnace to control the temperature that was increased by exothermic carbon combustion. Whereas, the curve for Pt/NiC (5 wt %) had no oscillation, indicating slower progress of the exothermic reactions. It should be noted that with increase in the Pt content, temperature for the weight decrease shifted to high temperature region. To reveal the difference of behavior of the catalysts weight loss curves of the catalysts compared to those for ion exchange resin (without loading of metal), which was started more than 400 °C. This means that carbon support combustion was promoted by Ni species during TGA because the weight loss was started around 300 °C. Therefore the disappearance of oscillation for Pt/NiC (5 wt %) indicated that the effect of Ni on combustion of carbon was probably suppressed by Pt or carbon combustion was progressed slowly by two steps: first to carbon monoxide and further to carbon dioxide with increase in the Pt content.

2.3.4. CHTR of Water-solubles over Pt/NiC

Figure 2.7 shows the results of CHTR of the water-solubles with NiC and Pt/NiC. The conversions achieved with the Pt/NiCs were well above 99%, while 98.4% by NiC. The yields of H_2, CH_4, and CO_2 were 5.5–8.1, 50.6–53.1 and 41.4–44.8%, respectively, which were in broad agreement with those from CHTR of phenol over NiC [16] and Ru [12] catalysts at 350 ºC and 20–21 MPa. As reported in literatures [14], CHTR of oxygenated organic compounds is believed to start from their decomposition to form CO and H_2 followed by water-gas shift ($CO + H_2O \rightarrow CO_2 + H_2$) and methanation ($CO + 3H_2 \rightarrow CH_4 + H_2O$) reactions occurring in parallel. Although H_2, CH_4, and CO_2 might also be produced directly by the decomposition, it was more plausible that those gases were formed by not single but series/parallel reactions as stated above. The product gas composition thus seemed to be determined mainly by thermodynamics. The total gas yield was more than 92% on a feedstock carbon basis. The remainder, < 8% of the feedstock solution, was caused mainly by dissolution of CO_2 in the product liquid as inorganic carbon species.

Improvement of the activity of NiC by the Pt impregnation was significant in considering reduction of TOC of the product liquid from 161 ppm (NiC) to 25 ppm (Pt/NiC, 1 wt %) and even to 6 ppm (Pt/NiC, 5 wt %). The Pt/NiC was thus effective to

totally remove water-solubles from the solution. Pt catalysts have been used in CHTR studies. For example, Cortright and co-workers [19] used Pt/γ-Al_2O_3 catalyst for CHTR of sugars and alcohols at temperatures near 220 ºC, and succeeded in producing H_2 in high yield. However, at high temperature range as employed in this study, other precious metals, such as Ru, Rh, and Ni show higher catalytic activities than Pt, producing primarily CH_4 as claimed by Elliot et al. [12,22]. In this study, Pt/$CeZrO_x$ catalyst, prepared according to the published method, was also examined for CHTR of the water-solubles but the conversion was only 50.7% [23]. The result roughly demonstrates that Pt alone did not have activity to totally convert the water-solubles into gas. Accordingly, the very low TOC of the liquid products from CHTR with the Pt/NiC was attributed to promotion of the activity of Ni by Pt or otherwise, activity of Pt toward a specific compounds that were refractory over NiC.

GC-MS analysis of the liquid product detected only a compound, acetone, for both NiC and Pt/NiC. This result evidenced almost all water-soluble organics were fully converted, since detection limit of the GC-MS was lower than several ppm-C. Phenol that is often used as a model compound seemed to be rather labile under the present CHTR conditions. To probe the catalyst performance, three compounds, i.e., acetone, acetol, and acetic acid, were selected and subjected individually to CHTR. Acetol and acetic acid were main compounds in the water-solubles (Figure 2.2). Aqueous solutions of these compounds were prepared at TOC of 500 ppm, and used for CHTR over NiC and Pt/NiC (1 wt %). The results are shown in Figure 2.8. Pt/NiC was more active than NiC for all of the three compounds. Acetic acid and acetol were completely converted, but leaving acetone in the solution. On the other hand, the conversion of acetone was incomplete even with Pt/NiC. It was concluded from these results that at least a portion of acetic acid and that of acetol were catalytically converted to acetone, which was more refractory than its precursors. Since acetic acid is rather stable even in the super critical condition [24], the formation of acetone took place from acetic acid under the catalysis to cause a reaction

$$2CH_3COOH \rightarrow CH_3COCH_3 + CO_2 + H_2O.$$

Acetol, which is produced mainly from the pyrolysis of cellulose [25], was thought to be dehydroxylated to form acetone

$$CH_3COCH_2OH + H_2 \rightarrow CH_3COCH_3 + H_2O.$$

Although it might be possible for acetone to be formed from other compounds included in water-solubles, it can be said that acetic acid and acetol were important precursors of acetone. With the use of Pt/NiC, acetone in the feedstock solution and that formed in-situ were reformed to gas nearly completely. This was a main reason why Pt/NiC gave the product liquid with TOC as low as 6 ppm.

Figure 2.9 compares XRD patterns of fresh catalysts and spent ones by CHTR of water-solubles. Broad peak at $2\theta = 44.8^{\circ}$ found in all patterns represents small particles of metallic Ni. No peak assigned to NiO occurred in the patterns of the fresh catalysts, while a portion of Ni of the spent NiC was present as NiO of that peaks appeared at 2θ = 37.3, 43.4 and 62.9º. As reported in the literature [14], Ni is oxidized primarily by water or O_2 dissolved in water. Loss of metallic Ni due to such oxidation lowers the catalytic activity. On the other hand, no formation of NiO was detected in spent Pt/NiC. This indicates that Pt promoted the resistance of Ni to the oxidation or oxidized Ni species were reduced with reducing agents such as CH_4, CO and H_2 by occurrence of Pt at higher rate than that of oxidation during CHTR, and is consistent with the result of TGA that is shown in Figure 2.6. It seems that CHTR had intensified the peaks for Ni and Pt of Pt/NiC slightly. Average crystallite sizes of Pt of the fresh and spent Pt/NiC were given as 14.1 and 14.7 nm, respectively, by analyzing the peaks at $2\theta = 39.8^{\circ}$ based on Scherrer equation (D (Å) = $K \cdot \lambda / (\beta \cos\theta)$). Thus, change on the size of Pt particles was, if any, insignificant, suggesting long-term stability of Pt/NiC.

Long-term catalytic activity of Pt/NiC was investigated. The feedstock was continuously supplied to the catalyst bed for 24 h, while TOC of the product liquid was measured every two hour (Figure 2.10). It is generally known that carbon supported metal catalysts loses activity with time due to sintering and/or phase transformation of metals, change of specific surface area, and decomposition of support. Such loss of the catalytic activity was, however, not the case of Pt/NiC, which maintained conversion of more than 99% (on TOC basis) over the period of 24 h. Rather, the conversion even increased from 99.7% of after 2 h to 99.9% of after 10 h. Although the reason of this was not clear, the result demonstrated maintenance of high activity of Pt/NiC. If there was real increase in catalyst activity was most likely caused by part of the carbon support which was covering some metal particles was gasified and the oxidized Ni

metals NiO may be reduced to Ni particles again during the reforming. As represented by Sample (b) in Figure 2.11, the product liquid was colorless within several hours from the beginning. However, it was tinged with a light ocher color and smoked with suspended matter after 10 h, as exampled by Sample (c). Filtration of the liquid gave a colorless solution as Sample (d) and residue (Sample (e)). Taken together with the maintenance of TOC of the product liquid below 10 ppm after 8 h (Figure 2.10), it was suspected that suspended matter was solid formed from water-soluble inorganics. Identification of this matter and clarification of mechanism of its formation was left in future work.

2.4. Conclusions

CHTR of water-solubles from the biomass pyrolysis was studied for aiming to develop catalysts that convert them into syngas rich in CH_4 and/or H_2 and produce organics-free water simultaneously. CHTR with NiC converted more than 98% of the dissolved organic carbon to CH_4 and CO_2 forming H_2 but allowing the product liquid to have TOC as high as 160 ppm. The catalytic performances of the five Me-NiCs were lower than NiC. The impregnation of Pt into NiC greatly improved the activity and the Pt/NiC enabled to decrease TOC of the product liquid to only 6 ppm that corresponded to the carbon conversion of 99.94%. Such a high activity was attributed to that for the reforming of the most refractory compounds, acetone, which was a component of the feedstock and formed from other major ones such as acetic acid and acetol. Pt played a role of preventing metallic Ni being oxidized during CHTR, avoiding activity loss of NiC, rather than that of converting refractory component over itself. A continuous CHTR run for a duration of 24 h demonstrated stability of Pt/NiC at temperature and pressure of 350 ºC and 20 MPa, respectively, under continuous feeding of the water-solubles with TOC of 10,000 ppm. This CHTR process demonstrates its promising application to develop a wastewater treatment. The significance of this study is the achievement of the strict limitation of environmental restriction to dispose the treated water to the environment.

Table 2.1. Product yields from the pyrolysis of biomass.

Yield [wt%]										Mass balance [%]
Gas					Condensables (Temp. for cold or hot traps [°C])				Char	
H_2	CO	CO_2	CH_4	C_2-C_4	-70	-40	0	> 170		
0.1	9.5	11.2	1.7	1.9	3.0	3.1	35.8[a]	10.5	24.2	101.1

[a] Water content: 62.6 wt %.

Table 2.2. Results of various types of catalysts examined.

Catalyst name	Conversion [%, mol/mol-C]
CoC	56
MoCoC	76
Pt/$CeZrO_2$/Al_2O_3	51
Cu/ZnO/C	24
NiC	98

Table 2.3. Properties of NiC and Pt/NiC.

Catalyst	S_{BET} [m^2 g^{-1}]	V_P[a] [cm^3 g^{-1}]	D_P[b] [nm]	Metal amount [wt %]
NiC	228	0.17	< 0.6	42.6
Pt/NiC (1 wt %)	253	0.20	< 0.6	46.2
Pt/NiC (5 wt %)	243	0.31	< 0.6	45.6

[a] Pore volume, [b] Peak diameter of micropore.

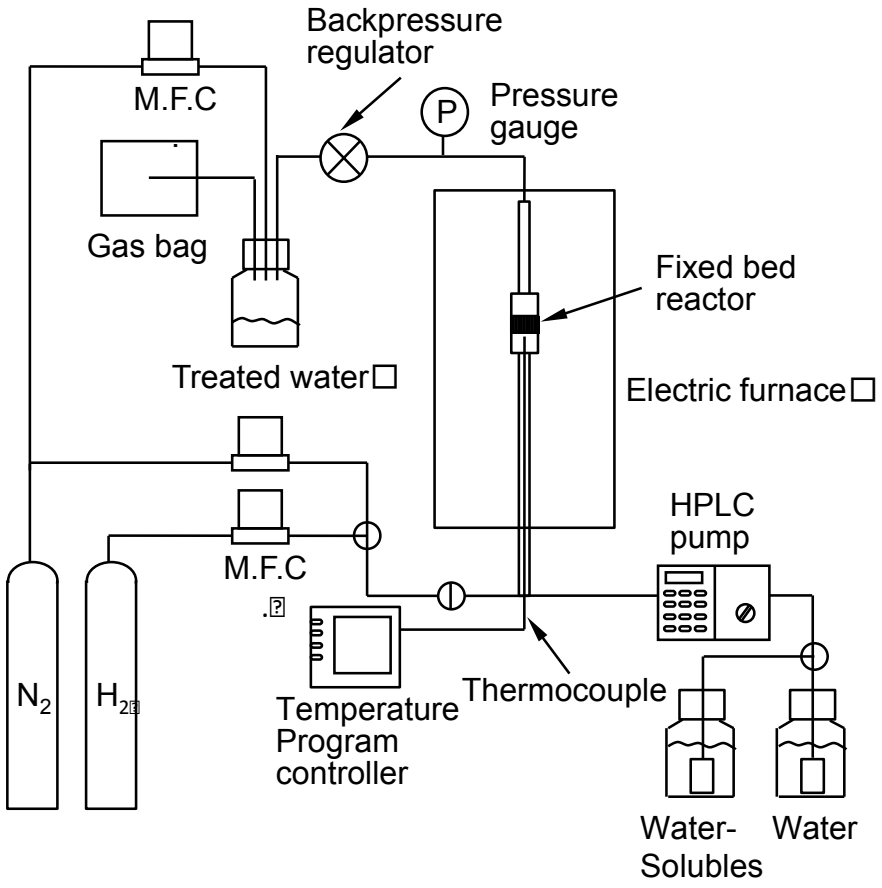

Figure 2.1. Experimental setup for CHTR.

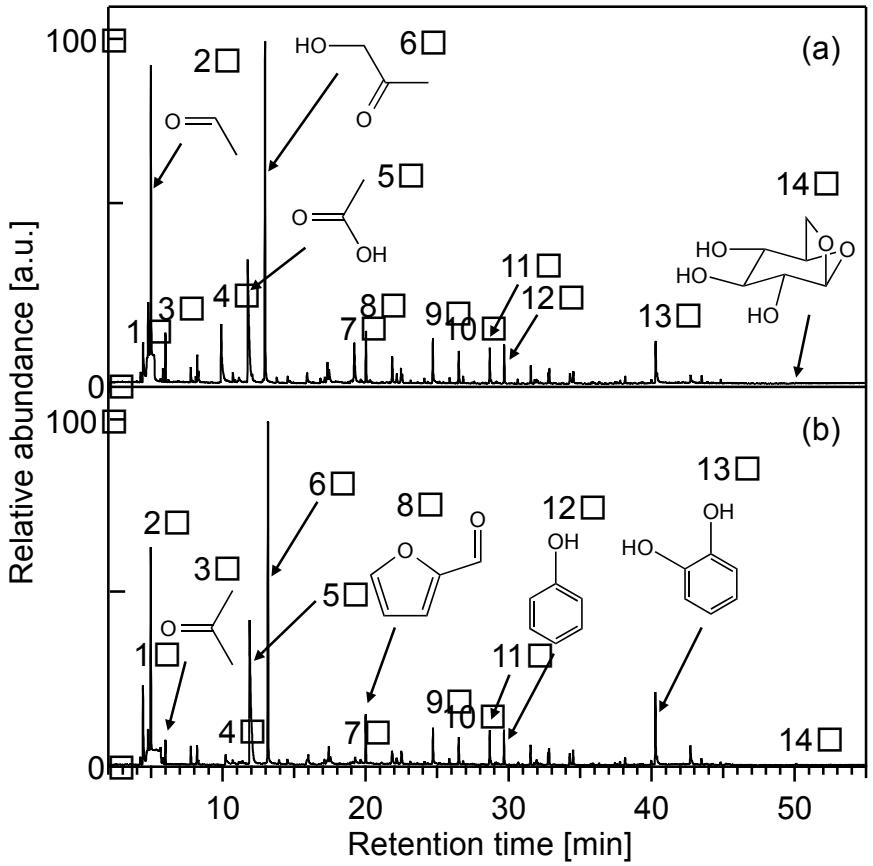

Figure 2.2. GC-MS chromatograms of (a) fresh feedstock, and (b) feedstock after storage for three months. The main peaks are assigned as follows: 1. Formaldehyde, 2. Acetaldehyde, 3. Acetone, 4. Acetaldehyde, hydroxyl-, 5. Acetic acid, 6. Acetol, 7. Butanedial, 8. Furfural, 9. 2-Cyclopenten-1-one, 2-hydroxy-, 10. Butyrolactone, 11. 1,2-Cyclopentanedione, 3-methyl-, 12. Phenol, 13. 1,2-Benzenediol, 14. Levoglucosan.

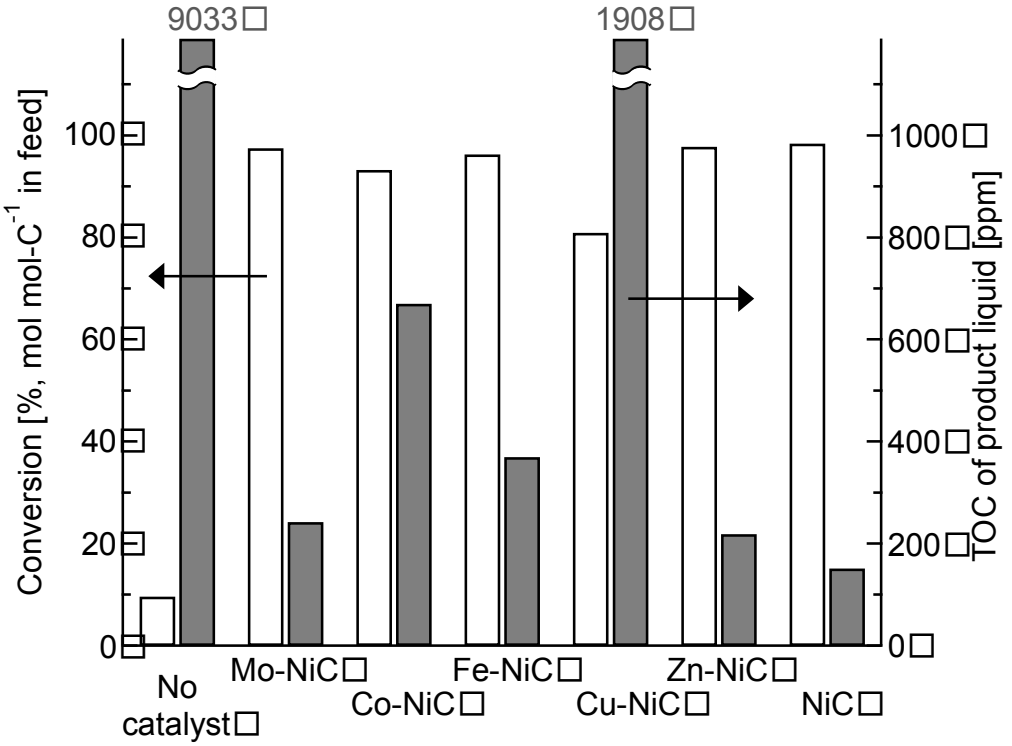

Figure 2.3. Conversion of water-solubles and TOC of the product liquid in the CHTR with NiC, Me-NiC, and no catalyst. Temperature; 350 ºC, Pressure; 20 MPa, and LHSV; 45 h^{-1}.

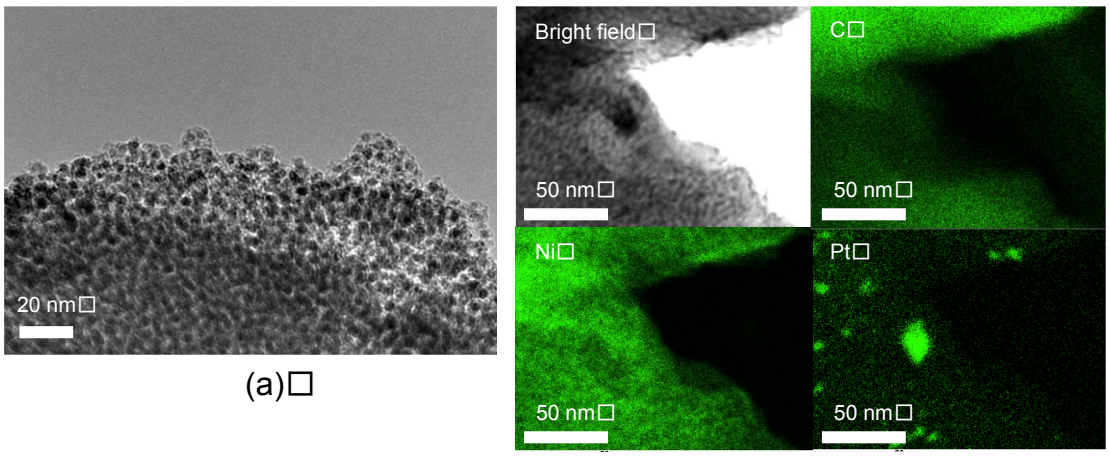

Figure 2.4. Result of TEM observation of NiC and Pt/NiC (5 wt %). (a) TEM image of NiC, and (b) bright field image and EDS mappings of Pt/NiC (5 wt %) catalyst using C Kα, Ni Kα and Pt Mα peaks at X-ray energies of 0.277, 7.471 and 2.048 keV, respectively.

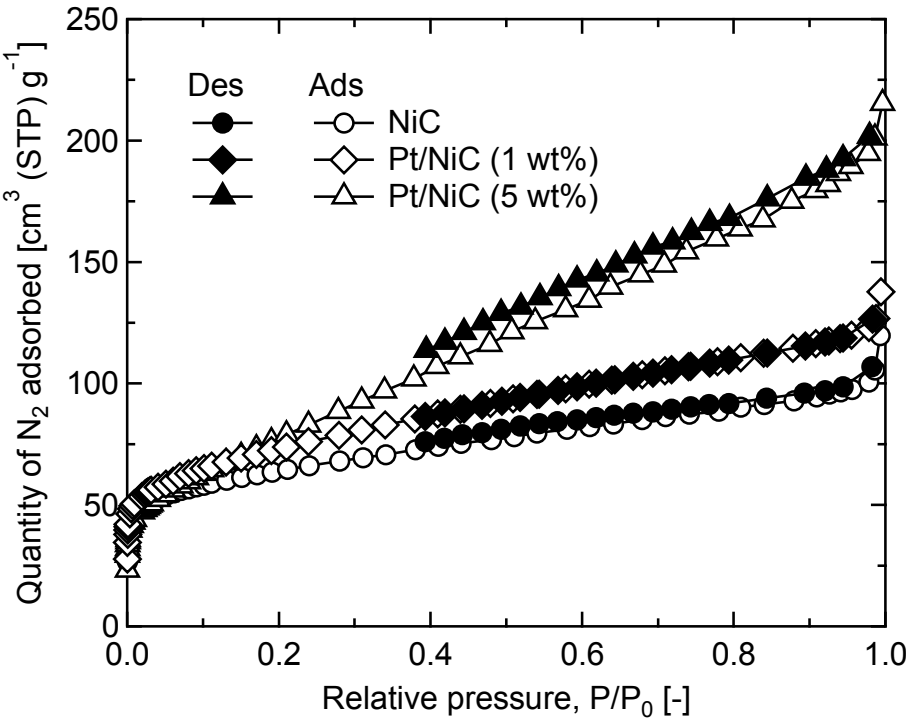

Figure 2.5. N_2 adsorption and desorption isotherms of NiC, Pt/NiC (1 wt %), and Pt/NiC (5 wt %).

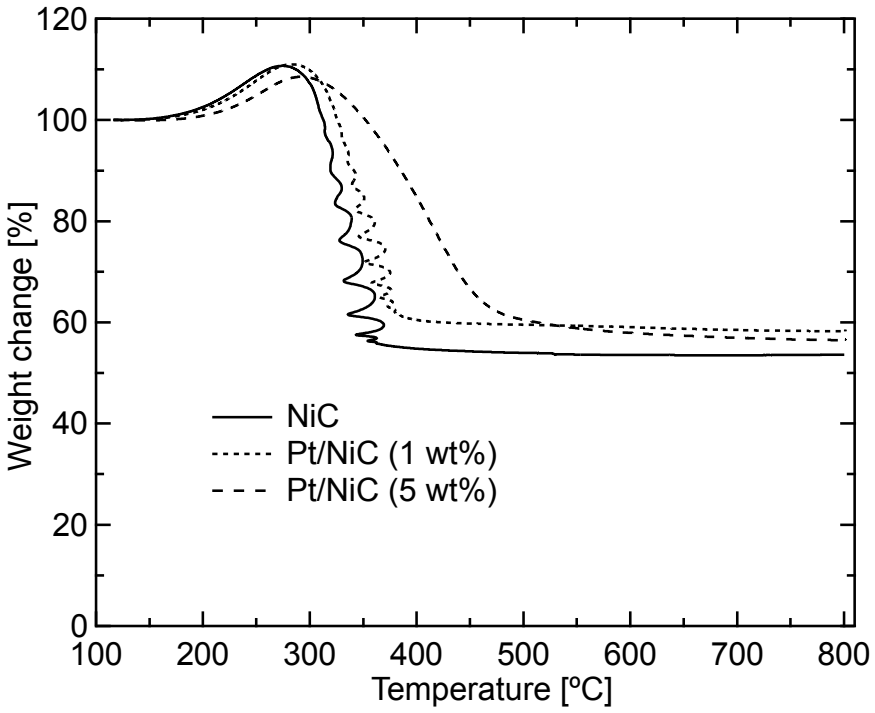

Figure 2.6. Weight change during heating of NiC and Pt/NiC in air. Initial sample mass; 10 mg, heating rate; 10 ºC min^{-1}, flow rate of air; 200 mL min^{-1}.

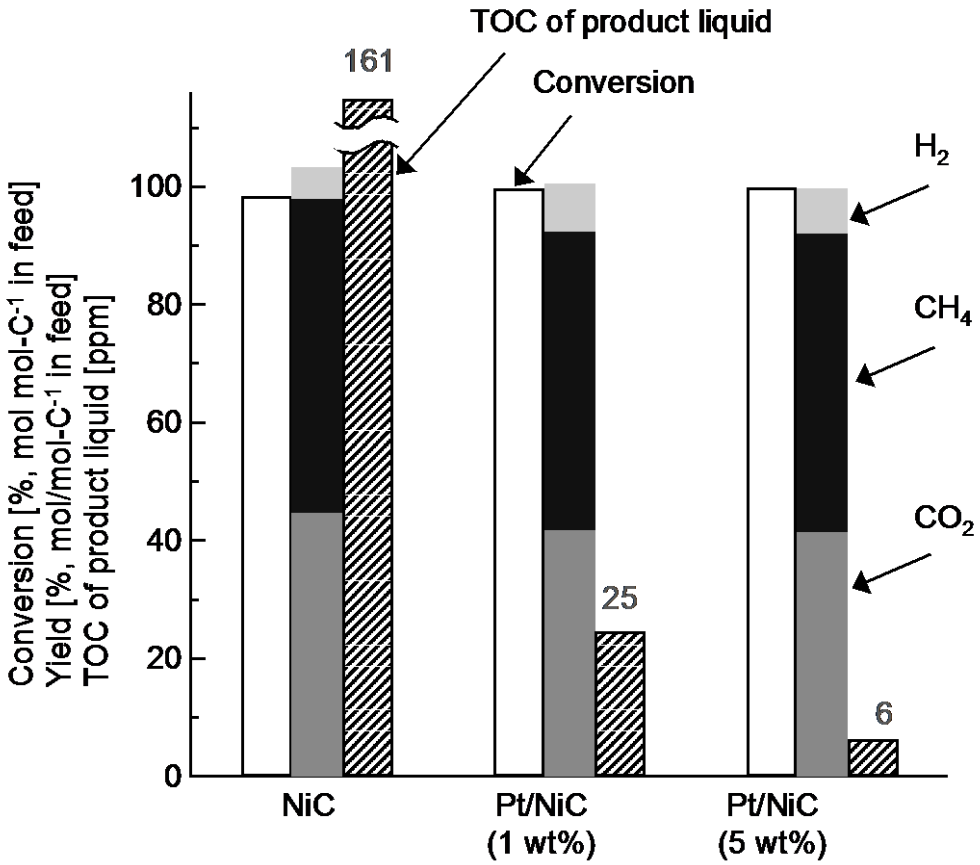

Figure 2.7. Results from CHTR of water-solubles over NiC and Pt/NiC. Temperature; 350 ºC, Pressure; 20 MPa, and LHSV; 45 h^{-1}.

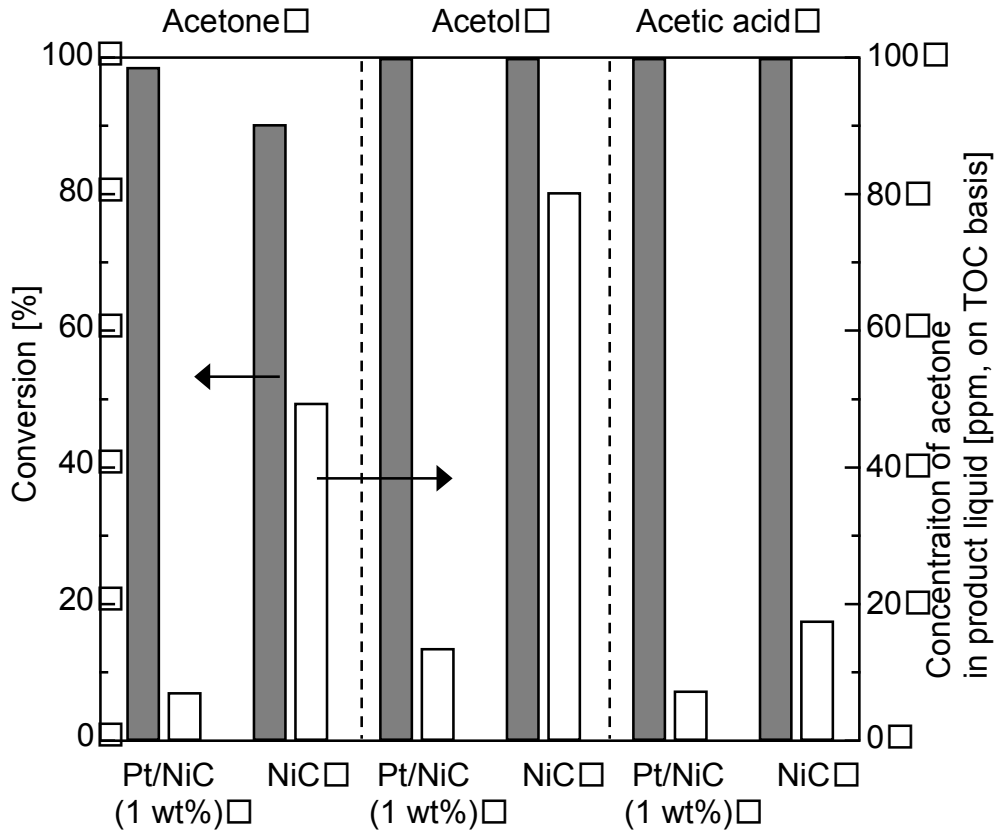

Figure 2.8. CHTR of acetone, acetol, and acetic acid over NiC and Pt/NiC; feedstock: aqueous solution containing 500 ppm (on TOC basis) of acetone, acetol, or acetic acid. Temperature; 350 ºC, Pressure; 20 MPa, and LHSV; 45 h^{-1}.

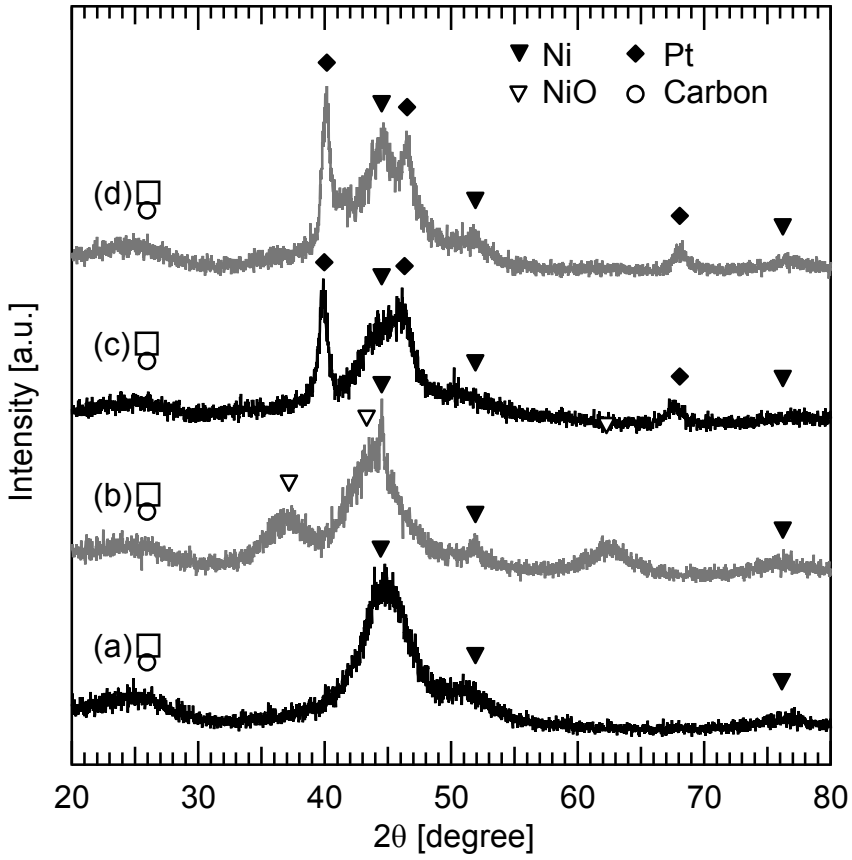

Figure 2.9. XRD patterns of catalysts; (a) fresh NiC, (b) spent NiC, (c) fresh Pt/NiC (5 wt %) and (d) spent Pt/NiC (5 wt %).

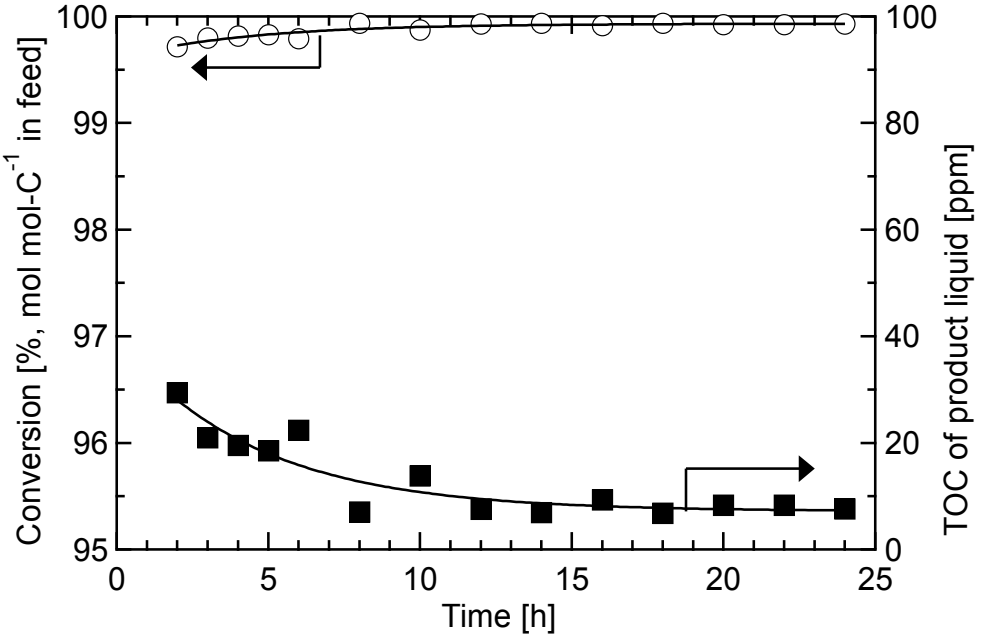

Figure 2.10. Result of long-term CHTR of water-solubles over Pt/NiC (1 wt %). Temperature; 350 ºC, Pressure; 20 MPa, and LHSV; 21 h^{-1}.

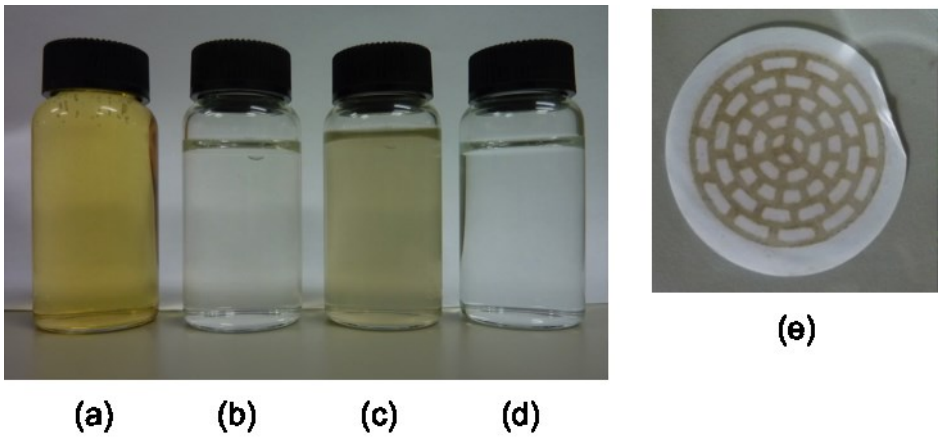

Figure 2.11. Photos of (a) feedstock solution, (b) product liquid collected at 2 h since the start of CHTR, (c) product liquid at 24 h, (d) product liquid at 22 h after filtration, and (e) residue filtered from the product liquid at 22 h.

2.5. References

1. McKendry P. *Energy production from biomass (part 1)-overview of biomass.* Bioresource Technology, 2002. 83: p. 37–46.
2. Zhang Q, Chang J, Wang T, Xu Y. *Review of biomass pyrolysis oil properties and upgrading research.* Energy Conversion and Management, 2007. 48(1): p. 87–92.
3. Lu Q, Li W-Z, Zhu X-F. *Overview of fuel properties of biomass fast pyrolysis oils.* Energy Conversion and Management, 2009. 50(5): p. 1376–1383.
4. Mullen CA, Boateng AA, Hicks KB, Goldberg NM, Moreau RA. *Analysis and comparison of bio-oil produced by fast pyrolysis from three barley biomass/byproduct streams.* Energy & Fuels, 2010. 24(1): p. 699–706.
5. Nonaka M, Hirajima T, Sasaki K. *Upgrading of low rank coal and woody biomass mixture by hydrothermal treatment.* Fuel, 2011. 90(8): p. 2578–2584.
6. Oasmaa A, Korhonen J, Kuoppala E. *Characterization of hydrotreated fast pyrolysis liquids.* Energy & Fuels, 2010. 24(9): p. 5264–5272.
7. Garcia L, French R, Czernik S, Chornet E. *Catalytic steam reforming of bio-oils for the production of hydrogen:effects of catalyst composition.* Applied Catalysis A: General, 2000. 201: p. 225–239.
8. Wang D, Czernik S, Chornet E. *Production of hydrogen from biomass by catalytic steam reforming of fast pyrolysis oils.* Energy & Fuels, 1998. 12: p. 19–24.
9. Guo Y, Wang SZ, Xu DH, Gong YM, Ma HH, Tang XY. *Review of catalytic supercritical water gasification for hydrogen production from biomass.* Renewable and Sustainable Energy Reviews, 2010. 14(1): p. 334–343.
10. Lu Y, Li S, Guo L, Zhang X. *Hydrogen production by biomass gasification in supercritical water over Ni/γAl_2O_3 and Ni/CeO_2-γAl_2O_3 catalysts.* International Journal of Hydrogen Energy, 2010. 35(13): p. 7161–7168.
11. Elliott DC, Baker EG, Symposium on Biotechnology for Fuels and Chemicals. *Upgrading biomass liquefaction products through hydrodeoxygenation*. Richland, Washington: Pacific Northwest Laboratory, 1984. 14: p. 159–174.

12. Elliott DC, Hart TR, Neuenschwander GG. *Chemical processing in high-pressure aqueous environments. 8. Improved catalysts for hydrothermal gasification.* Industrial & Engineering Chemistry Research, 2006. 45: p. 3776–3781.
13. Valle B, Gayubo AG, Alonso A, Aguayo AT, Bilbao J. *Hydrothermally stable HZSM-5 zeolite catalysts for the transformation of crude bio-oil into hydrocarbons.* Applied Catalysis B: Environmental, 2010. 100(1–2): p. 318–327.
14. Sharma A, Nakagawa H, Miura K. *A novel nickel/carbon catalyst for CH_4 and H_2 production from organic compounds dissolved in wastewater by catalytic hydrothermal gasification.* Fuel, 2006. 85(2): p. 179–184.
15. Sharma A, Nakagawa H, Miura K. *Uniform dispersion of Ni nano particles in a carbon based catalyst for increasing catalytic activity for CH_4 and H_2 production by hydrothermal gasification.* Fuel, 2006. 85(17–18): p. 2396–2401.
16. Sharma A, Saito I, Nakagawa H, Miura K. *Effect of carbonization temperature on the nickel crystallite size of a Ni/C catalyst for catalytic hydrothermal gasification of organic compounds.* Fuel, 2007. 86(7–8): p. 915–920.
17. Morimoto M, Nakagawa H, Miura K. *Hydrothermal extraction and hydrothermal gasification process for brown coal conversion.* Fuel, 2008. 87(4–5): p. 546–551.
18. Elliott DC, Hart TR. *Catalytic hydroprocessing of chemical models for bio-oil.* Energy & Fuels, 2009. 23: p. 631–637.
19. Cortright RD, Davda RR, Dumesic JA. *Hydrogen from catalytic reforming of biomass-derived hydrocarbons in liquid water.* Nature, 2002. 418: p. 964–967.
20. Oasmaa AJ, Korhonen J, Kuoppala E. *An approach for stability measurement of wood-based fast pyrolysis bio-oils.* Energy & Fuels, 2011. 25(7): p. 3307–3313.
21. Kudo S, Maki T, Miura K, Mae K. *High porous carbon with Cu/ZnO nanoparticles made by the pyrolysis of carbon material as a catalyst for steam reforming of methanol and dimethyl ether.* Carbon, 2010. 48(4): p. 1186–1195.
22. Osada M, Sato O, Watanabe M, Arai K, Shirai, M. *Water density effect on lignin gasification over supported noble metal catalysts in supercritical water.* Energy & Fuels, 2006. 20: p. 930–935.

23. Nousir S, Keav S, Barbier J Jr, Bensitel M, Brahmi R, Duprez D. *Deactivation phenomena during catalytic wet air oxidation (CWAO) of phenol over platinum catalysts supported on ceria and ceria–zirconia mixed oxides.* Applied Catalysis B: Environmental, 2008. 84(3–4): p. 723–731.
24. Watanabe M, Inomata H, Smith RL Jr, Arai K. *Catalytic decarboxylation of acetic acid with zirconia catalyst in supercritical water.* Applied Catalysis A: General, 2001. 219: p. 149–156.
25. Piskorz J, Radlein D, Scott DS. *On the mechanism of the rapid pyrolysis of cellulose.* Journal of Analytical and Applied Pyrolysis, 1986. 9: p. 121–137.

CHAPTER 3

CATALYTIC HYDROTHERMAL REFORMING OF VEGETABLE OIL FOR THE PRODUCTION OF BIOFUELS

3.1. Introduction

The search for alternatives to petroleum based fuels has led to the development of fuels from various sources. Biofuels, which collectively mean any fuels derived from biomass, are attracting considerable attention because of decreasing petroleum resources and the environmental consequences of exhaust emissions. The two major chemical pathways to biofuels are fermentation of starches to ethanol and transesterification of fatty acids from vegetable oils. However in both cases agricultural products are being produced as feedstocks for biofuels rather than as food. Triglycerides, which are esters from glycerol and three fatty acids, are the major component of vegetable/seed oils and animal fats. The direct use of triglycerides for a diesel engine is possible; however, problematic properties, such as high viscosity and low volatility, require them to be upgraded before use [1]. Techniques developed for this upgrading include transesterification [2–4], pyrolysis [5,6], emulsification with alcohol [7], and hydrotreatment [8].

The most common way has been transesterification, which produces alkyl esters of long-chain fatty acids termed biodiesel, whereas an emerging area is the conversion into straight-chain alkanes (*n*-alkanes), which is instead termed green diesel [9,10]. Green

diesel could be directly used or cracked/isomerized to more suitable fuels. Hydrotreatment is currently of the best way to produce selectively long-chain alkanes derived from the carbon chain in triglyceride/fatty acids. The conversion pathway roughly consists of the formation of fatty acids as the initiation step and the succeeding deoxygenation of the fatty acids. The second step, deoxygenation, is promoted by a catalyst and therefore, efforts have been made to understand comprehensively the reaction mechanism as well as to develop a catalyst to selectively produce green diesel [8,11–19]. The drawbacks of the process certainly include the consumption of hydrogen, of which the major part is currently produced from fossil fuels. There is further uncertainty in the way to process glycerol and impurities such as water and other organics in the oil. In the direct hydrotreatment of triglyceride, glycerol is supposed to be converted to propane through catalysis [20] or a β-elimination pathway [21], but detailed information on this is unavailable, probably because of the low selectivity. Another option is the two-step process, where glycerol is removed to the water phase after the hydrolysis of triglyceride followed by the deoxygenation of the fatty acid in the oil phase [22].

The present study proposes catalytic hydrothermal reforming (CHTR) as a method to convert triglyceride into alkanes, aiming at the development of a clean process. CHTR has been applied to the conversion of a wide variety of carbon resources (e.g., lignocellulosic biomass [23,24], biomass derivatives [25], coals [26,27] and microalgae [28]) into gas, liquid, and/or solid products, depending on the purpose. There have been proposed triglyceride deoxygenation schemes in which a catalytic or noncatalytic hydrothermal system is involved as a part of the reforming process. However, in any of the cases, hydrogen is used as an essential agent for deoxygenation. For example, Murata et al. [20] examined the catalytic conversion of jatropha oil in the presence of water but under a pressurized hydrogen atmosphere. Wang et al. [22] demonstrated continuous production of the mixture of *n*-alkanes from vegetable oil using a two-step system; noncatalytic hydrothermal step for the hydrolysis and a hydrotreatment step for the deoxygenation of fatty acids. Li et al. [29] examined the catalytic hydrothermal conversion of triglyceride for cracking and succeeded in the reduction of hydrogen required for postrefining by hydrotreatment.

The best source for the chemistry relevant to triglyceride CHTR is a series of works

by Fu et al. [30–32] on hydrothermal fatty acids decarboxylation. Saturated fatty acids were selectively deoxygenated to long-chain alkanes by a hydrothermal process over Pt/C, but the experiment with unsaturated ones resulted in low selectivity with modest yields of the hydrogenated fatty acids.

However, starting CHTR from triglycerides or corresponding oils and not from fatty acids makes the reaction system more complex; however, if the conversion selectively progresses, then it is possible to realize a process without any separation of the products that are immiscible from each other. Therefore, the CHTR of triglyceride has the potential to contribute to the reduction of energy required for the production of biofuels. Furthermore, the glycerol generated from triglyceride by hydrolysis as well as a part of the organic impurities would be catalytically gasified, and the resulting hydrogen, if produced, may contribute to the reactions associated with the deoxygenation of fatty acids. The removal of glycerol from the reaction phase can also accelerate hydrolysis, which is restricted by the chemical equilibrium.

The main objective of this work is to investigate the reactions occurring during CHTR of triglyceride mainly over Pt and Ni catalysts supported on carbon to describe the differences between their catalysis. The product fuels, not limited to liquid fuels, were evaluated in terms of the efficiency of their conversion to *n*-alkanes.

3.2. Experimental

3.2.1. Materials

Feedstock. A type of jatropha oil having the fatty acid composition shown in Table 3.1 was used as the feedstock for CHTR. Jatropha oil is one of the promising feedstocks for the production of biofuels from inedible biomass. The fatty acid composition fall within the ranges generally found in the extracted oil from jatropha curcas seeds [33]. Unsaturated fatty acids, oleic and linoleic acids, account for the majority of the composition of jatropha oil. Free fatty acids with a similar composition are contained at 2.4 wt % in total.

Assuming the constituent of the oil by triglyceride and free fatty acids, the empirical formula of the feedstock was calculated to be $C_{56.0}H_{101.0}O_{6.0}$ using the contents and

compositions. The theoretically available maximum yield of fatty acids is 94.8% on the basis of carbon, and that of heptadecane and pentadecane is 77.4 and 11.9%, respectively, when CHTR induces only decarboxylation and hydrogenation (of carbon with double bonds) after or along with the hydrolysis.

Catalysts. Six different types of catalysts that were supported on carbon were examined for the CHTR of jatropha oil. Pt/C and Pd/C were purchased from Wako Pure Chemical Industries. The others were prepared by a method similar to that developed by Nakagawa et al. [34], where ion-exchange resin was used as a precursor of the support carbon. The characteristics of the catalyst prepared with this method is a high and homogeneous loading of metals on the carbon support, with the maintenance of moderate dispersion of the particles. For NiC and Pt/NiC, details for the preparation are described elsewhere [25,35]. Strongly basic anion-exchange resin, PK308 (Mitsubishi Chemical), was used for the preparation of PtC-P and PdC-P after treatment with a NaOH aqueous solution. The resin was immersed in the aqueous solution of H_2PtCl_6 or H_2PdCl_4, stirred for 24 h, washed by deionized water, and finally carbonized at 500 ºC for 1 h under an atmospheric nitrogen stream. All catalysts were treated under an atmospheric stream of H_2 at 350 ºC for 3 h before use. For convenience, the metals attached on carbon by the impregnation method are described with slash in the catalyst names (e.g., Pt/C).

Table 3.2 lists the textural properties of catalysts. The BET surface area and pore volume/size for each catalyst were calculated from an N_2 adsorption isotherm recorded with Quantachrome NOVA 3200e. The metal contents were determined by a general carbon combustion. Dispersion of the metals was qualitatively confirmed by TEM images that were taken with JEOL, JEM-2100, as shown in Figure 3.1.

All catalysts had a micropore structure of the carbon support. In comparison with the commercially purchased Pt/C and Pd/C, the other homemade catalysts were characterized by lower porosities, larger metal particles, and higher metal contents. Pt of the Pt/NiC was loaded on NiC by an impregnation method. Although Pt could not be distinguished from Ni particles by the TEM image, it was confirmed by EDS mapping that Pt interspersed over NiC with the particle size of 6–8 nm, which was recorded with JEOL JED-2300T analyzer [25].

3.2.2. CHTR of jatropha oil

CHTR was performed in a 10 mL batch reactor made of SUS316 Swagelok fittings. A $^1/_2$ in. plug was connected by union with $^1/_2$–$^1/_8$ in. reducer. The end of reducer was connected to a ball valve having 41.3 MPa pressure resistance through a 20 cm length of $^1/_8$ in. tube for the product gas collection. Jatropha oil (120 mg), catalyst (80 mg), water (5 mL), and 0.1 MPa nitrogen gas (purity > 99.9999 vol %) were charged into the reactor. The CHTR was initiated by submerging the entire part of the reactor in a fluidized sand bath heated at a prescribed temperature, and then quenched by immersing it into an ice-water bath after a period of 0.5–5 h, which included the heating period of 10–15 min. The pressure in batch reactor was in a range 6–16.5 MPa according water saturated vapor pressure and in addition of pressure of products gases. With a similar reaction system and conditions, Fu et al. [30] showed that the reaction rate was not limited by the rate of reactant molecules diffusion through the catalyst pores using the Wilke–Change correlation for the catalytic hydrothermal conversion of fatty acids.

The gaseous products were thoroughly collected in a gas bag. A gas chromatograph equipped with a TCD (GL Sciences, Micro GC CP4900) was used for the quantification of H_2, CO, CO_2, and C_1–C_4 hydrocarbons. The products retained in the reactor, liquid and solid, were recovered with a given volume of tetrahydrofuran and subjected to gas chromatography–mass spectrometry (GC–MS) for identification on a PerkinElmer Clarus 600C and also to gas chromatography (GC) on a HP 6890 series GC for identification/quantification. The same capillary column (GL Sciences InertCap® 1 (methylpolysiloxane, 60 m, 0.25 mm i.d., 0.25 μm d.f.)) was employed for the GC–MS and GC. Detector/injector temperatures of 250/345 °C were commonly applied to the GC–MS and GC. The following chromatographic temperature program was used for analysis: holding at 40 °C for 5 min, heating to 325 °C at 4 °C min^{-1}, and a final holding at 325 °C for 20 min. The analysis aimed mainly at the quantification of fatty acids and *n*-alkanes, although pentane and hexane were excluded because of their poor reproducibility in quantification, but this did not influence the discussion of the present study. The chemical standards were purchased, enabling product identification and quantification. The prospective assignments of the peaks from compounds other than fatty acids and *n*-alkanes were conducted by relying on the NIST 08 MS library. The

yields of products were calculated on the basis of carbon involved in the jatropha oil.

TGA of the liquid/solid product was performed under flowing nitrogen (150 mL min^{-1}) on an SII Nano Technology EXSTAR TG/DTA 7200 to identify the presence of GC–MS undetectable matter. Water and tetrahydrofuran were removed from the collected product using a rotary evaporator operated at 55 °C and 130 mbar for several hours. A 3 mg portion of the resulting liquid/solid mixture was subjected to TGA. The temperature was ramped from 30 to 600 °C at a heating rate of 3 °C min^{-1}.

3.3. Results and Discussion

3.3.1. Catalyst performances in jatropha oil conversion

CHTR of the jatropha oil was performed with the purchased and homemade catalysts. Because of the difficulty in quantifying unconverted jatropha oil with the present experimental methodology, the yield of fatty acids was used as a measure of catalysis. The results are shown in Figure 3.2. Kusdiana et al. [36] demonstrated that the hydrolysis of triglyceride at 350 °C reaches a complete conversion within several minutes even in the absence of catalysts. This was confirmed in the present study by a high yield of fatty acids in the absence of catalyst, but the further conversion of the resulting fatty acids into *n*-alkanes rarely progressed in the absence of catalyst, as shown in Table 3.3. Thus the higher yield of fatty acids represents a lower catalysis for the conversion of fatty acids and vice versa. Therefore, the yields of fatty acids and *n*-alkanes can be used as a measure of catalysis.

Although this is not necessarily a fair comparison of catalytic metals because of the variety of their textural properties, the results clearly distinguish the characteristics of the individual catalysts from those of the others. Pt/C and NiC gave the lowest yields of fatty acids followed by Pt/NiC. The high activity of Pt is in qualitative agreement with a previous report on the deoxygenation of fatty acid [30]. Pd/C, which is a superior catalyst in the hydrotreatment of triglyceride and fatty acids [12], was less active under the present CHTR conditions. The homemade Pt and Pd catalysts (i.e., PtC-P and PdC-P) had a much weaker catalytic effect on the conversion even with a higher content of active metals. This was caused by their less porous structure, allowing the reactant to

access the active metals.

Table 3.3 summarizes the key results for the distribution of products from CHTR over Pt, Pd, and Ni catalysts. The *n*-alkanes were grouped into $C_{1–4}$, $C_{15,}$ C_{17} and $C_{7–14,16,18}$ to represent gaseous, decarboxylation of C_{16}, decarboxylation of C_{18} and other products, respectively. Compounds other than those listed in the table were also contained in the CHTR products, which are discussed in more depth later. For the Pt and Pd catalysts except for PdC-P, the most abundant hydrocarbon product was always heptadecane derived from C_{18} fatty acids. In contrast, the catalysis of NiC directed the production toward lower hydrocarbons, in particular methane. As is to be expected, Pt/NiC had catalysis derived from both Pt and Ni, resulting in the production of broadly distributed alkanes. However, because partial leaching of Pt was visually apparent from the color of the product solution and the succeeding deposition an of orange gel for only this catalyst, the result does not necessarily show an inherent and/or long-term catalytic activity of Pt/NiC. The leaching probably occurred by less-fixed Pt particles on Ni metals, not on the carbon support, because of the large content of Ni in the catalyst.

In terms of the activity and selectivity, Pt/C and NiC seemed to be the most effective for the CHTR of jatropha oil and therefore these catalyses were investigated in more detail. Figure 3.3 again confirms the difference in the reactions occurring in CHTR over these catalysts. However, for both catalysts, prominent peaks were observed from only *n*-alkanes among the detected hydrocarbons.

3.3.2. Main reactions in CHTR of jatropha oil over Pt/C

Pt/C was active even at 275 °C for the conversion of jatropha oil into mainly heptadecane, and the yield reached 40.8% at 350 °C (Figure 3.4 (a)). Figure 3.5 (a) indicates that the conversion is nearly completed within 1 h at 350 °C. It is generally believed that reactions of triglyceride deoxygenation leading to the formation of long-chain hydrocarbons include decarboxylation, decarbonylation, and hydrodeoxygenation, by which oxygen in triglyceride is converted to CO_2, CO, and water, respectively [17]. The negligible yield of C_{18} hydrocarbon (0.1% at 350 °C) rules out the possibility of the occurrence of hydrodeoxygenation or else it is considered that the atmosphere of highly compressed water does not favor the water-forming hydrodeoxygenation. Mäki-Arvela

et al. [12] reported that decarbonylation is the main route for the formation of heptadecane from stearic acid ethyl ester under a hydrogen atmosphere over Pd/C, where heptadecane was formed directly from the ester. This means that decarbonylation, if this is the case, directly produces the long-chain hydrocarbon from triglyceride. However, in CHTR, the formation of fatty acid was confirmed at lower temperatures (Figure 3.6), and the yield decreased with temperature along with an increase in the heptadecane yield. The temporal changes of the yields at 350 °C in Figures 3.2 and 3.5 also show the formation of fatty acids before that of *n*-alkanes. Accordingly, it can be stated that heptadecane was formed by the catalytic decarboxylation of fatty acids, which are generated from jatropha oil by hydrolysis, for the present reaction in hydrothermal water.

Taking into consideration the fatty acid composition in the jatropha oil, the yield of heptadecane above 40%, corresponding to a selectivity of 52% (mol/mol C_{18} fatty acids), is high. Concerning the catalytic hydrothermal deoxygenation of monounsaturated fatty acid oleic acid, over Pt/C, Fu et al. [30,31] reported that the molar yield and selectivity of heptadecane were less than 20% at 330 °C, because of the slower rate of decarboxylation and side reactions, such as conversion into unidentified heavy products. Linoleic acid, having one more carbon double bond, resulted in worse selectivity, whereas saturated stearic acid could be converted to heptadecane with a selectivity of about 90%.

The content of saturated C_{18} fatty acid in jatropha oil is only 7.4% on the basis of carbon. However, the composition of the product fatty acids from CHTR at 275 °C is clearly higher than this value, where stearic acid is dominant among the C_{18} fatty acids (Figure 3.6). In other words, it is suggested that hydrogenation of carbon with double bonds occurred before and/or after the release of fatty acids from triglyceride by the hydrolysis.

The authors of the above-cited literature [27] found that linoleic acid was sequentially hydrogenated to stearic acid via oleic acid by hydrogen generated from partial cracking and reforming of hydrocarbons; however, the total yield of stearic acid and heptadecane was no more than 30% in their case. A larger extent of hydrogenation observed in the present jatropha oil CHTR would be explained by the presence of glycerol that is generated in hydrolysis simultaneously with fatty acids. In fact, glycerol

can be a source of hydrogen because the Pt catalyst is active enough for gasification at the present temperatures between 275–350 °C [37]. An additional CHTR experiment with glycerol instead of jatropha oil demonstrated the formation of gas that was rich in hydrogen with a composition; 62.5% H_2, 7.6% CH_4, and 29.3% CO_2 in mol. Figure 3.7 shows the molar yields of the gaseous products. In CHTR for 1 h, the yields of H_2 and CO_2 were 3.1 and 3.9%, respectively. With the assumption of a complete gasification of glycerol (5.2%-C in feedstock) and the adaptation of the above-mentioned gas composition, the available hydrogen from glycerol is 8.5% (mol/mol-C in feed) if it is not consumed. The difference between the yields of hydrogen, 5.4%, possibly reveals a portion of hydrogen that is consumed by in situ hydrogenation of unsaturated fatty acids. In fact, the hydrogen required for the complete hydrogenation of unsaturated acids in jatropha oil is theoretically 6.3%.

Another possible cause of the advanced hydrogenation is the use of triglyceride as feedstock and not fatty acids. When released from the triglyceride structure, unsaturated fatty acids suffer from reactions over Pt/C, leading to their conversion into heavier byproducts [31]. Conversely, before the release, the carboxyl group, which might be easily subjected to attack by reactive species, is protected by an ester bond to glycerol. Therefore, if hydrogenation is allowed to occur before the hydrolysis, particularly at low temperatures, more unsaturated fatty acid in triglyceride can be converted to saturated ones followed by hydrolysis. The literature lends some support to this hypothesis: Snåre et al. [14] found that oleic acid methyl ester was selectively hydrogenated to stearic acid methyl ester under a pressurized hydrogen atmosphere over Pd/C, whereas the experiment with oleic acid resulted in a much greater production of byproducts other than stearic acid and heptadecane. In addition, Gabrovska et al. [38] observed a gradual progress of linoleic acid hydrogenation over Ni catalysts even at 145 °C without the release from triglyceride. However, the effect of the use of triglycerides as the feedstock could not be confirmed because of the unavailability of data on glycerides in this study.

3.3.3. Main reactions in CHTR of jatropha oil over NiC

Thus, PtC is effective for the production of liquid fuel, heptadecane, which is a typical target product for hydrotreatment processes of triglycerides. However, NiC

produced fuel gas composed mainly of methane, as seen in Figures 3.4, 3.5, and 3.7, as well as Table 3.3. It is known that Ni catalysts are active in hydrotreatment processes, but the catalysis generally works toward mainly the production of long-chain alkanes as with the Pd and Pt catalysts. For instance, in work by Gong et al. [17], the yields of liquid and gaseous hydrocarbons from a jatropha oil were 83.9 and 5.6 wt %, respectively, over $NiMoP/Al_2O_3$ under 3 MPa hydrogen stream at 350 °C, which means that triglyceride was hardly cracked into lower hydrocarbons such as methane in the absence of water. It seems even in the hydrothermal medium that the thermal or catalytic cracking of jatropha oil cannot account for the methane formation because of the insignificant yield of hydrocarbons other than methane.

The yield of CO_2 gives insight pertaining to the main reaction over NiC. The theoretical maximum yield of CO_2 from glycerol and fatty acid decarboxylation is 10.6%. The much higher yield obtained from CHTR over NiC (e.g., 21.6% at 350 °C for 1 h; Figure 3.7), indicates that the reaction is associated with oxidation.

The following is a plausible reaction pathway:

(1) hydrolysis of triglyceride to form fatty acid (RCH_2COOH);

(2) formation of hydrocarbon by decarboxylation (RCH_3);

(3) oxidation by water ($RCH_3 + H_2O \rightarrow RH + CO + 2H_2$);

(4) methanation ($CO + 3H_2 \rightarrow CH_4 + H_2O$) and water-gas shift ($CO + H_2O \rightarrow H_2 + CO_2$).

By the repetition of step (3), hydrocarbon such as heptadecane continuously loses its carbon as carbon monoxide. A selective and rapid progression of the oxidation step presumably caused the low yield of higher carbon number *n*-alkanes.

The product from CHTR of the jatropha oil over Pt/NiC contained a broader range of *n*-alkanes (Table 3.3). This result is indicative of the role of Pt to provide an active hydrogen to the hydrocarbon, terminating the loss of carbon. The hydrocarbon thus produced was relatively stable in the presence of Pt against oxidation by water over Ni, as seen from the product distribution. In other words, the result of the Pt/NiC test gives a certain credibility to the mechanism that the formation of the hydrocarbon was initiated from the decarboxylation.

The activity of NiC was demonstrated also in our previous study of CHTR of water-soluble organics derived from biomass pyrolysis [25], where the gasification was nearly

completed within 1 min of liquid residence time over the catalyst bed at 350 °C. Although it depends on the organic species, the rate of the conversion of the present jatropha oil over NiC was also thought to be high because of a similar reaction mechanism [25]. However, the yields of gaseous product gradually increased with time even after 1 h of the reaction (Figure 3.5). This was caused by the decomposition and gasification of more persistent organic substances found in the residual liquid, of which the details are discussed later.

3.3.4. Reuse of Pt/C and NiC

Because the information provided by CHTR in the batch reactor was insufficient to discuss the maintenance of catalyst activity, CHTR tests were repeated three times under the same conditions with a reuse of the catalysts. The results are shown in Figure 3.8 for Pt/C and NiC. For both catalysts, the distribution of the product was well reproduced with deviations of 0.6 and 2.3% for heptadecane (Pt/C) and methane (NiC), respectively. These results confirm the maintenance of catalysis, at least enough for the reaction under the present conditions, as well as the reproducibility of our experimental data.

Table 3.4 shows the textural properties of the catalysts after the reuse three times. The porous structures of the support carbon, which influence the activity of the catalysts as indicated by PtC-P and PdC-P (Table 3.3), were moderately maintained for both catalysts. It is noteworthy that the content of Pt, measured by the combustion of carbon, was reduced by 32%. A possible cause of the reduction in Pt content other than the leaching of Pt is the inclusion of a compound derived from jatropha oil in spite of washing with tetrahydrofuran. Figure 3.9 shows the mass loss curves of fresh and three-times reused Pt/C during the combustion. The mass loss of the reused Pt/C started at a lower temperature and completed at a higher temperature, indicating the presence of a material not contained in the fresh one. Nevertheless, the reproducible catalyst performance shows that such a change in the structural property has an insignificant influence on the catalytic activity.

3.3.5. Liquid/solid product distribution

n-Alkanes, fatty acids, and CO_2 account for only 61.6 and 80.1% of the carbon in the feedstock for CHTR over Pt/C and NiC, respectively, at 350 °C for 1 h. These are the values of carbon balance typically observed in experiments under similar reaction conditions. Such a poor carbon recovery shows the presence of other products, in other words, byproducts. Table 3.5 shows examples of the products identified in this study, where the yield of liquid/solid was calculated from the mass after evaporation of water and solvent. The evaporation could be associated with the loss of a small amount of volatile hydrocarbon products.

GC–MS detectable byproducts included 1-methyldecyl-benzene and 8-heptadecene with the highest peak area for Pt/C and NiC, respectively. The CHTR over Pt/C involved at least isomerization, cracking, and aromatization as side reactions, whereas the detected peaks were from only *n*-alkanes and alkenes for NiC. Regardless of the experiment, there was little or no peaks from compounds having a carbon number of more than 18 except for a slight amount of fatty acid esters. However, judging from the peak areas, the amount of GC–MS detectable byproducts was not enough to explain the entire portion of carbon, especially for Pt/C products.

To find qualitatively GC–MS undetectable products, TGA under an inert atmosphere (in N_2) of liquid/solid products was performed (Figure 3.10). Because of the difficulty in a homogeneous collection of the sample, the results do not necessarily represent a mass distribution of the products. For the Pt/C product, there were four peaks at 159, 210, 304 and 446 °C. By comparison with the peaks of the reference materials in Figure 3.10 (b), the peak at the lowest temperature was assigned to the main product, pentadecane and heptadecane as well as byproducts having molecular weights similar to them. The two peaks at 304 and 446 °C undoubtedly show the presence of heavy byproducts. The peak temperatures of fatty acids were close to that of the remaining peak but slightly higher (palmitic acid = 226 °C and C_{18} fatty acids = 236–242 °C at the peak). Therefore, it is possible that the peak at 210 °C was also derived partially from GC-MS undetectable products. A similar TG profile was observed for NiC products, with an additional peak at a higher temperature of 557 °C. In addition, there were residues remaining after heating to 600 °C with yields of 2.4 and 5.5 wt %

for Pt/C and NiC products, respectively. No residue remained for the reference samples even in the case of jatropha oil.

A detailed mechanism for the formation of these heavy byproducts is still not clear. As discussed earlier, a part of the linoleic and oleic acids, which were not hydrogenated, was the potential source of the heavy byproducts. Impurities in jatropha oil known collectively as gum substances may have an influence, but their content is very low.

3.3.6. Performance of CHTR as a method for jatropha oil conversion

Figure 3.11 summarizes the reactions that are plausible in the CHTR of jatropha oil described together with the heating values of the main product (methane or pentadecane/heptadecane) per unit mass of the feedstock. The advantages of CHTR over hydrotreatment, which is attracting attention as a method for triglyceride conversion, would include the following features.

Two options are available depending on the catalyst, namely, the production of fuel gas or liquid fuel. Fuel gas was originally not a target product of hydrotreatment; however, the present study has identified fuel gas production as an attractive option with a high recovery of chemical energy from the feedstock as well as selectivity. For liquid fuel production, the selectivity to pentadecane/heptadecane, was lower, which was mainly due to the formation of byproducts. To make the CHTR competitive with hydrotreatment, it is required to suppress the side reactions arising from unsaturated fatty acids.

Glycerol from triglyceride hydrolysis is converted to gas including hydrogen, and this contributes to the acceleration of hydrolysis and the in situ hydrogenation of unsaturated fatty acids, leading to more *n*-alkane products. For hydrotreatment, a portion of glycerol is converted into propane [20,21], which is to be used in a separated process as a fuel gas.

CHTR requires neither additional solvent nor reagents such as hydrogen and methanol. The activity of the catalyst in hydrothermal water in turn indicates the possibility of the use of wastewater containing organics. In other words, the process may be accompanied by the cleanup of wastewater (by the gasification of organics), or more specifically the additional organics can be a source of methane and hydrogen,

leading to a more feasible process. For example, water containing water-soluble organics derived from biomass pyrolysis [25,39] or hydrothermal treatment [40] is a potential source of wastewater. Hydrogen generated from the organic wastes would contribute to the increase in *n*-alkanes yields.

The main drawbacks of CHTR come from the operational problems related to high pressure (e.g., about 17 MPa or even more). Given the reaction with a fixed bed reactor as an example of a flow system, the solid products would not be allowed in the effluent because it causes the plugging of the flow channel downstream of the reactor. Therefore, a near complete removal of the compound, which becomes solid at the decreased temperature, such as fatty acids, would be required for its practical use.

3.4. Conclusions

Among the catalysts examined, Pt/C and NiC had the highest activities for the conversion of the jatropha oil under in subcritical water. Two options with these catalysts have been suggested for the production of liquid and gas fuel with these catalysts. The main products of CHTR over Pt/C were pentadecane and heptadecane, which were derived from the decarboxylation of the corresponding fatty acids with the total yield of more than 46.3% at 350 °C. Hydrogen generated by the catalytic gasification of glycerol possibly contributed to the enhancement of the yield through the partial hydrogenation of unsaturated fatty acids. Ni/C had a different manner of catalysis, resulting in the selective formation of methane with a higher recovery of energy. It is plausible that the methane formation was caused by the repetition of the reactions between oxidation and radical formation of hydrocarbon, leading to the continuous loss of carbon as carbon monoxide. It has also been demonstrated that the activities of Pt/C and Ni/C were maintained during their three times repeated use, whereas the heavy byproducts were deposited onto the carbon support. The avoidance of the formation of such heavy products is therefore a most important subject for future studies. This study is signifying an option to use wastewater. The significance of this study is that no necessity of external hydrogen or other chemicals for this reforming process.

Table 3.1. Fatty acid composition of feedstock jatropha oil

FA [a]	Formula	Composition [b] [mol %]
Palmitoleic acid (C16:1)	$C_{16}H_{30}O_2$	1.2
Palmitic acid (C16:0)	$C_{16}H_{32}O_2$	13.7
Margaric acid (C17:0)	$C_{17}H_{34}O_2$	0.1
Linoleic acid (C18:2)	$C_{18}H_{32}O_2$	39.7
Oleic acid (C18:1)	$C_{18}H_{34}O_2$	39.0
Stearic acid (C18:0)	$C_{18}H_{36}O_2$	6.3

[a] The information in parenthesis denotes the number of carbon and the number of double bonds, respectively. [b] Compositions were determined by analysis after transesterification according to the method reported in reference 3.

Table 3.2. Textural properties of catalysts used for jatropha oil CHTR

Catalysts	Metal content [wt %]	S_{BET} [$m^2\ g^{-1}$]	V_p[a] [$cm^3\ g^{-1}$]	r_p[b] [nm]
Pt/C	Pt 6.8	1280	1.11	1.7
Pd/C	Pd 10.9	943	0.53	1.1
NiC	Ni 46.2	182	0.10	1.1
Pt/NiC	Ni 45.8 (Pt 1wt %)	219	0.11	1.0
PtC-P	Pt 39.7	46	0.04	2.4
PdC-P	Pd 29.5	34	0.04	1.9

[a] V_p = total pore volume at $p/p_0 = 0.99$. [b] r_p = mean pore radius (= $2V_p/S_{BET}$).

Table 3.3. Yields of *n*-alkanes and fatty acids from the CHTR of jatropha oil at 350 °C for 1h over different catalysts

	Yield [%-C]				
Catalysts	**C_{1-4}**	**$C_{7-14, 16, 18}$**	**C_{15}**	**C_{17}**	**Fatty acids**
No catalyst	0	0.2	<0.1	<0.1	80.9
Pt/C	1.2	1.4	5.5	40.8	7.6
Pd/C	0.3	0.4	0.7	6.2	66.7
NiC	54.5	2.0	0.4	1.0	0.7
Pt/NiC	19.0	3.6	1.6	5.6	21.6
PtC-P	0.2	0.3	0.4	3.8	48.3
PdC-P	0	<0.1	<0.1	<0.1	83.3

Table 3.4. The textural properties of the catalysts reused three times at 350 °C for 1h

Catalysts	Metal content [wt %]	S_{BET} [m^2 g^{-1}]	V_p [cm^3 g^{-1}]	r_p [nm]
Pt/C used	Pt 4.6	1039	0.99	1.9
NiC used	Ni 46.9	187	0.10	1.1

Table 3.5. Distribution of identified products from CHTR of jatropha oil at 350 °C for 1h

Products	Pt/C	NiC
Gas [%-C]	**6.1**	**76.0**
Liquid/solid[a] [%-C]	**93.8**	**17.7**
GC-MS detectable compounds [%-C]		
$C_{7–18}$ *n*-Alkanes	47.9	3.4
Fatty acids	7.6	0.7
Other compounds[b] [%, relative area]		
iso-Alkanes	1.6	—
Alkenes	3.0	8.9
Aromatics	5.0	—
Alcohols	0.8	—
Fatty acid esters	—	0.3
GC-MS undetectable compounds [%-C]	27.9	4.4
Gas + Liquid/solid [%-C]	**99.9**	**93.7**

[a] Liquid/solid is a residue after the removal of water and tetrahydrofuran from the recovered product. The carbon content was presumed to be the same as that of jatropha oil.

[b] Compounds detected in the GC–MS analysis are indicated as a peak area ratio of each compound to pentadecane + heptadecane.

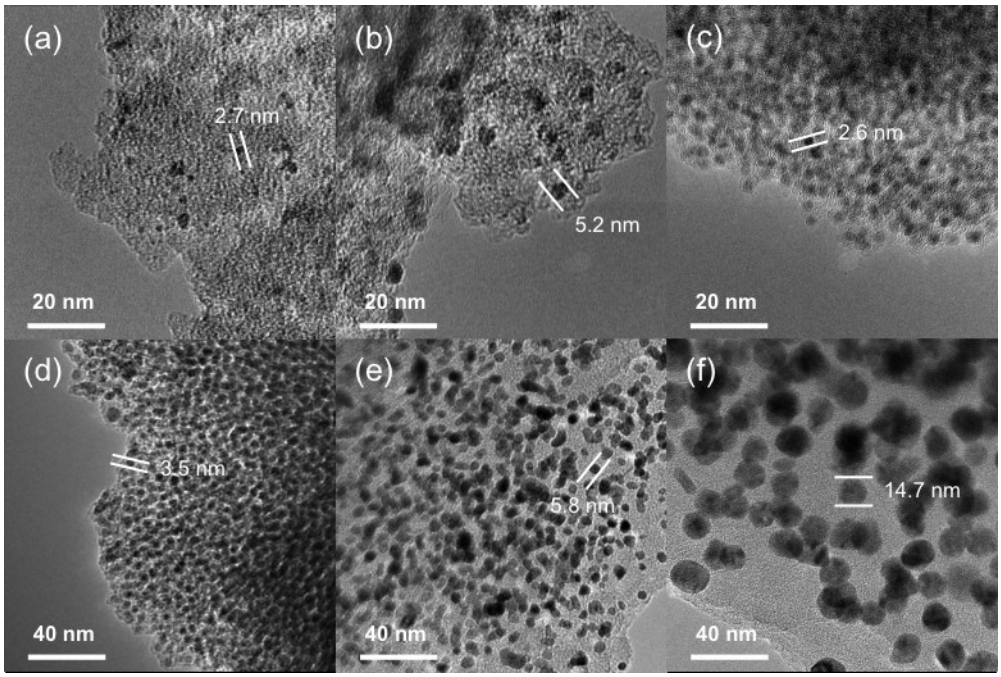

Figure 3.1. TEM images of the catalysts; (a) Pt/C, (b) Pd/C, (c) NiC, (d) Pt/NiC, (e) PtC-P, and (f) PdC-P.

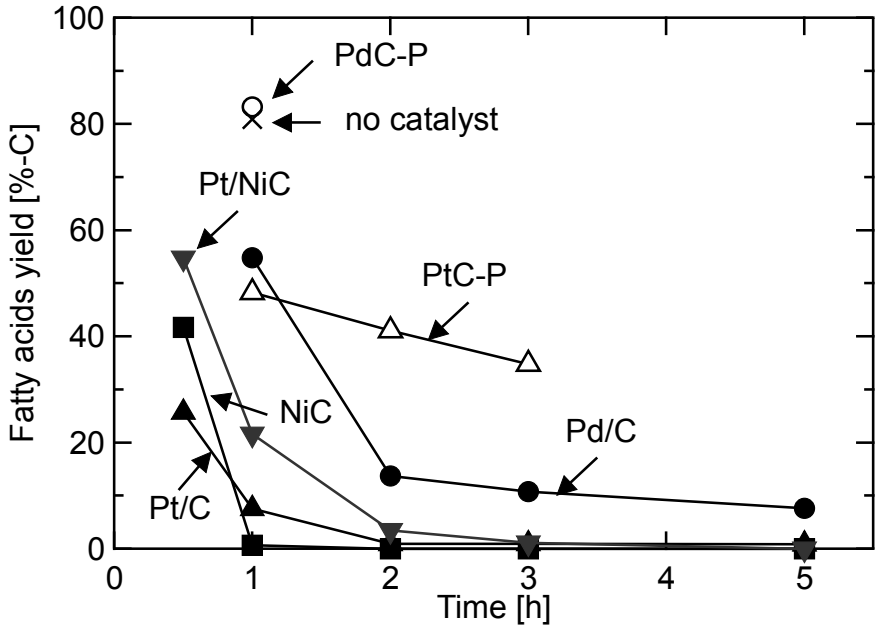

Figure 3.2. Effect of catalysts on the yield of fatty acids as a function of time for jatropha oil CHTR at 350 ºC.

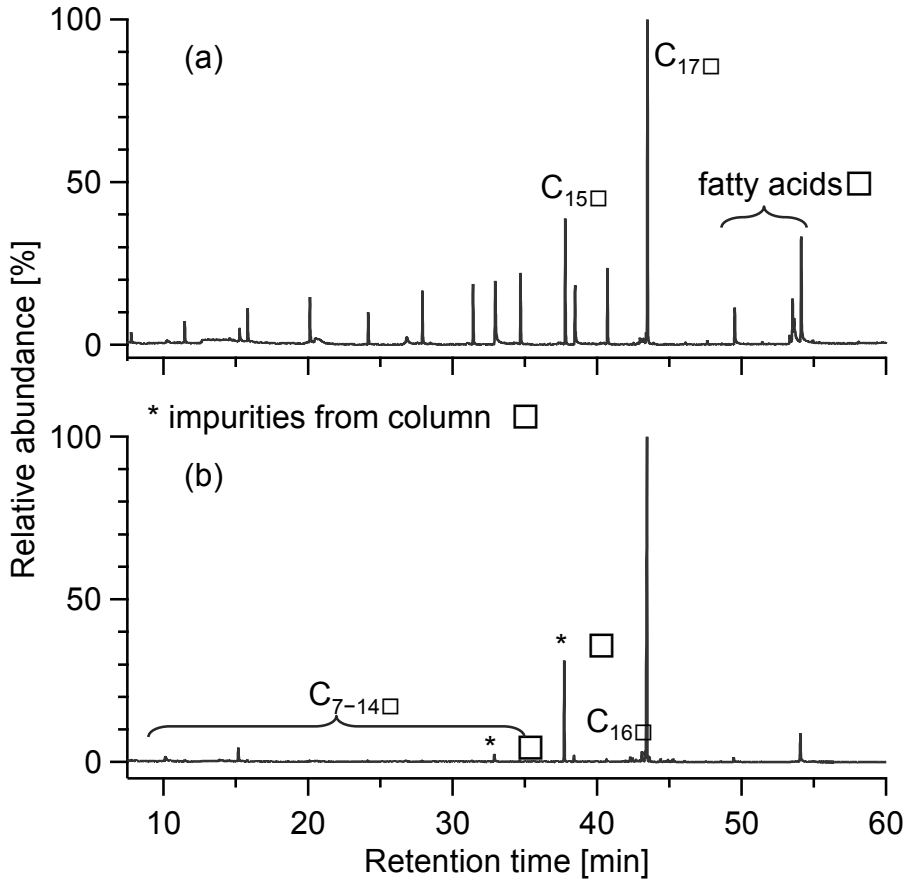

Figure 3.3. Typical GC–MS chromatograms of the liquid product from jatropha oil CHTR at 350 ºC for 1 h over (a) NiC and (b) Pt/C.

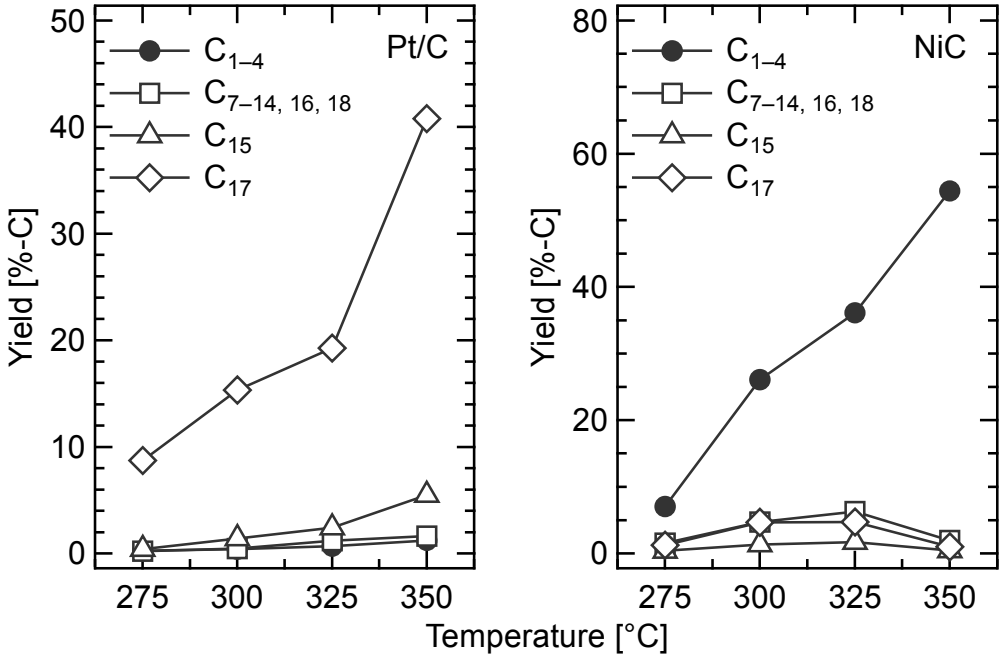

Figure 3.4. Yields of *n*-alkanes at different temperatures from jatropha oil CHTR for 1 h over Pt/C and NiC.

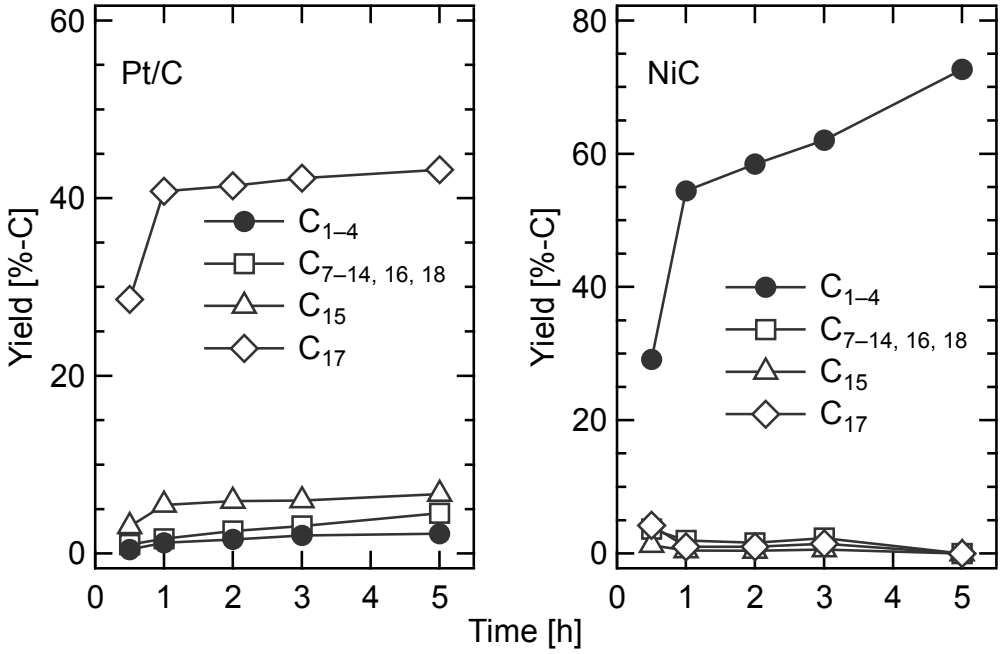

Figure 3.5. Temporal change in the *n*-alkanes yields from jatropha oil CHTR at 350 ºC over Pt/C and NiC.

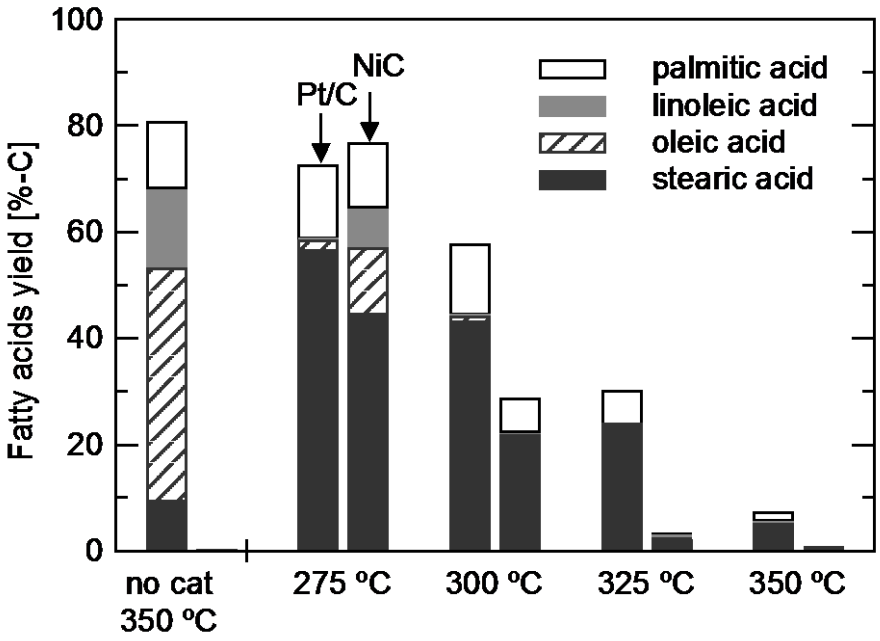

Figure 3.6. Change in the fatty acids yield and composition with temperature from jatropha oil CHTR for 1 h.

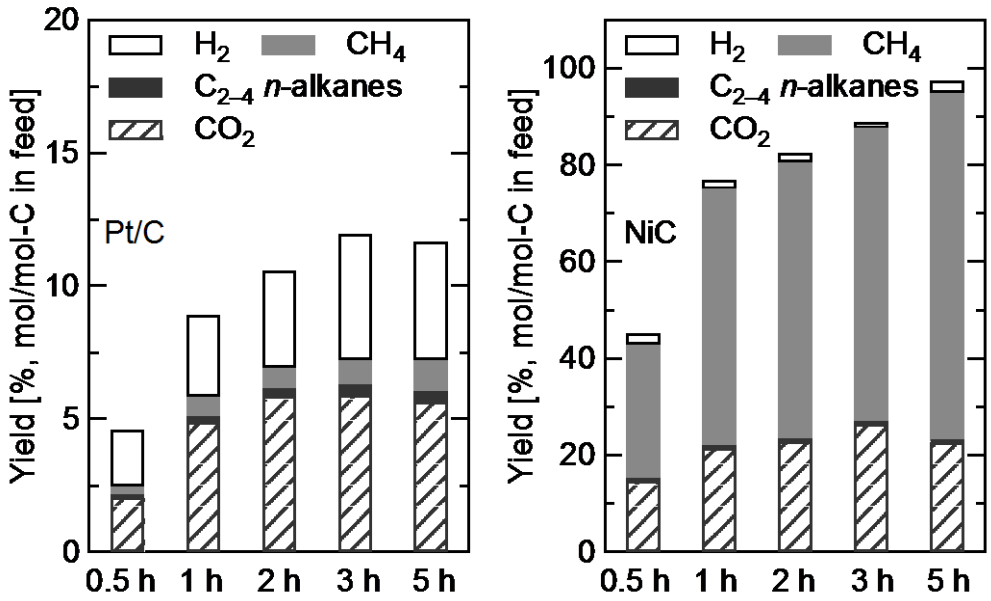

Figure 3.7. Temporal change in the **y**ield of gas products from jatropha oil CHTR at 350 ºC over Pt/C and NiC.

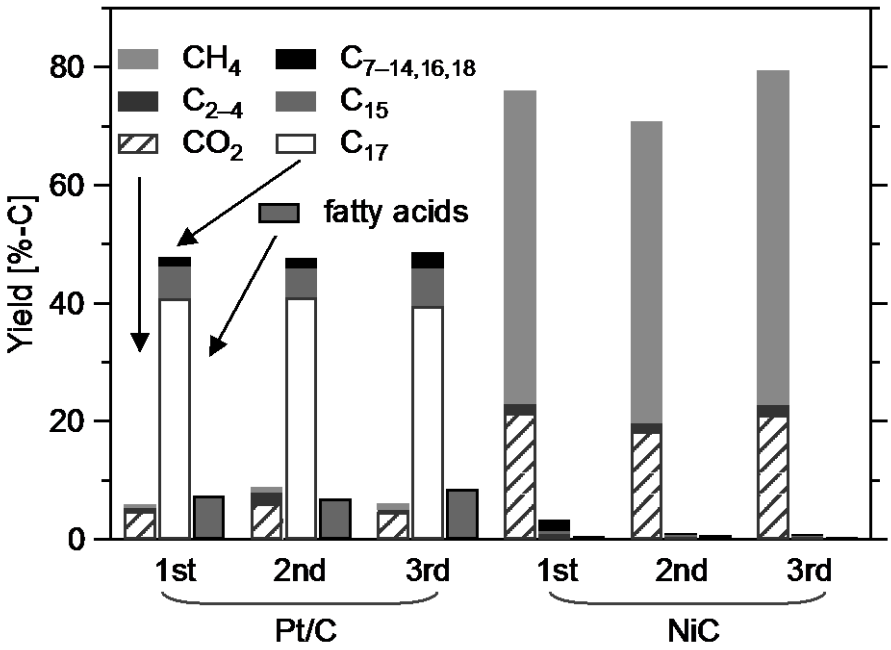

Figure 3.8. Reuse **(**three times) of Pt/C and NiC for jatropha oil CHTR at 350 ºC for 1 h.

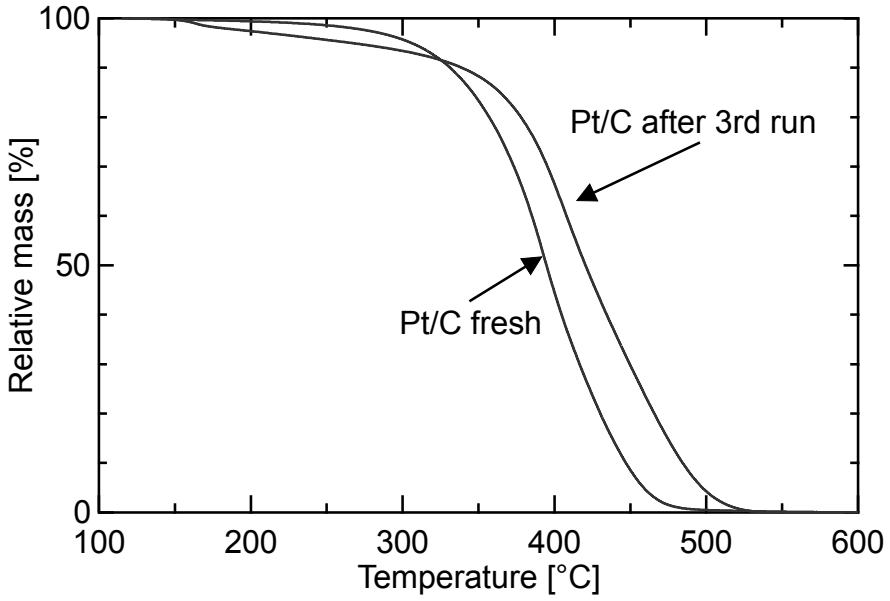

Figure 3.9. TGA of the catalysts during combustion (air 150 mL min^{-1} and a heating rate of 3 °C min^{-1}).

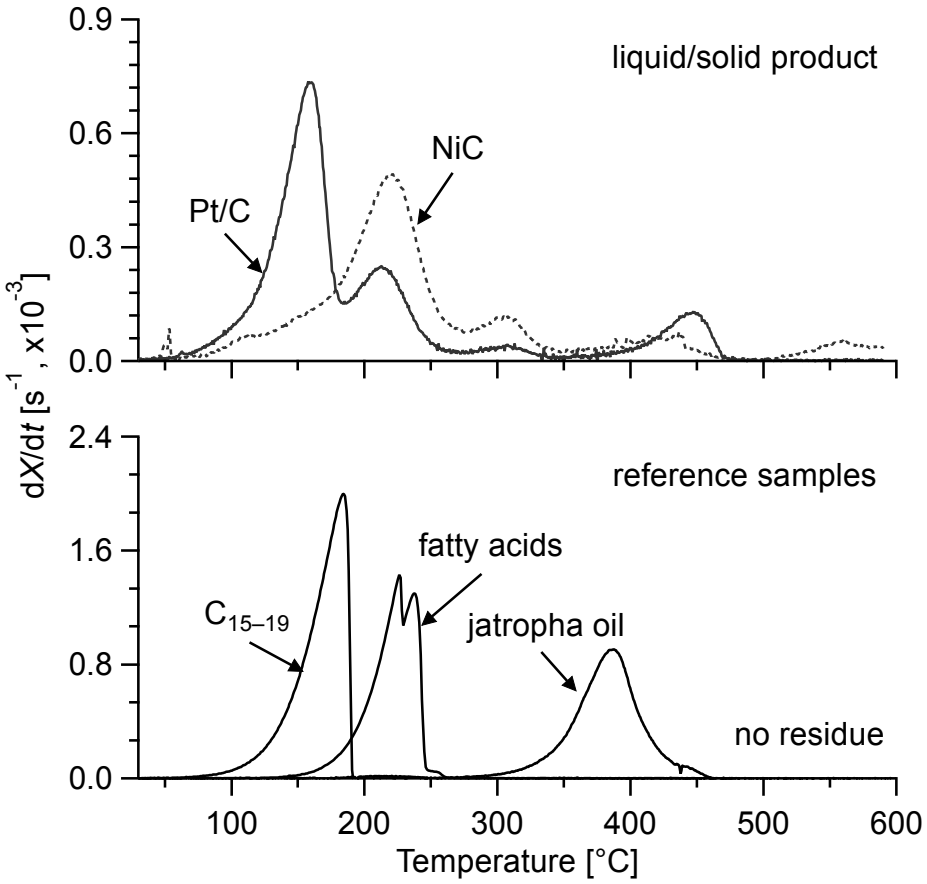

Figure 3.10. Rate of mass loss (X = normalized mass) fo the liquid/solid product of jatropha oil CHTR at 350 ºC in N_2 for 1 h over Pt/C and NiC and reference samples (an equal volume mixture of $C_{15–19}$ *n*-alkanes, an equal mass mixture of palmitic, linoleic, oleic, and stearic acids, and jatropha oil).

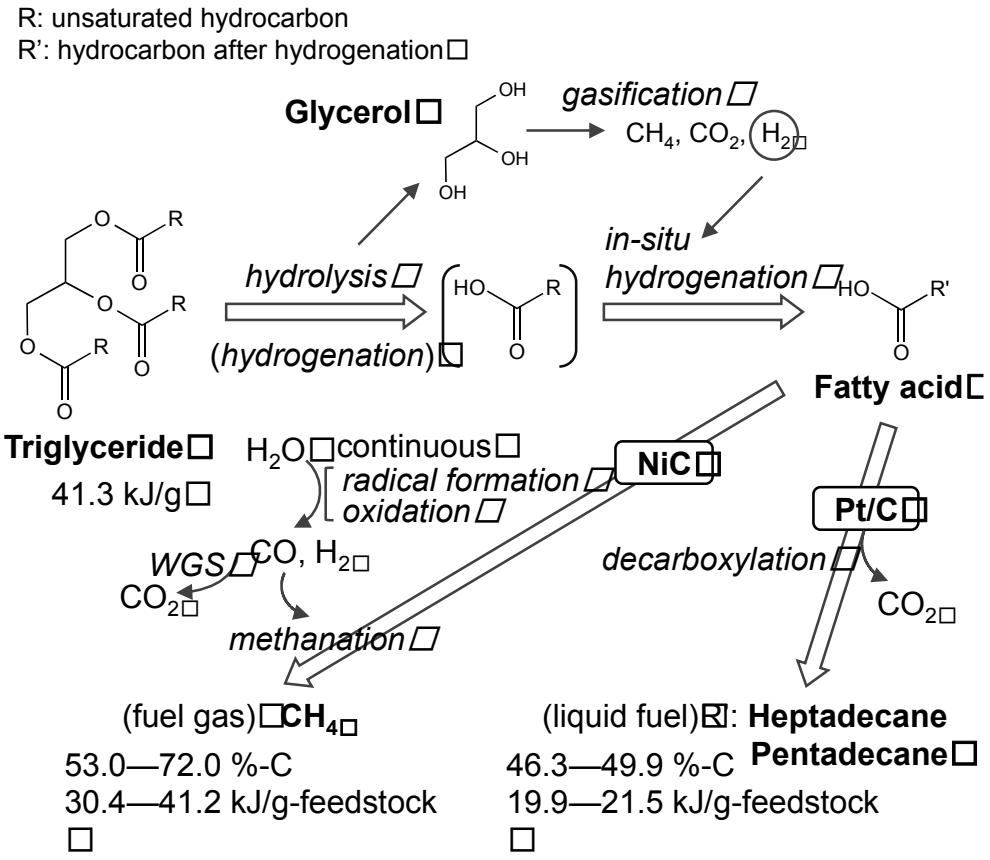

Figure 3.11. Main pathways and products of jatropha oil CHTR at 350 ºC for 1–5 h. Heating values of the main products are expressed as the HHV. The heating value of the feedstock was calculated from the elemental composition using the Dulong formula: (J/g, 338.3C + 1442(H – O/8)).

3.5. References

1. Huber GW, Iborra S, Corma A. *Synthesis of transportation fuels from biomass: Chemistry, catalysts, and engineering.* Chemical Reviews, 2006. 106: p. 4044–4098.
2. Ma F, Hanna MA. *Biodiesel production-a review.* Bioresource Technology, 1999. 70: p. 1–15.
3. Abreu FR, Lima DG, Hamú EH, Wolf C, Suarez PAZ. *Utilization of metal complexes as catalysts in the transesterification of Brazilian vegetable oils with different alcohols.* Journal of Molecular Catalysis A: Chemical, 2004. 209(1–2): p. 29–33.
4. Helwani Z, Othman MR, Aziz N, Fernando WJN, Kim J. *Technologies for production of biodiesel focusing on green catalytic techniques: A review.* Fuel Processing Technology, 2009. 90(12): p. 1502–1514.
5. Lima DG, Soares VCD, Ribeiro EB, Carvalho DA, Cardoso ÉCV, Rassi FC, Mundim KC, Rubim JC, Suarez PAZ. *Diesel-like fuel obtained by pyrolysis of vegetable oils.* Journal of Analytical and Applied Pyrolysis, 2004. 71(2): p. 987–996.
6. Maher KD, Bressler DC. *Pyrolysis of triglyceride materials for the production of renewable fuels and chemicals.* Bioresource Technology, 2007. 98(12): p. 2351–2368.
7. Gerpen JV, Knothe G. *The Biodiesel Handbook.* Eds. AOCS Press: Champaign, IL, 2005.
8. Stumborg M, Wong A, Hogan E. *Hydroprocessed vegetable oils for diesel fuel improvement.* Bioresource Technology, 1996. 56: p. 13–18.
9. Smith B, Greenwell HC, Whiting A. *Catalytic upgrading of triglycerides and fatty acids to transport biofuels.* Energy & Environmental Science, 2009. 2(3): p. 262–271.
10. Serrano-Ruiz JC, Ramos-Fernández EV, Sepúlveda-Escribano A. *From biodiesel and bioethanol to liquid hydrocarbon fuels: new hydrotreating and*

advanced microbial technologies. Energy & Environmental Science, 2012. 5(2): p. 5638–5652.

11. Kubičková I, Snåre M, Eränen K, Mäki-Arvela P,.Murzin DY. *Hydrocarbons for diesel fuel via decarboxylation of vegetable oils.* Catalysis Today, 2005. 106(1–4): p. 197–200.
12. Mäki-Arvela P, Kubičková I, Snåre M, Eränen K, Murzin DY. *Catalytic deoxygenation of fatty acids and their derivatives.* Energy & Fuels, 2007. 21: p. 30–41.
13. Rozmysłowicz B, Mäki-Arvela P, Tokarev A, Leino A-R, Eränen K, Murzin DY. *Influence of hydrogen in catalytic deoxygenation of fatty acids and their derivatives over Pd/C.* Industrial & Engineering Chemistry Research, 2012. 51(26): p. 8922–8927.
14. Snåre M, Kubičková I, Mäki-Arvela P, Chichova D, Eränen K, Murzin DY. *Catalytic deoxygenation of unsaturated renewable feedstocks for production of diesel fuel hydrocarbons.* Fuel, 2008. 87(6): p. 933–945.
15. Simakova I, Simakova O, Mäki-Arvela P, Simakov A, Estrada M, Murzin DY. *Deoxygenation of palmitic and stearic acid over supported Pd catalysts: Effect of metal dispersion.* Applied Catalysis A: General, 2009. 355(1–2): p. 100–108.
16. Kubička D, Kaluža L. *Deoxygenation of vegetable oils over sulfided Ni, Mo and NiMo catalysts.* Applied Catalysis A: General, 2010. 372(2): p. 199–208.
17. Gong S, Shinozaki A, Shi M, Qian EW. *Hydrotreating of jatropha oil over alumina based catalysts.* Energy & Fuels, 2012. 26(4): p. 2394–2399.
18. Snåre M, Kubičková I, Mäki-Arvela P, Eränen K, Murzin DY. *Heterogeneous catalytic deoxygenation of stearic acid for production of biodiesel.* Industrial & Engineering Chemistry Research, 2006. 45: p. 5708−5715.
19. Santillan-Jimenez E, Morgan T, Lacny J, Mohapatra S, Crocker M. *Catalytic deoxygenation of triglycerides and fatty acids to hydrocarbons over carbon-supported nickel.* Fuel, 2013. 103: p. 1010–1017.
20. Murata K, Liu Y, Inaba M, Takahara I. *Production of synthetic diesel by hydrotreatment of jatropha oils using Pt−Re/H-ZSM-5 catalyst.* Energy & Fuels, 2010. 24(4): p. 2404–2409.

21. Morgan T, Santillan-Jimenez E, Harman-Ware AE, Ji Y, Grubb D, Crocker M. *Catalytic deoxygenation of triglycerides to hydrocarbons over supported nickel catalysts.* Chemical Engineering Journal, 2012. 189–190: p. 346–355.
22. Wang W-C, Thapaliya N, Campos A, Stikeleather LF, Roberts WL. *Hydrocarbon fuels from vegetable oils via hydrolysis and thermo-catalytic decarboxylation.* Fuel, 2012. 95: p. 622–629.
23. Matsumura Y, Minowa T, Potic B, Kersten S, Prins W, Vanswaaij W, Vandebeld B, Elliott D, Neuenschwander G, Kruse A. *Biomass gasification in near- and supercritical water: Status and prospects.* Biomass and Bioenergy, 2005. 29(4): p. 269–292.
24. Azadi P, Farnood R. *Review of heterogeneous catalysts for sub- and supercritical water gasification of biomass and wastes.* International Journal of Hydrogen Energy, 2011. 36(16): p. 9529–9541.
25. Idesh S, Kudo S, Norinaga K, Hayashi J-i. *Catalytic hydrothermal reforming of water-soluble organics from the pyrolysis of biomass using a Ni/Carbon catalyst impregnated with Pt.* Energy & Fuels, 2012. 26(1): p. 67–74.
26. Morimoto M, Nakagawa H, Miura K, *Hydrothermal extraction and hydrothermal gasification process for brown coal conversion.* Fuel, 2008. 87(4–5): p. 546–551.
27. Yamaguchi D, Sanderson PJ, Lim S, Aye L. *Supercritical water gasification of Victorian brown coal: Experimental characterization.* International Journal of Hydrogen Energy, 2009. 34(8): p. 3342–3350.
28. Minowa T, Yokoyama S-y, Kishimoto M, Okakura T. *Oil production from algal cells of Dunaliella tertiolecta by direct thermochemical liquefaction.* Fuel, 1995. 74: p. 1735–1738.
29. Li L, Coppola E, Rine J, Miller L, Walker D. *Catalytic hydrothermal conversion of triglycerides to non-ester biofuels.* Energy & Fuel, 2010. 24 (2), p. 1305–1315.
30. Fu J, Lu X, Savage PE. *Catalytic hydrothermal deoxygenation of palmitic acid.* Energy & Environmental Science, 2010. 3(3): p. 311–317.
31. Fu J, Lu X, Savage PE. *Hydrothermal decarboxylation and hydrogenation of fatty acids over Pt/C.* ChemSusChem, 2011. 4(4): p. 481–486.

32. Fu J, Shi F, Thompson LT, Lu X, Savage PE. *Activated carbons for hydrothermal decarboxylation of fatty acids.* ACS Catalysis, 2011. 1(3): p. 227–231.

33. Vaknin Y, Ghanim M, Samra S, Dvash L, Hendelsman E, Eisikowitch D, Samocha Y. *Predicting Jatropha curcas seed-oil content, oil composition and protein content using near-infrared spectroscopy—A quick and non-destructive method.* Industrial Crops and Products, 2011. 34(1): p. 1029–1034.

34. Nakagawa H, Watanabe K, Harada Y, Miura K. *Control of micropore formation in the carbonized ion exchange resin by utilizing pillar effect.* Carbon, 1999. 37: p. 1455–1461.

35. Sharma A, Nakagawa H, Miura K. *A novel nickel/carbon catalyst for CH_4 and H_2 production from organic compounds dissolved in wastewater by catalytic hydrothermal gasification.* Fuel, 2006. 85(2): p. 179–184.

36. Kusdiana D, Saka S. *Two-step preparation for catalyst-free biodiesel fuel production.* Applied Biochemistry and Biotechnology, 2004. 115: p. 781–791.

37. Cortrigh RD, Davda RR, Dumesic JA. *Hydrogen from catalytic reforming of biomass-derived hydrocarbons in liquid water.* Nature, 2002. 418: p. 964–967.

38. Gabrovska M, Krstić J, Edreva-Kardjieva R, Stanković M, Jovanović D. *The influence of the support on the properties of nickel catalysts for edible oil hydrogenation.* Applied Catalysis A: General, 2006. 299: p. 73–83.

39. Chakinala AG, Chinthaginjala JK, Seshan K, van Swaaij WPM, Kersten SRA, Brilman DWF. *Catalyst screening for the hydrothermal gasification of aqueous phase of bio-oil.* Catalysis Today, 2012. 195(1): p. 83–92.

40. Karagoz S, Bhaskar T, Muto A, Sakata Y. *Comparative studies of oil compositions produced from sawdust, rice husk, lignin and cellulose by hydrothermal treatment.* Fuel, 2005. 84(7–8): p. 875–884.

CHAPTER 4

CATALYTIC HYDROTHERMAL REFORMING OF BIOMASS-DERIVED MATERIAL IN ALKALINE MEDIA

4.1. Introduction

Gasification is a most important technology for the utilization of low-rank carbonaceous solid fuels such as biomass and lignite (or brown coal). Current issues associated with environmental and resource constraints require the development of technologies for the efficient conversion of such solid fuels with minimized loss of their original chemical energy, which is theoretically achievable by the gasification at lower temperature with minimized or no use of oxygen [1]. Steam gasification has been typically a major focus of the research in this field. It is in fact possible to accomplish complete gasification of biomass by steam at a temperature as low as 700 °C with a careful consideration of the reaction chemistry involving catalysis [2] Sub- or supercritical water gasification has a potential to realize the process at far lower temperatures because of unique physical and chemical properties of hot compressed water. The presence of active catalysts accelerates the conversion of organics with water, i.e., catalytic hydrothermal reforming (CHTR), and typically produces methane and carbon dioxide as the thermodynamically favored products. The recovery of chemical energy by CHTR is theoretically around 100% because of balance between endothermic H_2/CO formation and exothermic CH_4 formation from the H_2/CO. Other advantages of CHTR over conventional gasification

are no need of either use of O_2, drying of feedstock, or generation of steam, which brings about large energy penalty. An important technological challenge of the hydrothermal processes is the delivery of solid feedstock to a highly pressurized reactor. Although the gasification should be performed in flow reactors from a practical point of view, the nature of biomass and lignite, which is less soluble in water, limits the application of CHTR to continuous reactors with feeding of aqueous solution containing water-soluble organics and/or necessitates the use of batch reactors. A solution of this problem is, as suggested by Matsumura et al.[3] the use of viscous solid feedstock/water slurry.

The present study proposes a new scheme to effectively apply CHTR to conversion of biomass and lignite, which is shown in Figure 4.1. Biomass and lignite are first subjected to treatment in aqueous alkaline solution at elevated temperatures for their complete or partial dissolution. For the biomass, lignin or the lignin and hemicellulose are dissolved into an alkaline solution, leaving the cellulose as solid for further processing to paper and/or valuable chemicals. It is also known that a substantial portion of lignite can be extracted by aqueous alkaline solutions [4–6]. The lignin or lignite as a solute of the alkaline water is then converted to gas by CHTR using heterogeneous catalysts. One option, especially for the lignin, is to depolymerize it to monomeric phenols by non-catalytic hydrothermal reforming (HTR). After liquid-liquid extraction of the phenols, the remaining high molecular organics are gasified by CHTR. Complete gasification of the organics makes the aqueous alkaline solution recyclable.

Traditional Kraft pulping process, also known as sulfate process, involves delignification of wood with an alkaline solution (cooking liquor) that consists mainly of NaOH and Na_2S. The resultant solution of the lignin, so called black liquor, is afterward burned for steam generation and recovery of the alkali chemicals. On the other hand, the alkaline solution of the proposed process needs to meet some requirements as follows: 1) The use of sulfur species, such as Na_2S, should be avoided due to an intolerance of CHTR catalysts toward sulfates [7] 2) For a simple recycling of the solution, the alkali salt should be a carbonate because carbon dioxide from CHTR inevitably makes the solution rich in carbonate ions [8] 3) CHTR should be operated at temperature well below the critical point temperature of water because the solubility of alkali salts in water dramatically decreases at near critical conditions (e.g., solubility of

Na_2CO_3 decreases from 0.3 mol L^{-1} at 350 °C to less than 0.002 mol L^{-1} at 400 °C) [9,10] The salts, if precipitated during CHTR, stick to catalysts and reactor wall and then cause plugging of the flow channel. The concentration of alkali salts, therefore, should be low, but high enough to dissolve the feedstock.

The alkali salt is recently a focus of attention as a type of catalyst for hydrothermal gasification of biomass. Series of works by some research groups [8,11–19] on supercritical water gasification of biomass showed that the addition of alkali salts, sodium or potassium hydroxide in particular, leads to a selective production of H_2 by removal of CO_2 and catalysis toward water-gas shift. Alkalis in black liquor also catalyze the gasification of dissolved organics [20,21]. Meanwhile, in those studies, it seems that the alkali salts are regarded as consumable additives, but not as reusable catalysts. It is known that, in comparison with cellulose, hemicellulose, and their derivatives, lignin is substantially harder to gasify under supercritical water conditions even with the presence of active heterogeneous catalysts [22]. Formation of char by polymerization due to reactions such as condensation in the course of heating-up is one of the reasons for the low gasification efficiency. An alkaline environment is thought to be effective to suppress the char formation, because hydroxyl groups in the lignin are stabilized and protected by an ionic interaction with alkali metal cation. Conversely, CHTR are required to gasify such a stabilized organic macromolecule.

There has been a wide range of studies on heterogeneous catalysts for gasification of organics in hydrothermal environment [23–31] Elliott et al. [25] identified nickel, ruthenium and rhodium as catalytically active/stable metals and monoclinic zirconia, rutile titania and carbon as stable support under subcritical conditions. Although less information is available for their catalysis under alkaline hydrothermal water conditions [7,18,32–35] Sealock et al. [36] reported that the presence of alkali metals was detrimental to destruction and gasification of organic compounds by nickel catalysts. The negative effects of the alkali were confirmed by Elliot et al. [35], where CHTR with a Ni/Al_2O_3 catalyst at 350 °C was not enough to effectively gasify phenol that was in the form of sodium phenolate. Onwudili and Williams [18] examined supercritical water gasification of glucose in a batch reactor at 550 °C using Ru/Al_2O_3 and CaO (1.07 M) as catalysts. The yield and composition of product gas gradually changed in the course of two-time reuse of the ruthenium catalyst, although they did not report on the

change in the structural property of catalyst. In our opinion, oxide supports such as Al_2O_3 and SiO_2 is unavailable to the reactions in alkaline medium because of their potential to meltdown to form salts with alkali metals, e.g., sodium aluminate ($NaAlO_2$). Our choice for the catalyst support was, therefore, carbon. This work primarily aimed to demonstrate complete gasification of lignin dissolved in aqueous alkaline solution by CHTR under subcritical conditions in a continuous reactor. According to discussion above, Na_2CO_3 and carbon-supported ruthenium and nickel catalysts were chosen as the alkali salt and catalysts for CHTR, respectively. Catalyst activities/deactivation, recovery of chemical energy, and recyclability of the alkaline solution were investigated to examine the potentiality of the proposed process. Furthermore, production of monomeric phenols by HTR of lignin, which is an option in the scheme (Figure 4.1), was also investigated.

4.2. Experimental

4.2.1. Materials

Feedstock material. A type of lignin derived from bamboo was kindly supplied by Sanuki Kasei Co., Ltd., Japan and used as the raw material without any purification. The lignin sample had a molecular weight of about 14,000 (according to the product specification) and composed of 61.2 wt % C, 5.8 wt % H, 0.3 wt % N, 32.4 wt % O (by difference), 0.3 wt % ash, and < 0.1 wt % sulfur. Analytical characterization of the lignin by a common nitrobenzene oxidation method [37] revealed the ratio of aromatic nuclei in the structure: syringyl (S)/guaiacyl (G)/*p*-hydroxyphenyl (H) = 26.2/48.0/26.8 % on a molar basis.

Catalyst Preparation and Characterizations. Ru/C-5%, Pd/C-10%, Rh/C-5%, $Ni(NO_3)_2{\cdot}6H_2O$, $Pd(NO_3)_2$, $RuCl_3$, Trinitratonitrosyl ruthenium (II) in nitric acid solution (50%) and activated charcoal were purchased from Wako Pure Chemical Industries. PtC-3% and sodium carbonate (Na_2CO_3) were purchased from Aldrich and Kanto Chemical Co.Inc. Carbon-supported nickel and ruthenium catalysts for flow-type CHTR experiments were prepared by an impregnation or an ion exchange-carbonization method [38]. An activated charcoal (granular) was crushed, sieved to 0.5–1.0 mm,

sonicated in water for the removal of fines, dried in vacuo and used as the carbon support. Ru-N/AC, Ru-Cl/AC and Ni/AC were prepared by incipient wetness impregnation of the charcoal with acetone solution of trinitratonitrosyl ruthenium (II), ruthenium (III) chloride and nickel (II) nitrate, respectively, subsequent drying at 100 °C for 1 h and final reduction at 400 °C in a 20% H_2 flow for 3 h. Ni-C was prepared by the ion exchange-carbonization method developed by Nakagawa et al. [38]. Briefly, an ion-exchange resin (WK-11, Mitsubishi Chemical) loaded with Ni^{2+} from nickel nitrate aqueous solution was carbonized at 500 °C under a N_2 flow for 1 h.

BET surface areas, S_{BET}, of the catalysts were calculated from the isotherms measured by N_2 adsorption at 77 K with a Quantachrome NOVA 3200e after drying at 200 °C for 3 h under high vacuum. XRD patterns were measured by an X-ray diffractometer (TTR III, Rigaku) equipped with a Cu Kα radiation source at a voltage and current of 50 kV and 300 mA, respectively. A TEM observation was conducted with a JEOL, JEM-2100F at an accelerating voltage of 200 keV. Metal particle size distributions were obtained from more than 200 particles in the TEM images. TGA was conducted using a SII Nano Technology EXSTAR TG/DTA 7200.

4.2.2. CHTR and product analysis

A solubility of the lignin in Na_2CO_3 aqueous solution at 35 °C was investigated at 35 °C and ambient pressures. The resulting solution (or suspension) was filtered through a membrane filter with a pore size of 0.45 μm, and the solubility was determined by the weight of residue on the filter. Figure 4.2 shows the experimental setup used for CHTR. A total of 1.2 g of catalyst was charged in the reactor assembled from Swagelok fittings that were made of SUS316. A lignin solution with a total organic carbon concentration (TOC) = 5,000 ppm (mg of C L^{-1}) in 0.1 M Na_2CO_3 aqueous solution was used as the feedstock solution for CHTR, unless otherwise noted. Before CHTR experiment, the catalysts were treated in a flow of 0.1 M Na_2CO_3 aqueous solution (0.5 mL min^{-1}) at 350 °C and 20 MPa for 2 h, and that of water for 0.5 h. Later, the lignin solution was fed continuously to the reactor at a rate of 0.5 mL min^{-1} for a prescribed period of 0.7–10 h. The flow rate typically corresponded to WHSV of 0.2 h^{-1}. The configuration of the reactor, as depicted in Figure 4.2, enabled contact of the hot solution with the

catalyst bed immediately after the entrance to the reactor. The effluent stream passing through the cooler, sintered SUS-made filter, and backpressure regulator was led to the glass bottle as the gas-liquid separator and the liquid collector. The gaseous product was purged with 50 mL min^{-1} N_2 out of the glass bottle and then collected in the gasbag. CHTR was quenched by replacing the flow of the lignin solution with that of water. After 30 min duration, the reactor was cooled down by immersing it in iced water. The entire part of the flow was purged with N_2, washed with water, and then with acetone to collect deposited char and coke. The amounts of carbon contained in each wash solution were determined from the TOC measured by an analyzer (Shimadzu, TOC-5000A) and mass of carbon in the residue after evaporation of acetone, respectively. The char and coke thus collected were collectively referred to as deposits. The amount of coke deposited on the catalyst was determined from the change in its mass. The gaseous products collected in the gasbag were analyzed by general gas chromatography. A portion of the liquid effluent was acidified to pH 1 with 1 N aqueous solution of hydrochloric acid, filtered, and subjected to a TOC measurement. Carbon in precipitate of the acidification was taken into account in the calculation of TOC, assuming that its carbon content was the same as that of the lignin, i.e., 61.2 wt %. The chemical composition of organic compounds in the liquid effluent was measured by gas chromatography–mass spectrometry (GC-MS) with a PerkinElmer Clarus SQ8 that was equipped with a capillary column, TC-1701 [14% cyanoprophylphenyl–86% dimethylsiloxane, 60 m, 0.25 mm inner diameter, and 0.25 μm film thickness (df)]. Detector and injector temperatures were 250 and 345 °C, respectively. The following chromatographic temperature program was used: holding at 40 °C for 5 min, heating to 250 °C at 4 °C min^{-1}, and final holding at 250 °C for 20 min. Hydrothermal reforming (HTR) and CHTR of the lignin was performed in batch reactor that consisted of a SUS 316 tube bomb with an internal volume of 10 mL. The reactor head was fitted to a gas sampling tube with two high-pressure valves. A 5 mL of a 0.5 M Na_2CO_3 solution of the lignin with a TOC of 10,000 ppm and 1.0 MPa nitrogen gas (purity > 99.9999 vol %) were charged into the reactor. The HTR was initiated by submerging the reactor in a fluidized sand bath heated at a prescribed temperature and then quenched by the immersion into an iced water bath after 1.5 h of the aging. After the collection of gaseous product, the resultant solution was filtered, and the filtrate was extracted with 5

mL dichloromethane and three times repetition. Monomeric phenols in the extract were quantitatively analyzed by GC–MS. The solid residue of the filtration was washed with water and then dried to obtain its mass.

4.3. Results and Discussion

4.3.1. Dissolution of lignin.

Figure 4.3 presents the effect of Na_2CO_3 concentration on the solubility of lignin and pH of the solutions with/without lignin. The lignin was almost insoluble in pure water. The addition of Na_2CO_3 increased the solubility, and 0.1 M Na_2CO_3 was enough to completely dissolve 5,000 ppm of carbon, corresponding to 8.14 g-lignin L^{-1}. The decrease in pH by the lignin dissolution was arisen from acidic functionalities of the lignin. The dissociation of the acidic groups under certain alkaline conditions provides enough salvation energy for solubilization to take place. The result suggested that pH of over 10 was necessary for the dissociation of phenols as the acid. The lignin solubility in the 0.1 M Na_2CO_3 aqueous solution was up to 13,000 ppm-TOC. Although the increasing Na_2CO_3 concentration leaded to more dissolution of lignin around ambient temperature, its solubility is limited under subcritical conditions, as mentioned previously.

4.3.2. CHTR of lignin for the production of phenolic compounds

Lignin is a potential feedstock not only for fuel gas that is a target product of this study, but also valuable chemicals such as phenols and BTX. The base-catalyzed depolymerization (BCD) is one of the methods to produce chemicals, enabling the controlled hydrolysis of lignin macromolecules mainly by cleaving ether bonds [39–41], often employing NaOH as the base.

Figure 4.4 compares GC-MS chromatogram of the phenolic compounds which were extracted by dichloromethane from the product liquid from the HTR conducted at 250 °C for 1 h with lignin dissolved in water (Figure 4.4 (a)) to chromatogram of that in alkali solution (Figure 4.4 (b)) respectively. A range of monomers of phenolic compounds derived from lignin was identified in the product liquid from the HTR of

lignin dissolved in water. However, when alkali solution was used as solvent of lignin, the product liquid from CHTR was consisted of phenolic compounds which were formed more selectively, especially phenol and guaiacol with highly increased yield, whereas yields of other monomers were decreased. In particular, it can be seen that yields of 4-ethylphenol, 4-ethylguaiacol, benzofuran, syringol, vanillin and syringaldehyde were drastically decreased due to presence of alkali salt (Na_2CO_3). It was clear that alkali salts additives also had an effect during lignin decomposition as catalyst not only as solvent. Figure 4.5 shows the yields of solid residue (char) and monomeric phenols from the product liquid from the hydrothermal reforming of the lignin using Na_2CO_3 without solid catalyst. The lignin was less soluble to pure water even at elevated temperatures, resulting in the highest char yield and low yield/selectivity of monomeric phenols. The dissolution in the Na_2CO_3 aqueous solution stabilized the lignin, and, therefore, the yield of char was only 3.2%-C after 1.5 h at 175 °C. The char yield increased with temperature and reached 37.8%-C at 250 °C. As seen in some reports [39–41] BCD product consist mainly of phenol, guaiacol and syringol, which are compounds derived at least from the cleavage of β-O-4 linkage and 5-5 linkage of lignin units. The yields of the three major phenols largely depend on the original structure of the lignin, i.e., S/G/H ratio. The major compounds included in other phenols were 4-acetylsyringol, followed by 4-methyl-/ethyl-phenols, but the yield was at most 0.5%-C. With the maximum at 250 °C, the total yield of monomeric phenols decreased with temperature due to their repolymerization. The monotonous increase in the yield of phenol shows the occurrence of demethoxylation of guaiacol and syringol. The total yields of monomeric phenols were comparable to that reported in literatures on BCD of lignin using NaOH [41], although the difference of feedstock lignin should be taken into account. It was believed that strong basicity was important in BCD of lignin, and NaOH has therefore been employed in the previous studies [42]. The alkali hydroxide is converted to carbonate, of which conversion back to the hydroxide requires energy consuming processes. On the other hand, the present result suggested that Na_2CO_3, which is a weaker base, was also effective for the monomeric phenols production. Thus Na_2CO_3 plays important roles in HTR that are to protect the lignin and

its derivatives against repolymerization and catalyze reactions to selectively cleave the ether and other types of linkages.

The yields of monomeric phenols from the hydrothermal reforming of the lignin using Na_2CO_3 without heterogeneous catalyst was high enough but at the same time char yield was too high (>30%-C). Consequently different types of catalysts were examined for the production of phenolic compounds simultaneously for preventing or minimizing formation of char. The results of CHTR with various catalysts at 275 °C for 1 h are shown in Figure 4.6. But on the other hand, yields of gases and char of selected catalysts were dissimilar. Rh/C and Pt/C were most effective to produce monomeric phenols but at the same time char yield was significantly high, even more than that in CHTR without solid catalyst. Lignin contains many oxygen functional groups, when lignin depolymerizes in subcritical water ether and ester bonds are easily hydrolyzed and phenolic compounds and aldehydes are formed. These hydrolysis products and intermediate products from hydrothermal reforming cross-link with each other to form a heavy material or char. Hence the main reason of formation char is repolymerization of product monomers and intermediate compounds formed during CHTR. In addition to these polymers of organics, it was found that char was consisted of inorganic salts (carbonates), tars and corrosion products [43]. Disadvantages connected to the use of alkali salts have seen such as increase in char yield and ash content. It was confirmed that Na_2CO_3, which was used as solvent in this study, was affected not only yields of gases, but also gas composition. Although yield of phenolics was the lowest among the examined catalysts, the production of hydrogen was improved in CHTR with using Ru/C. The mechanisms of depolymerization over selected catalysts were different. There was important difference between mechanisms to form the phenolic products obtained using various catalysts. Without catalyst phenol, guaiacol and syringol were the major monomers, whereas for Pd/C 4-methylphenol, 4-ethylphenol and 4-ethylguaiacol were dominant. When using no catalyst cleavages of linkages between monomers of lignin were usually occurred on α–aryl, 5–5, 4–O–5 and ether bond, however in case with Pd/C linkages cleavages were took place mainly on β–O–4, β–1, β–5 and β–β bonds. Similar results found by Pepper et al. [44] when their group was studied the influence of a number of catalysts on softwood lignin hydrogenation. In

other words, capabilities of those catalysts to cleave of linkages between of methoxylated phenylpropane monomers were different.

Among these catalysts Pd/C was selected for the further assessment by reason of its capability to minimize char yield simultaneously fine performance to produce phenolic compounds. The effect of reaction temperature, residence time on the yield and composition were explored for the selected catalyst. Figure 4.7 presents yields of products from CHTR with Pd/C catalyst at temperatures ranging 225-300 °C. Phenol, guaiacol, 4-methylphenol, 4-ethylphenol, 4-ethylguaiacol, syringol were identified as main monomeric phenols in product liquid from CHTR with Pd/C. The yields of those monomeric phenols were decreased with the increasing reaction temperatures, from 12.9%-C at 225 °C to 5.5%-C at 300 °C. Ye et al. [45] obtained similar results in hydrothermal degradation of cornstalk lignin in ethanol-water media. In contrast char yields were reduced with temperatures. This significant decrease of char probably resulted from thermal depolymerization of the lignin. Temporal changes of yields of phenolic compounds at 275 °C, at which char yield was lowest, are shown in the Figure 4.8. To produce more phenolics compounds, shorter CHTR reaction period was revealed as a best option. The highest yield of phenolics was 13.1%-C in CHTR for the residence time of 30 min. It was obviously that the yields of phenolic compounds were decreasing over the reaction time, probably due to gasification and repolymerization. The HTR and CHTR produced low yields of gaseous products. The highest yield for HTR was 0.4%-C at 300 °C, indicating that a major part of organics (and inorganic species) from lignin was retained in the liquid phase. Therefore, after liquid-liquid extraction of the monomeric phenols using water-insoluble solvent, the Na_2CO_3 solution containing oligomer-rich fraction of lignin was ideally subjected to the CHTR for the production of fuel gas and regeneration of the alkaline solution.

4.3.3. CHTG of lignin for the production of fuel gases

Catalysts activities and cold gas efficiency (CGE). CHTR of the dissolved lignin was performed in a continuous flow reactor using several types of ruthenium and nickel catalysts. Table 4.1 lists textural properties of catalysts for the CHTR. High surface areas of Ru-N/AC, Ru-Cl/AC, and Ni/AC derived from that of the support activated

carbon, S_{BET} = 1,250 m^2 g^{-1}. Properties of NiC were agreed well with those in the previous report [26]. Although one may anticipate the plugging of the flow channel by the formation of char/coke, as seen in batch reactor experiments (Figure 4.2), their formations can be significantly suppressed by high heating rate. In contrast to the slow heating rate of batch reactor (30–50 °C min^{-1}, measured), the solution was rapidly heated up through a microtube (ID = 0.9 mm) before the entrance into catalyst bed in the continuous flow reactor system. The heating rate was roughly estimated to be 110 °C min^{-1} by the calculation of enthalpy balance equations assuming a constant flow rate, density, viscosity, and heat capacity of the solution and overall heat transfer coefficient at 0.5 mL min^{-1}, 1.0 g cm^{-3}, 0.001 Pa s, 4.0 kJ kg^{-1} K^{-1}, and 1.0 kJ m^{-2} s^{-1} K^{-1}, respectively. Even with a high heating rate of the feed, more and less amount of char/coke would deposit on the reactor, flow channel, and catalyst surface unless the catalyst activity was extremely high. The deposit was, therefore, quantified as an important indicator of the catalytic activity. The performance of CHTR is given by its cold gas efficiency (CGE), which is defined by the heating value of cold producer gas divided by that of the feedstock lignin.

The table 4.2 shows the results of CHTR runs (1–8) with duration of 0.7–2 h. Ru-N/AC and Ru-Cl/AC showed highest catalytic activities toward gasification of lignin in the runs 1 and 3, respectively, with high yields of gaseous product, low TOC concentrations and small amounts of deposits on reactor and flow channel. The produced gas consisted mainly of CH_4, followed by CO_2 and H_2. The other hydrocarbons and CO were rarely detected in the analysis by GC. Different from supercritical water gasification using alkali hydroxides [8,11–19], the present CHTR conditions did not provide selectivity to H_2 formation due to insignificant catalytic activity of Na_2CO_3 toward water-gas shift. CGEs for the runs 1 and 3 were 86.7–87.9% on HHV basis. These efficiencies are much higher than gross cold gas efficiencies for CH_4 production from woody biomass by conventional gasification combined with methanation of syngas, 53–71%-HHV [46]. It is, however, noted that the efficiencies for the runs 1 and 3 were lower than those expected from the stoichiometry of full CHTR of the lignin. This is discussed in detail later.

Yamaguchi et al. [28] examined supercritical water gasification of lignin in batch reactor using ruthenium catalysts prepared from ruthenium (III) nitrosylnitrate and ruthenium (III) chloride, corresponding to Ru-N/AC and Ru-Cl/AC of this study, respectively. They found lower catalytic activity in the latter one because of the larger ruthenium metal particles and poisoning by chloride. In this study, XRD patterns from Ru-N/AC and Ru-Cl/AC (Figure 4.9) indicated a partial existence of larger ruthenium for Ru-Cl/AC, while TEM analysis showed average sizes of Ru particles of both catalysts very similar to each other as seen in Figure 4.10 (a) and (d). Within the present experimental conditions, such insignificant difference had little influence on the performance of CHTR.

The catalytic activity of Ni/AC was very low, and the yield of gaseous product was similar level to that of AC. However, this was not necessarily attributed to low activity of nickel as a catalyst for CHTR. CHTR over Ni-C produced gaseous product with yields comparable to those over Ru catalysts. Relatively large Ni particles and insufficient Ni content were the main reasons for such low activity of Ni/AC. For the Ni-C, despite high yields of gaseous products, TOC in the liquid effluent and the amount of deposits were both higher than those of Ru catalysts. The insufficient removal of TOC was apparent from that the liquid effluent was a brown-colored suspension. Furthermore, XRD patterns of both Ni catalysts after the CHTR (Figure 4.9) involved peaks arisen from NiO that had no or little activity [26]. Baker et al.[34] and Elliott et al.[35] investigated CHTR of phenol, *p*-cresol, and benzoic acid in alkaline conditions applying a Ni/Al_2O_3 catalyst and found the conversions were much lower than those in neutral or acidic solution. Significant negative effects of the alkali were attributed to stabilization of the acidic compounds in the form of phenolate and carboxylate, inhibiting the mechanism by which the compounds were converted to gas in the presence of the Ni catalyst. The present results for Ni/AC and Ni-C suggests another mechanism, i.e., deactivation of Ni in the presence of alkali.

The Ru catalysts, thus, successfully reformed lignin into gaseous product at 350 °C, leading to more than 98% removal of organic carbon from the aqueous phase. Assuming the stoichiometry of CHTR of the lignin ($C_{100}H_{112.5}O_{39.9}$) as in eq. (1) and the complete conversion, the yields of CH_4, CO_2, and H_2 (y_{CH4}, y_{CO2}, and y_{H2}, respectively)

are given as functions of H_2O consumption, α, as depicted in Figure 4.11. The α value is determined by chemical equilibrium at the reaction conditions. The CGE calculated from the yields is theoretically in a range from 101% on HHV basis with the minimum consumption of H_2O (α) up to 114%. However, CGEs for the runs 1 and 3, 86.7–87.9%, were out of the range.

$$C_{100}H_{112.5}O_{39.9} + \alpha H_2O \rightarrow y_{CH4}CH_4 + y_{CO2}CO_2 + y_{H2}H_2 \quad (1)$$

Figure 4.11 also demonstrates theoretical yields of the gases from CHTR of phenol according to eq. (2).

$$C_{100}H_{100.0}O_{16.7} + \alpha H_2O \rightarrow y_{CH4}CH_4 + y_{CO2}CO_2 + y_{H2}H_2 \quad (2)$$

The CH_4, CO_2, and H_2 yields from phenol in the runs 4 and 5 are plotted against α that are determined from the CH_4/H_2 ratios. The run 4, which was performed in the absence of Na_2CO_3, gives the gas yields in good agreement with the calculated by eq. (2). The run 5 gives CH_4/H_2 yields equivalent to those for the run 4, while clearly lower CO_2 yield due to dissolution of a portion of CO_2 in the alkaline solution in a form of either carbonate or bicarbonate ion. The present Ru catalysts were thus active enough to convert phenol regardless of the alkalinity of water at 350 °C. A most probable explanation of the lower CH_4 and H_2 yields from the runs 1 and 3 were carbon deposition onto the surface of the Ru catalysts and reactor wall, the former of which was more important. The CH_4/H_2 yields from the runs 1 and 3 were described by the following stoichiometry that assumed deposition of 13.3% and 14.8% of the lignin carbon were deposited as $CH_{0.5}$, respectively.

$$C_{100}H_{112.5}O_{39.9} + 41.0H_2O \rightarrow 13.3CH_{0.5} + 46.3\ CH_4 + 40.4CO_2 + 2.7H_2 \quad (3)$$

$$C_{100}H_{112.5}O_{39.9} + 39.7H_2O \rightarrow 14.8CH_{0.5} + 45.4\ CH_4 + 39.8CO_2 + 2.9H_2 \quad (4)$$

The amounts of coke were roughly in agreement with those determined from the net mass gain of Ru-N/AC and Ru-Cl/AC, 9.2 and 12.7% on the lignin carbon basis, respectively. In accordance with the coke formation, surface areas of them (Table 4.1) decreased by 13 and 11%, respectively. Thus, the incomplete conversions of the lignin in the runs 1 and 3 were probably due to deposition of coke over the catalysts.

Longer-term catalytic activity of Ru-N/AC. CHTR of lignin was performed with longer reaction periods (Table 4.2, the runs 9 and 10) with Ru-N/AC. Images in Figure 4.12 display the liquid effluents from each run that were sampled every 100 min.

At 350 °C, the Ru-N/AC maintained the catalytic activity throughout the run with duration of 10 h, resulting in the steady reduction of TOC of the solution from 5,000 ppm to around 70 ppm. Analysis of the spent catalyst by TEM (Figure 4.10 (b)) and XRD (Figure 4.9) revealed maintenance of Ru particle sizes within a range 1–3 nm. The mass of the catalyst increased by 5.7 wt % corresponding to 6.4% on the lignin carbon basis, which was lower than that in the run 1, 9.2%-C. This is indicative of decrease in the rate of coke deposition over the catalyst with the run time due to simultaneous occurrence of the coke gasification. As a result, the catalyst maintained its surface area at a high level, 840 m^2 g^{-1}. Such suppression of the coke deposition leads to a maintenance of the catalytic activity as well as an achievement of higher yields of CH_4 and H_2, in other words, higher CGE.

CHTR at 300 °C, which was applied to the run 10, resulted in a gradual deactivation of Ru-N/AC. At the beginning of the CHTR, the catalyst was active enough to reform the lignin into gaseous product (Table 4.2, Run 2), but the TOC of the liquid effluent increased with time. The total yield of monomeric of phenols also increased from below detection limit for the first sample (0–100 min) to 7.6%-C for the last one (300-400 min). This shows that the deactivated catalyst could not afford to gasify the phenols. Figure 4.13 compares GC-MS chromatograms of dichloromethane extracts from the product solution of HTR at 250 °C and that of CHTR at 300 °C in the last period. A characteristic of the CHTR product was abundance of cresols and ethylphenols. There were less methoxy groups in the product compounds due to the high temperature. The yields of phenol, cresols, and ethylphenols were 1.5, 1.5 and 2.4%-C, respectively. The reaction pathways for the formations of cresols and ethylphenols possibly involve hydrogenation to remove hydroxyl group in the propanoid chain as well as β-O-4 cleavage. Ye et al. [47] demonstrated that 4-ethylphenolics were selectively produced from corn stalk lignin by hydrogenolysis in the presence of Ru/C catalyst.

The char/coke deposits occurred in the run 10 with yield of 3.4%-C causing mass gain of the catalyst of 11.2 wt %. Although the spent catalyst had a Ru particle size similar to that of fresh one, the surface area significantly decreased from 1145 to 339 m^2 g^{-1}. Figure 4.14 compares the rate of relative mass change during TGA of catalysts under a flow of air. The temperature was raised at a slow heating rate, 2 °C min^{-1}, to avoid

ignition. There is only a single peak for AC around 600 °C, indicating a homogeneous nature of the carbon material. Peaks of Ru-N/AC are distributed and appeared at lower temperatures. This is ascribed to catalysis of Ru to provide oxygen for combustion of carbon support (AC) and coke deposits. The rate profile for the spent catalyst from the run 1 is similar to that for the fresh one. The use of the catalyst in the run 9 for a much longer period seems to shift the dominant peak to a higher temperature side, but have little influence on the peak at the lowest temperature. Considering the maintenance of catalytic activity at 350 °C, it is reasonable to assign the peak at the lowest temperature (around 250 °C) to the combustion of carbon/coke in the vicinity and/or on the surface of Ru particles. On the other hand, the CHTR at 300 °C (run 10) clearly increases the intensity of the first peak. This result explains that the deactivation of Ru-N/AC in CHTR at 300 °C was caused by the coke formation on the Ru particle to hinder the reforming of the lignin. It is therefore important to maintain a balance between deposition and gasification of the coke over the Ru particles for avoiding the catalyst deactivation.

Recuperation of Na_2CO_3 aqueous solution. The recyclability of the alkaline aqueous solution was investigated with a portion of the liquid effluent from Run 9. The pH decreased from 10.6 of the feedstock solution to 8.7 after the CHTR, because of the lignin-derived carbonate ions. Bubbling helium through the solution recovered the basicity enough to prepare the lignin solution with the TOC at 5,000 ppm. Evaporation of water from the liquid effluent and the subsequent calcination of the residue recovered Na_2CO_3 with a negligible loss. The purity of the recovered one was confirmed by the XRD pattern as shown in Figure 4.15.

4.4. Conclusions

HTR and CHTR of the lignin dissolved in Na_2CO_3 aqueous solution have been investigated. The entire portion of the lignin was dissolved into 0.1 M Na_2CO_3 solution at the concentration of 5,000 ppm, and the solution was used for CHTR. In HTR at 250 °C, the alkaline nature of the lignin solution enabled suppression of its conversion to char as well as BCD into monomeric phenols with yield of 8.4%-C. Alternatively,

use of Pd/C catalyst in CHTR of lignin dissolved in alkaline solution was produced phenolic compounds with the highest yield of 13.1%-C at 275 °C. It was demonstrated that the present CHTR over the Ru catalysts at 350 °C converted the dissolved lignin to CH_4, CO_2, and H_2 with CGE of 86.7–87.9% on HHV basis and the rate of TOC removal over 98% even under the severe alkaline conditions. A portion of carbon of the lignin was deposited over the catalysts, which gave lower yield of the major product, CH_4, than expected from the stoichiometry of full gasification of the lignin. A Ru catalyst, Ru-N/AC, showed catalyst durability of at least 10 h with maintenance of TOC removal rate as high as 98.6%, where the deposition of coke over the catalyst was suppressed in the later period of the duration. Characterization of the fresh and spent catalysts confirmed that higher CH_4 yield and TOC removal were associated with less amount of coke deposit over Ru particles. The Na_2CO_3 solution after CHTR was almost free from organics and recuperated by removal of the lignin-derived carbonate ions by aeration. Consequently it increases performance and efficiency of the hydrothermal process. The importance of this work is efficient reforming of the lignin producing fuel gas rich in methane with high CGE.

Table 4.1. The textural properties of fresh and spent catalysts.

Catalyst	Fresh					After CHTR					
	S_{BET} [$m^2\ g^{-1}$]	V_p[a] [$cm^3\ g^{-1}$]	r_p[b] [nm]	Metal content[c] [wt%]	D_m[d] [nm]	Run[e]	S_{BET} [$m^2\ g^{-1}$]	V_p [$cm^3\ g^{-1}$]	r_p [nm]	Metal content[f] [wt%]	D_m [nm]
Ru-N/AC	1145	0.50	0.9	7.4	2.3	1	994	0.45	0.9	7.2	
						2	946	0.43	0.9	7.3	
						9	818	0.37	0.9	7.2	1.9
						10	339	0.19	0.9	6.6	2.3
Ru-Cl/AC	1148	0.51	0.9	6.5	1.7	3	1021	0.46	0.9	6.7	2.1
Ni/AC	1168	0.51	0.9	5.9	5.1	6	820	0.37	0.9	5.6	
Ni-C	178	0.11	1.2	47.6	3.5	8	202	0.12	1.2	45.0	3.6

[a] Total pore volume at $p/p_0 = 0.99$. [b] Mean pore radius ($= 2V_p/S_{BET}$). [c] Metal contents were determined by general carbon combustion. [d] Mean volume diameter (MV) of metal particles determined from their sizes of more than 200 particles in the TEM images. [e] Please see Table 2 for conditions of each run. [f] Catalysts after CHTR contained coke from lignin.

Table 4.2. Conditions and products of CHTR.

Run	1	2	3	4	5	6	7	8	9[a]	10[a]
Conditioins										
Sample	Lignin	Lignin	Lignin	Phenol	Phenol	Lignin	Lignin	Lignin	Lignin	Lignin
Catalyst	Ru-N /AC	Ru-N /AC	Ru-Cl /AC	Ru-Cl /AC	Ru-Cl /AC	Ni/AC	AC	Ni-C	Ru-N /AC	Ru-N /AC
TOC [ppm]	5,000	5,000	5,000	10,000	10,000	5,000	5,000	5,000	5,000	5,000
Na_2CO_3 conc. [M]	0.1	0.1	0.1	0	0.1	0.1	0.1	0.1	0.1	0.1
WHSV [h^{-1}]	0.2	0.2	0.2	0.3	0.3	0.2	0.2	0.2	0.2	0.2
Temp. [°C]	350	300	350	350	350	350	350	350	350	300
Time [h]	2.0	2.0	2.0	0.7	0.7	2.0	2.0	1.0	10.0	7.0
Products										
Gas yield [%, mol/mol-C in feed]										
H_2	2.7	0.7	2.9	2.7	3.4	1.7	1.3	4.7		
CO	< 0.1	< 0.1	< 0.1	< 0.1	< 0.1	< 0.1	< 0.1	< 0.1		
CO_2	19.3	11.4	19.2	41.1	32.6	0.5	0.5	24.9		
CH_4	46.3	31.5	45.4	54.3	54.5	0.8	0.7	46.1		
C_2H_6	0	0	0	0	< 0.1	0	0	0		
TOC of liq. effluent [ppm]	78	109	36	30	54	1938	2297	290		
Deposits [%-C]	0.6	2.0	0.3			4.8	11.3	13.2	0.5	3.6
Cat. mass change [wt %]	+2.4	+10.9	+3.4			+15.0[b]	+14.7	+3.3[b]	+5.7	+11.2
C total[c] [%-C]	76.6	86.6	78.3	95.4[d]	87.2[d]	94.5	98.5	n.d.[e]		
CGE [%-HHV]	87.9	59.4	86.7			2.5	2.0	89.3		

[a] Gas products were not analyzed. [b] Catalyst mass change involved oxidation of metallic nickel. [c] C total is sum of gas, TOC, deposits, and cat. mass change. [d] C total from gas yield. [e] Not determined because of unavailability of data for cat. mass change by coke deposition.

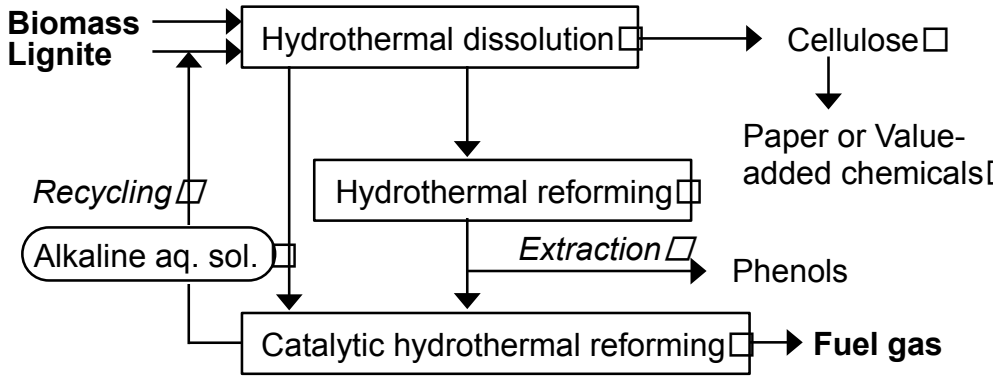

Figure 4.1. Conceptual diagram of biomass and lignite conversion using aqueous alkaline medium.

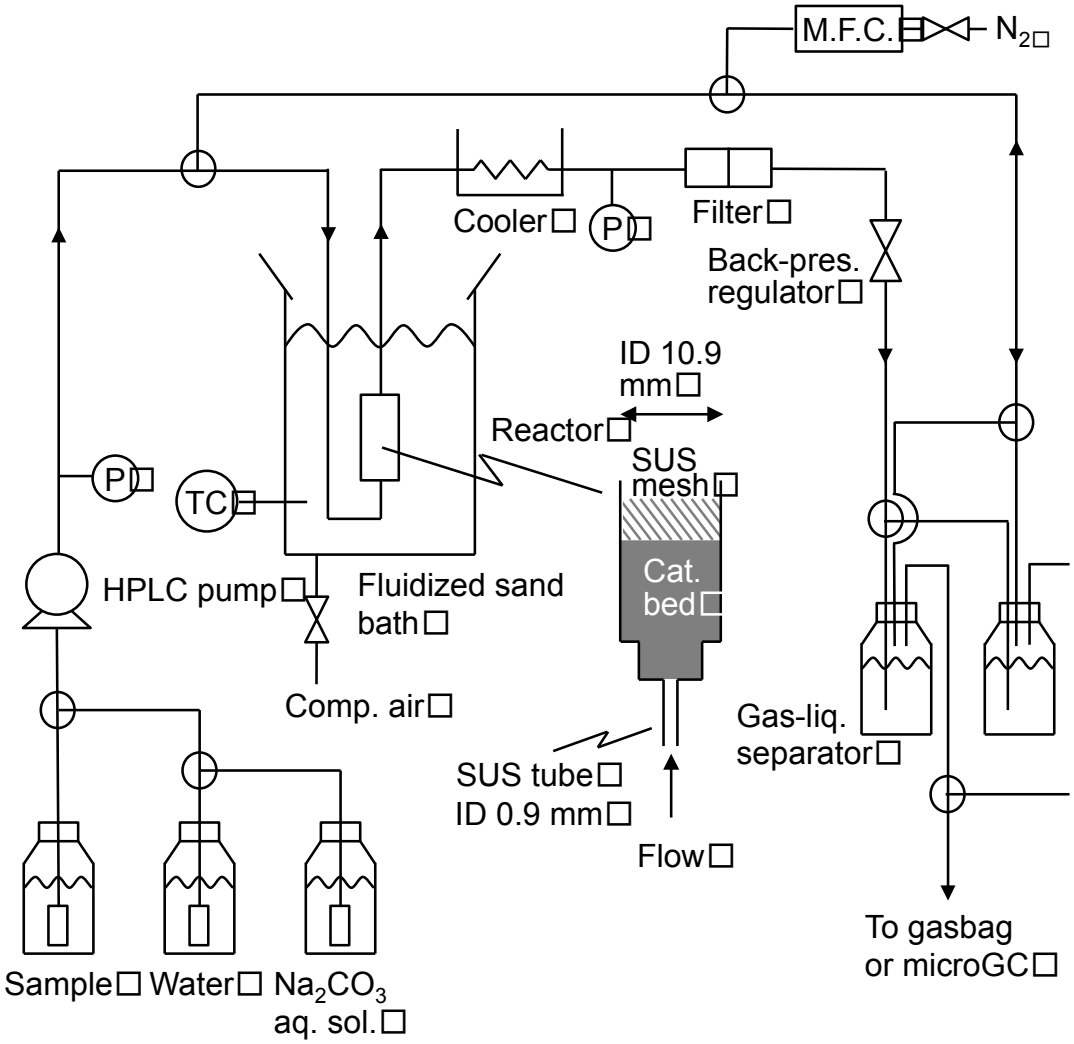

Figure 4.2. Schematic diagram of experimental setup for CHTR of lignin dissolved in Na_2CO_3 aqueous solution.

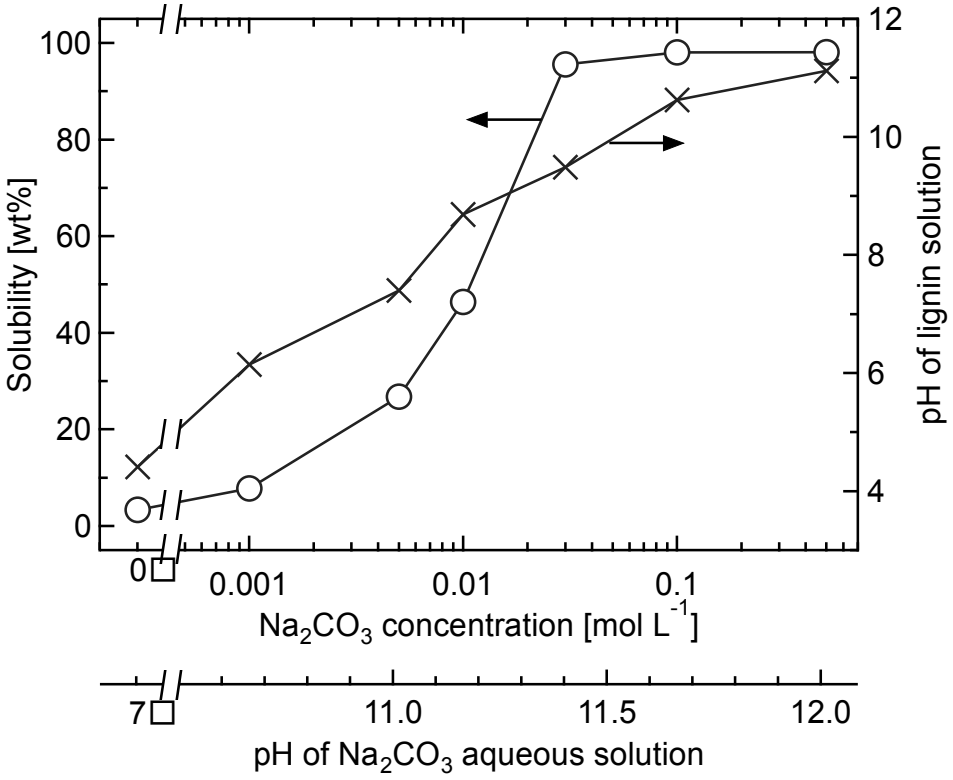

Figure 4.3. Solubility of 8.14 g lignin per liter of water or Na_2CO_3 aqueous solutions (corresponding to 5,000 ppm of lignin solution by the complete dissolution) at 35 °C.

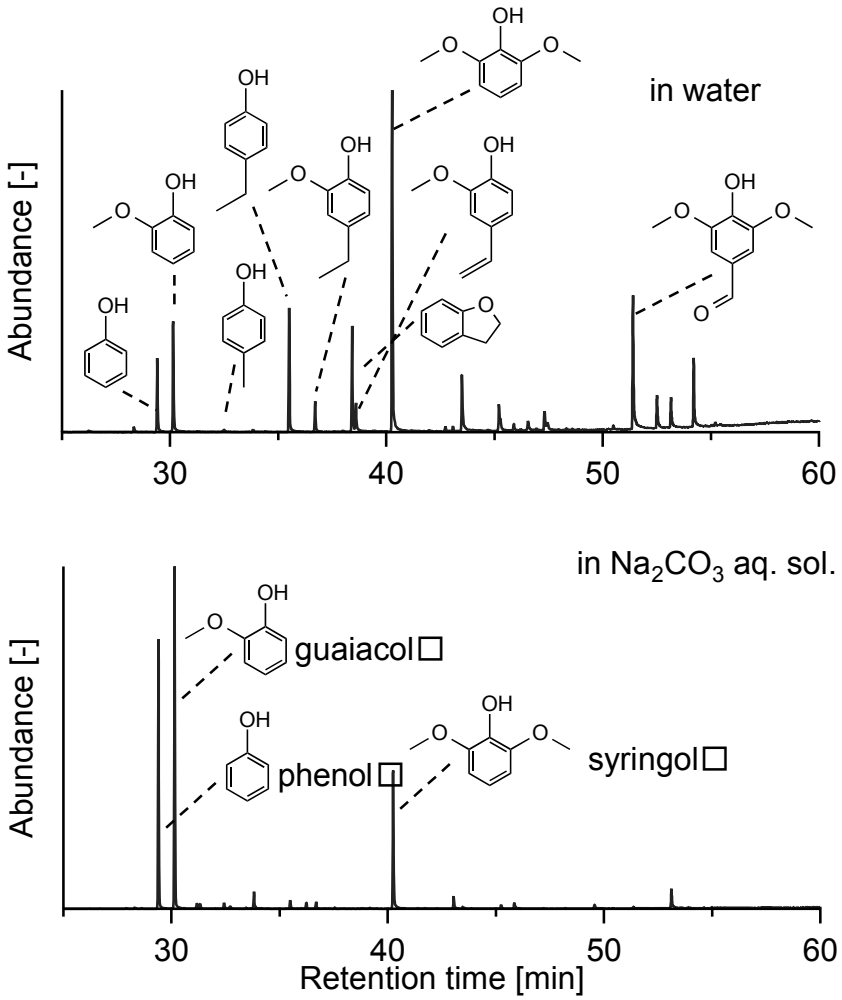

Figure 4.4. GC-MS chromatograms of the product liquids from HTR with lignin dissolved in water and in alkali solution at 250 °C for 1h.

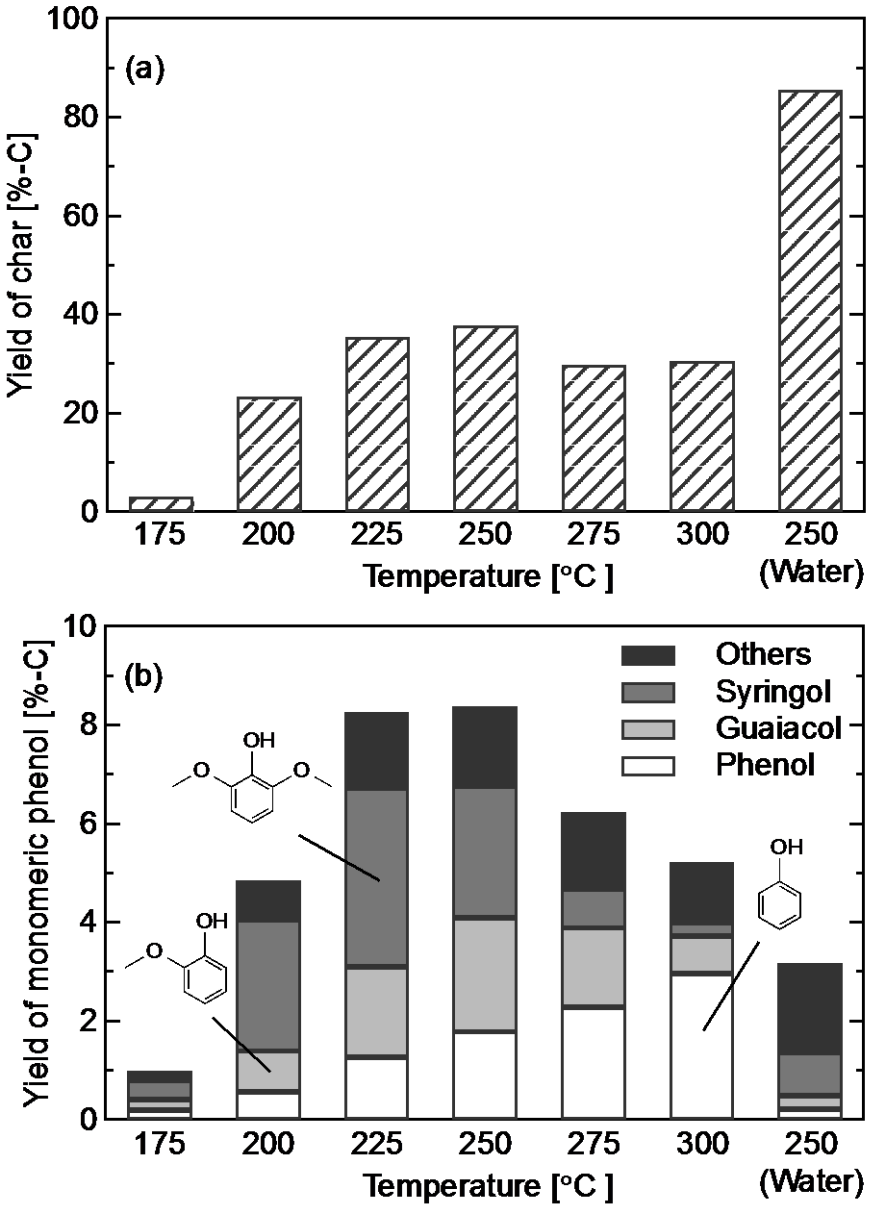

Figure 4.5. HTR of lignin using Na_2CO_3 aqueous solution in batch reactor. Conditions: lignin 80 mg (10,000 ppm), 0.5 M Na_2CO_3 aqueous solution 5 mL (reactor vol. 10 mL) and reaction for 1.5 h.

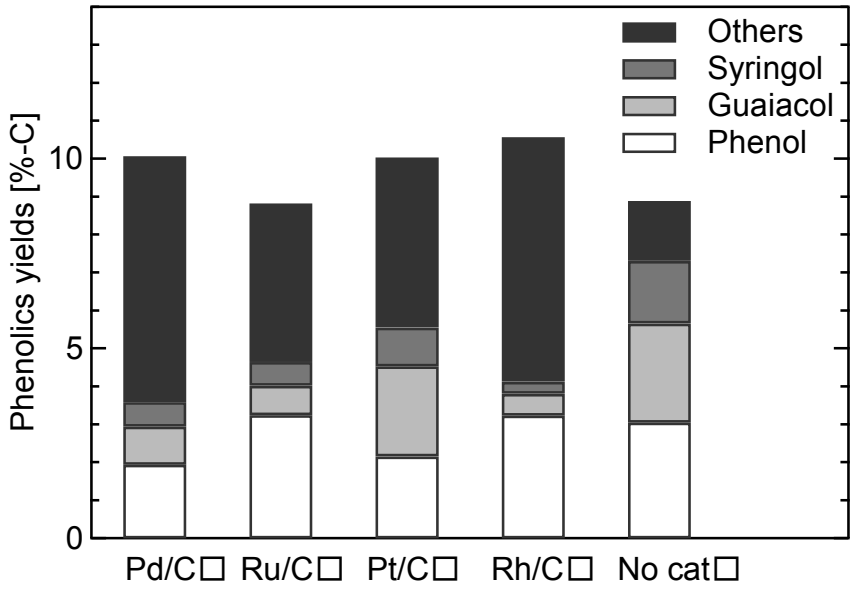

Figure 4.6. Performance of the various catalysts in CHTR at 275 °C for 1h.

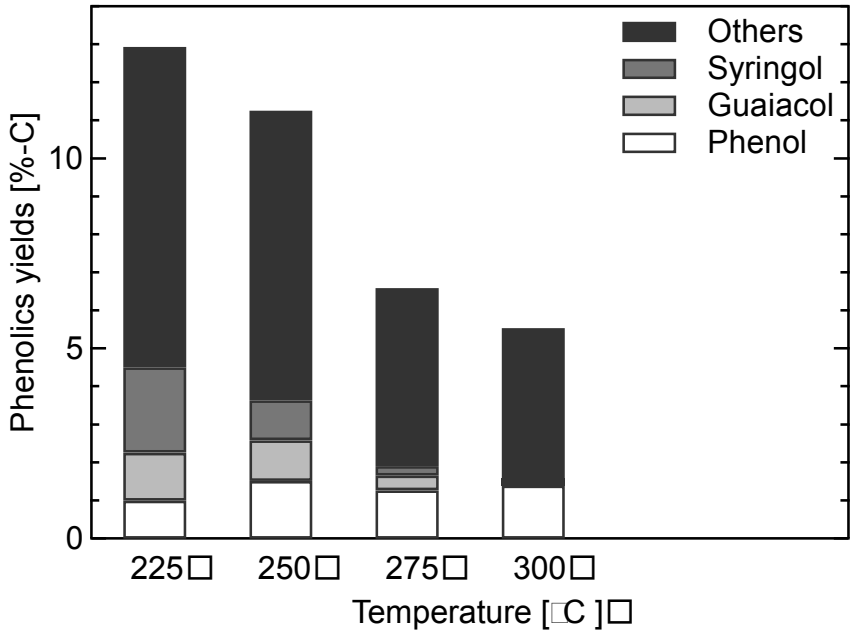

Figure 4.7. Monomeric phenols yields from CHTR with Pd/C at different temperatures for 1.5 h.

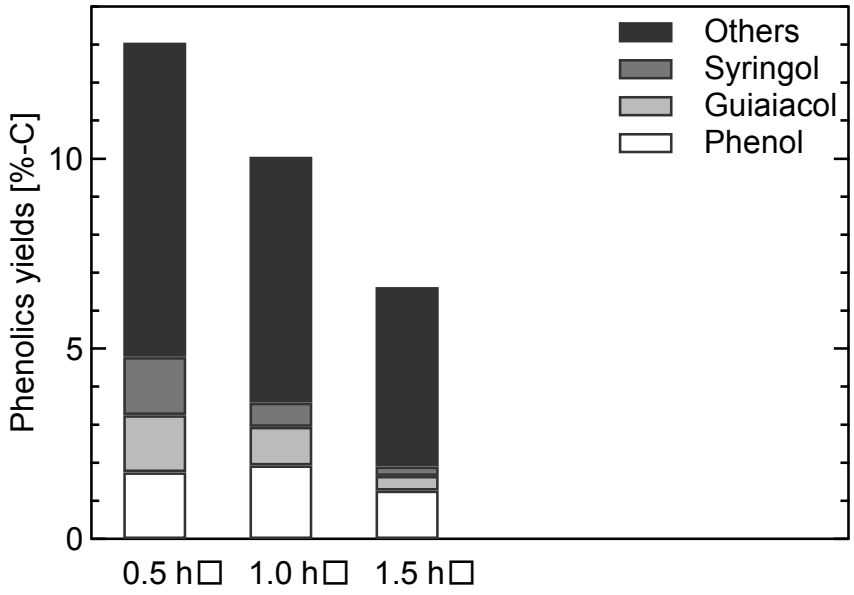

Figure 4.8. Temporal change of monomeric phenols yields from CHTR with Pd/C catalyst at 275 °C

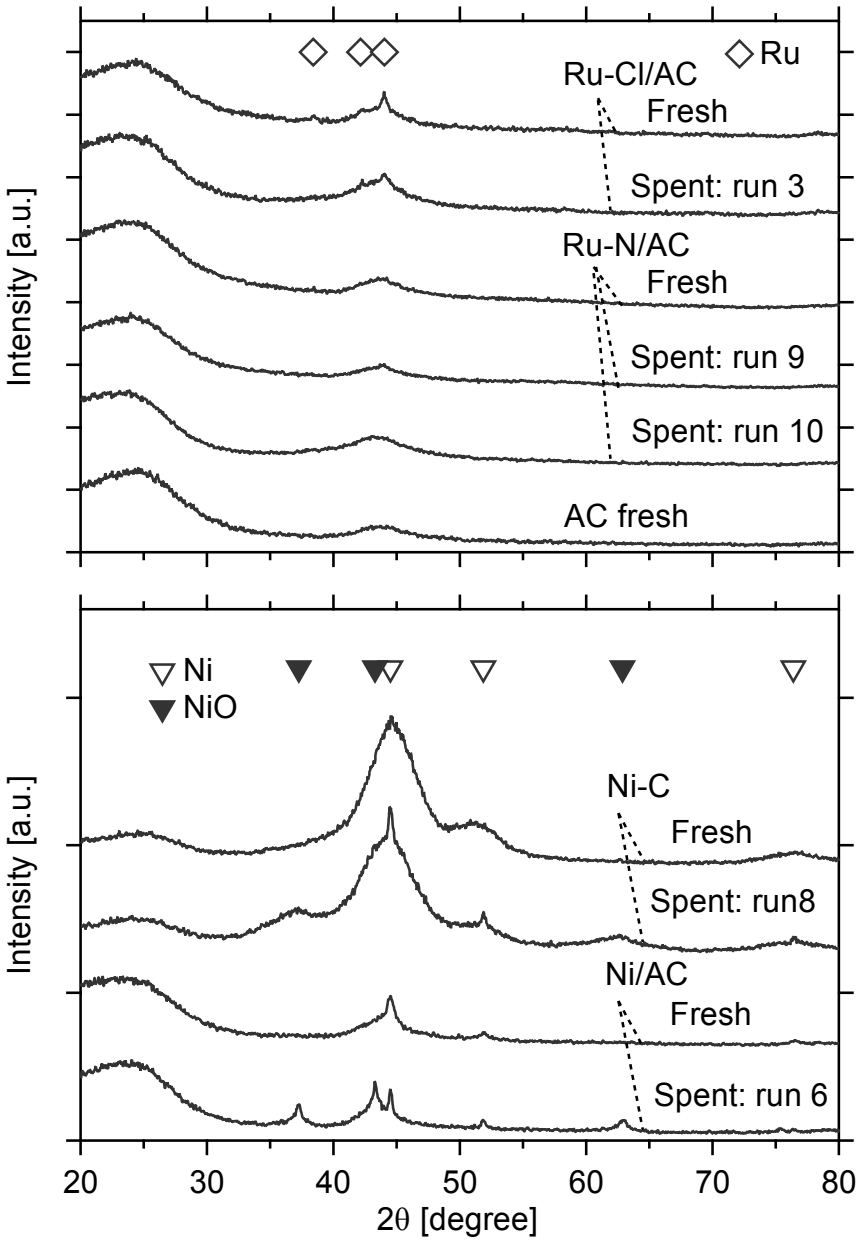

Figure 4.9. XRD patterns of fresh and spent catalysts.

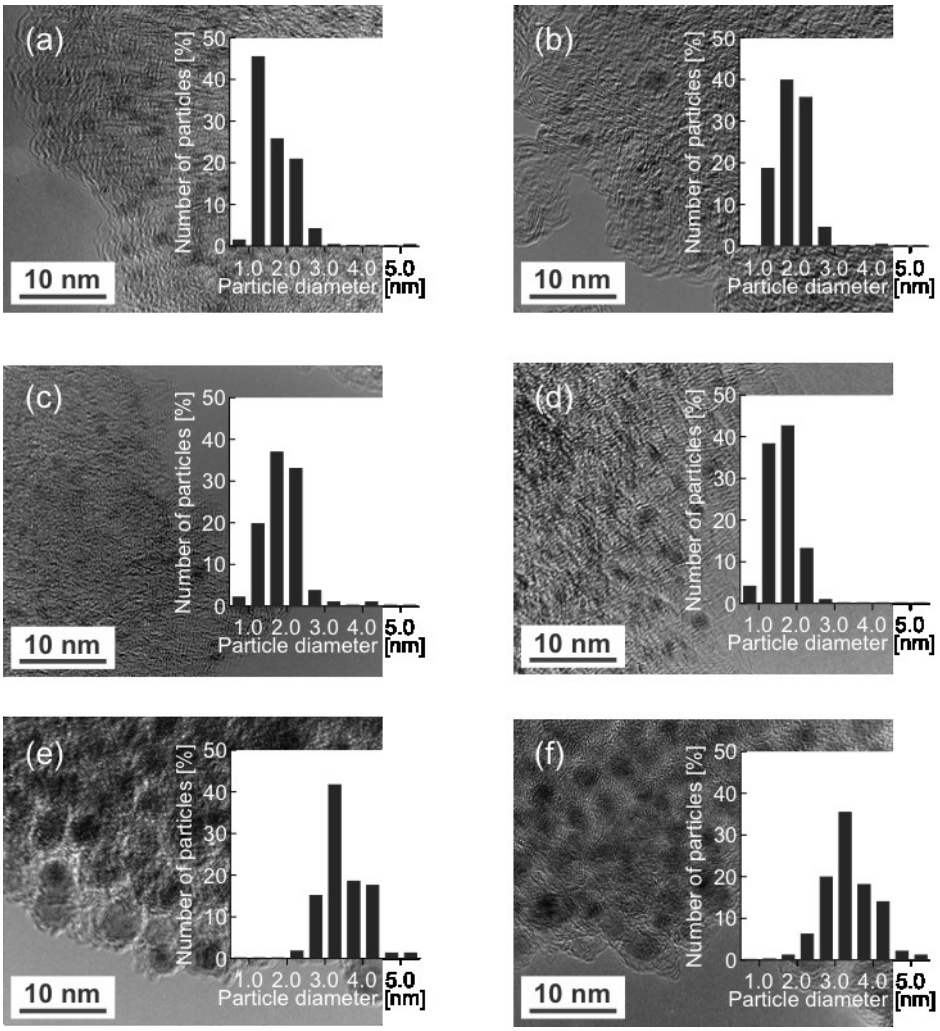

Figure 4.10. TEM images and histograms of metal particle size distribution of (a) fresh Ru-N/AC, (b) Ru-N/AC spent: run 9, (c) Ru-/N/AC spent: run 10, (d) fresh Ru-Cl/AC, (e) fresh Ni-C, and (f) Ni-C spent: run 8.

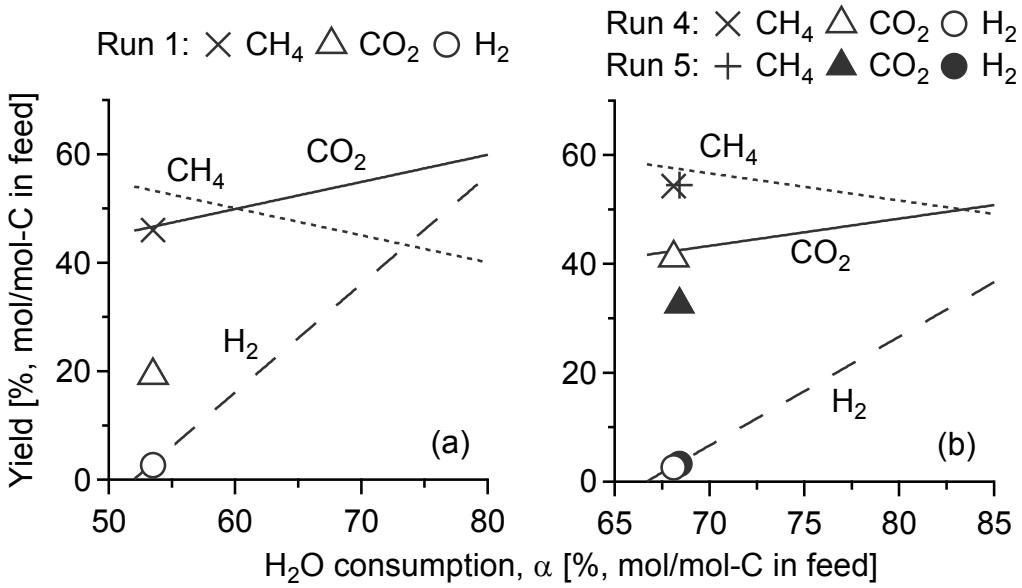

Figure 4.11. Yields of gaseous products according to eqs. (1) and (2) at complete conversion of (a) lignin and (b) phenol as a function of α. Plots in each figure show yields obtained from experiments.

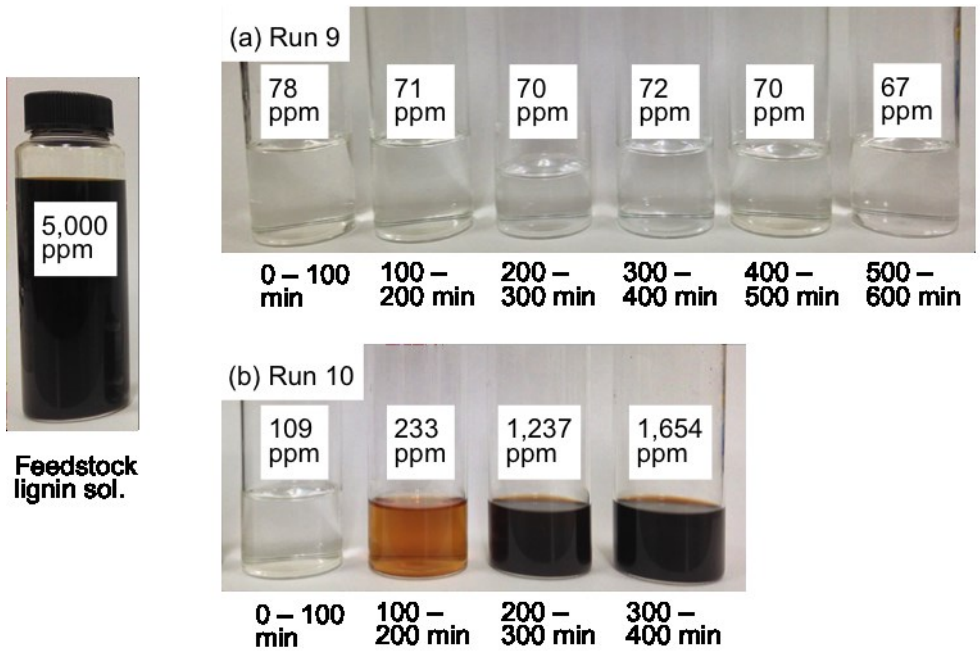

Figure 4.12. Photos and TOC concentrations of liquid effluents that were sampled every 100 min during CHTR of lignin using Ru-N/AC at (a) 350 °C and (b) 300 °C.

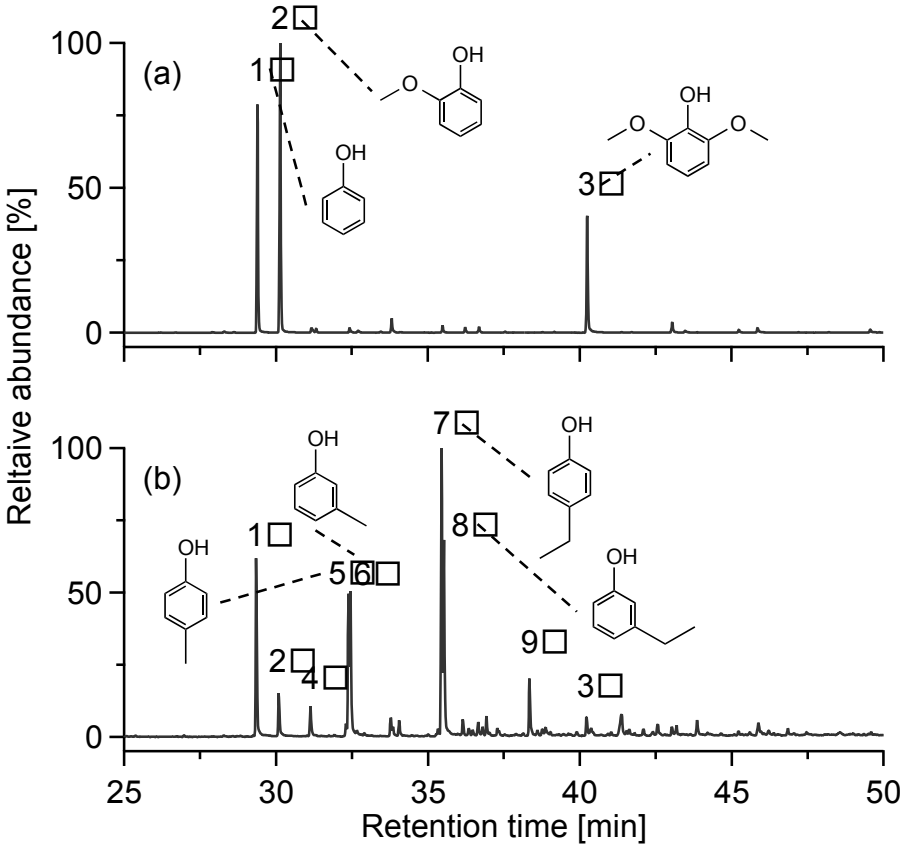

Figure 4.13. GC-MS chromatograms of dichloromethane extracts from (a) product liquid of HTR at 250 °C and (b) liquid effluent of CHTR run 10 at 300–400 min. The main peaks are assigned as follows: 1: phenol, 2: guaiacol, 3: syringol, 4: *o*-cresol, 5: *p*-cresol, 6: *m*-cresol, 7: 4-ethylphenol, 8: 3-ethylphenol, and 9: 3-propylphenol.

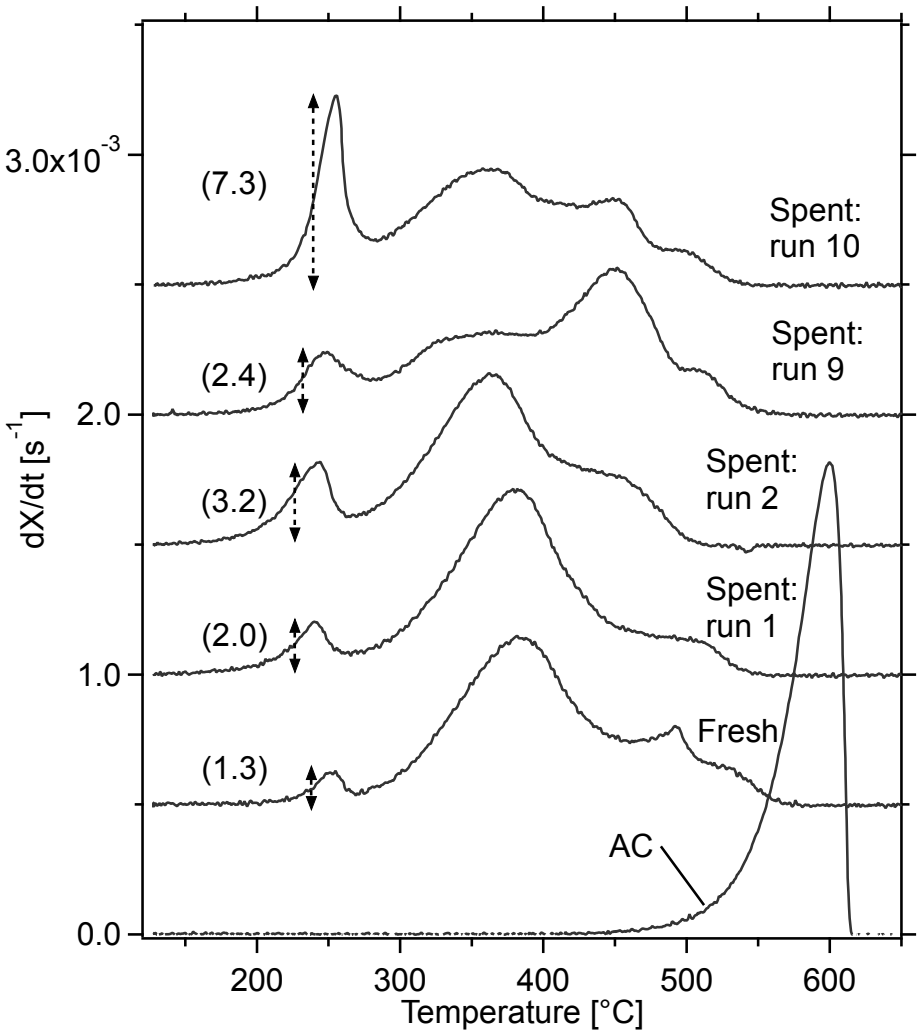

Figure 4.14. TGA of fresh/spent Ru-N/AC and fresh AC at heating rate of 2 °C min^{-1} in stream of flowing air (150 mL min^{-1}). Figure in parentheses is height of peak at 239–254 °C in units of $\times 10^{-4}$ s^{-1}.

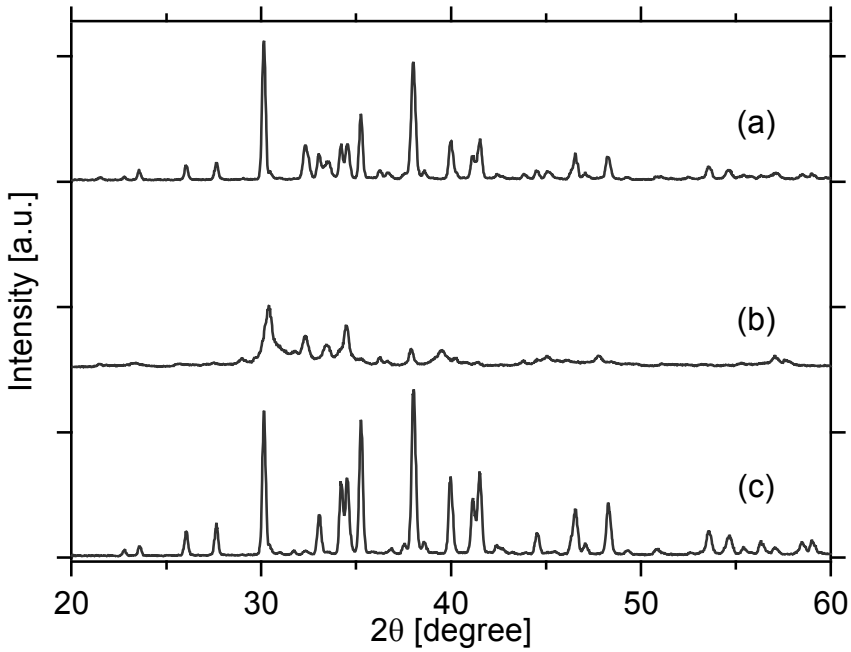

Figure 4.15. XRD patterns of (a) original Na_2CO_3 and the ones recovered from liquid effluent from CHTR run 9 by water evaporation (b) before and (c) after calcination at 300 °C.

4.5. References

1. Hayashi J-i, Hosokai S, Sonoyama N. *Gasification of low-rank solid fuels with thermochemical energy recuperation for hydrogen production and power generation.* Process Safety and Environmental Protection, 2006. 84 (6): p. 409–419.
2. Sueyasu T, Oike T, Mori A, Kudo S, Norinaga K, Hayashi J-i. *Simultaneous steam reforming of tar and steam gasification of char from the pyrolysis of potassium-loaded woody biomass.* Energy & Fuels, 2012. 26 (1): p. 199–208.
3. Matsumura Y, Minowa T, Potic B, Kersten S, Prins W, Vanswaaij W, Vandebeld B, Elliott D, Neuenschwander G, Kruse A. Antal MJ Jr. *Biomass gasification in near- and super-critical water: Status and prospects*. Biomass and Bioenergy, 2005. 29 (4): p. 269–292.
4. Kasehagen L. *Action of aqueous alkali on a bituminous coal*. Industrial & Engineering Chemistry, 1937. 29 (5): p. 600–604.
5. van Bodegom B, van Veen JAR, van Kessel GMM, Sinnige-Nijssen MWA, Stuiver HCM. *Action of solvents on coal at low temperatures*. Fuel, 1984. 63 (3): p. 346–354.
6. Kashimura N, Hayashi J-i, Li C-Z, Sathe C, Chiba T. *Evidence of poly-condensed aromatic rings in a Victorian brown coal.* Fuel, 2004. 83 (1): p. 97–107.
7. Waldner MH, Krumeich F, Vogel FJ. *Synthetic natural gas by hydrothermal gasification of biomass. Selection procedure towards a stable catalyst and its sodium sulfate tolerance*. Journal of Supercritical Fluids, 2007. 43 (1): p. 91–105.
8. Onwudili JA, Williams PT. *Role of sodium hydroxide in the production of hydrogen gas from the hydrothermal gasification of biomass.* International Journal of Hydrogen Energy, 2009. 34 (14): p. 5645–5656.
9. Waldeck WF, Lynn G, Hill AE. *Aqueous solubility of salts at high temperatures. Solubility of sodium carbonate from 50 to 3480°.* Journal of American Chemical Society, 1932. 54 (3): p. 928–936.
10. Khan MS, Rogak SN. *Solubility of Na_2SO_4, Na_2CO_3 and their mixture in supercritical water.* Journal of Supercritical Fluids, 2004. 30 (3): p. 359–373.

11. Kruse A, Meier D, Rimbrecht P, Schacht M. *Gasification of Pyrocatechol in Supercritical Water in the Presence of Potassium Hydroxide*. Industrial & Engineering Chemistry Research, 2000. 39 (12): p. 4842–4848.
12. Watanabe M, Inomata H, Osada M, Sato T, Adschiri T, Arai K. *Catalytic effects of NaOH and ZrO_2 for partial oxidative gasification of n-hexadecane and lignin in supercritical water.* Fuel, 2003. 82 (5): p. 545–552.
13. Sınağ A, Kruse A, Rathert J. *Influence of the heating rate and the type of catalyst on the formation of key intermediates and on the generation of gases during hydropyrolysis of glucose in supercritical water in a batch reactor.* Industrial & Engineering Chemistry Research, 2003. 43 (2): p. 502–508.
14. Muangrat R, Onwudili JA, Williams PT. *Influence of alkali catalysts on the production of hydrogen-rich gas from the hydrothermal gasification of food processing waste*. Applied Catalysis B: Environmental, 2010. 100 (3–4): p. 440–449.
15. Madenoğlu GT, Boukis N, Sağlam M, Yüksel M. *Supercritical water gasification of real biomass feedstocks in continuous flow system.* International Journal of Hydrogen Energy, 2011. 36 (22): p. 14408–14415.
16. Muangrat R, Onwudili JA, Williams PT. Bioresour. Technol. 2011, 102 (10), 6331–6335.
17. Onwudili JA, Lea-Langton AR, Ross AB, Williams PT. *Alkaline subcritical water gasification of dairy industry waste (Whey).* Bioresource Technology, 2013. 127: p. 72–80.
18. Onwudili JA, Williams PT. *Hydrogen and methane selectivity during alkaline supercritical water gasification of biomass with ruthenium-alumina catalyst.* Applied Catalysis B: Environmental, 2013. 132–133: p. 70–79.
19. Xu ZR, Zhu W, Gong M, Zhang HW. *Direct gasification of dewatered sewage sludge in supercritical water. Part 1: Effects of alkali salts.* International Journal of Hydrogen Energy, 2013. 38 (10): p. 3963–3972.
20. Sricharoenchaikul V. *Assessment of black liquor gasification in supercritical water.* Bioresource Technology, 2009. 100 (2): p. 638–643.

21. Cao C, Guo L, Chen Y, Guo S, Lu Y. *Hydrogen production from supercritical water gasification of alkaline wheat straw pulping black liquor in continuous flow system.* International Journal of Hydrogen Energy, 2011. 36 (21): p. 13528–13535.
22. Azadi P, Khan S, Strobel F, Azadi F, Farnood R. *Hydrogen production from cellulose, lignin, bark and model carbohydrates in supercritical water using nickel and ruthenium catalysts.* Applied Catalysis B: Environmental, 2012. 117–118: p. 330–338.
23. Huber GW, Shabaker JW, Dumesic JA. *Raney Ni-Sn catalyst for H_2 production from biomass-derived hydrocarbons.* Science, 2003. 300 (5628): p. 2075–2077.
24. Osada M, Sato T, Watanabe M, Adschiri T, Arai K. *Low-temperature catalytic gasification of lignin and cellulose with a ruthenium catalyst in supercritical water.* Energy & Fuels, 2003. 18 (2): p. 327–333.
25. Elliott DC, Hart TR, Neuenschwander GG. *Chemical processing in high-pressure aqueous environments. 8. Improved catalysts for hydrothermal gasification.* Industrial & Engineering Chemistry Research, 2006. 45 (11): p. 3776–3781.
26. Sharma A, Nakagawa H, Miura K. *Uniform dispersion of Ni nano particles in a carbon based catalyst for increasing catalytic activity for CH_4 and H_2 production by hydrothermal gasification.* Fuel, 2006. 85 (17–18): p. 2396–2401.
27. Morimoto M, Nakagawa H, Miura K. *Hydrothermal extraction and hydrothermal gasification process for brown coal conversion*. Fuel, 2008. 87 (4–5): p. 546–551.
28. Yamaguchi A, Hiyoshi N, Sato O, Osada M, Shirai M. *Lignin gasification over supported ruthenium trivalent salts in supercritical water.* Energy & Fuels, 2008. 22 (3): p. 1485–1492.
29. Lu Y, Li S, Guo L, Zhang X. *Hydrogen production by biomass gasification in supercritical water over $Ni/\gamma Al_2O_3$ and Ni/CeO_2-γAl_2O_3 catalysts*. International Journal of Hydrogen Energy, 2010. 35 (13): p. 7161–7168.

30. Shirai M, Hiyoshi N, Murakami Y, Osada M, Sato O, Yamaguchi A. *Supercritical water gasification of organosolv lignin over a graphite-supported ruthenium metal catalyst.* Chemistry Letters, 2012. 41 (11): p. 1453–1455.
31. Yamaguchi A, Hiyoshi N, Sato O, Shirai M. *Gasification of organosolv-lignin over charcoal supported noble metal salt catalysts in supercritical water*. Topics in Catalysis, 2012. 55 (11–13): p. 889–896.
32. Fang Z, Minowa T, Smith RL, Ogi T, Koziński JA. *Liquefaction and gasification of cellulose with Na_2CO_3 and Ni in subcritical water at 350 °C.* Industrial & Engineering Chemistry Research, 2004. 43 (10): p. 2454–2463.
33. Dolan R, Yin S, Tan Z. *Effects of headspace fraction and aqueous alkalinity on subcritical hydrothermal gasification of cellulose.* International Journal of Hydrogen Energy, 2010. 35 (13): p. 6600–6610.
34. Baker EG, Sealock LJ Jr. *Catalytic Destruction of hazardous organics in aqueous solutions,* PNL-6491-2; Pacific Northwest Laboratory: Richland, WA, 1988.
35. Elliott DC, Sealock LJ Jr, Baker EG. *Chemical processing in high-pressure aqueous environments. 3. Batch reactor process development experiments for organics destruction.* Industrial & Engineering Chemistry Research, 1994. 33 (3): p. 558–565.
36. Sealock LJ, Elliott DC, Baker EG, Butner RS. *Chemical processing in high-pressure aqueous environments. 1. Historical perspective and continuing developments.* Industrial & Engineering Chemistry Research, 1993. 32 (8): p. 1535–1541.
37. Rodrigues Pinto PC, Borges da Silva EA, Rodrigues AE. *Insights into oxidative conversion of lignin to high-added-value phenolic aldehydes.* Industrial & Engineering Chemistry Research. 2011, 50 (2), 741–748.
38. Nakagawa H, Watanabe K, Harada Y, Miura K. *Control of micropore formation in the carbonized ion exchange resin by utilizing pillar effect.* Carbon, 1999. 37 (9): p. 1455–1461.
39. Nenkova S, Vasileva T, Stanulov K. *Production of phenol compounds by alkaline treatment of technical hydrolysis lignin and wood biomass.* Chemistry

of Natural Compounds, 2008. 44(2): p. 182−185.

40. Radoykova T, Nenkova S, Stanulov K. *Production of phenol compounds by alkaline treatment of poplar wood bark.* Chemistry of Natural Compounds, 2010. 46(5): p. 807−808.

41. Beauchet R, Monteil-Rivera F, Lavoiea JM. *Conversion of lignin to aromatic-based chemicals (L-chems) and biofuels (L-fuels).* Bioresource Technology, 2012. 121: p. 328–334

42. Miller JE, Evans L, Littlewolf A, Trudell DE. *Batch microreactor studies of lignin and lignin model compound depolymerization by bases in alcohol solvents.* Fuel, 1999. 78 (11): p. 1363−1366.

43. Rönnlund I, Myreen L, Lundqvist K, Ahlabeck J, Westerlund T. *Waste to energy by industrially integrated supercritical water gasification – Effects of alkali salts in residual by-products from the pulp and paper industry.* Energy, 2011. 36(4): p. 2151–2163.

44. Pepper JM, Lee YW. *Lignin and related compounds. I. A comparative study of catalysts for lignin hydrogenolysis.* Canadian Journal of Chemistry, 1968. 47: p. 723−727.

45. Ye Y, Fan J, Chang J. *Effect of reaction conditions on hydrothermal degradation of cornstalk lignin.* Journal of Analytical and Applied Pyrolysis, 2012. 94: p. 190−195.

46. van der Meijden CM, Veringa HJ, Rabou LPLM. *The production of synthetic natural gas (SNG): A comparison of three wood gasification systems for energy balance and overall efficiency.* Biomass and Bioenergy, 2010. 34 (3): p. 302–311.

47. Ye Y, Zhang Y, Fan J, Chang J. *Selective production of 4-ethylphenolics from lignin via mild hydrogenolysis.* Bioresource Technology, 2012. 118: p. 648–651.

CHAPTER 5

GENERAL CONCLUSIONS

For the development of sustainable society from the viewpoints of reduction in environmental burden and finding resources alternative to depleting fossil fuels, utilization of biomass resources is expected to be one of the most promising solutions. Bioenergy has a potential to provide the major part of the required renewable energy provisions in the future. In order to popularize and radicate the use of biomass, which has unfavorable properties such as low bulk density and high moisture content, a compact system is required to achieve a concept of local production for local consumption of the resources. Key factors for the miniaturization of the conversion system are to progress the reaction faster and at lower temperatures. To meet this challenge one of the expectant avenues for biomass processing is the use of catalytic hydrothermal reforming, which is a technology to reform the resources under high temperature and pressure in the presence of catalysts. Recently the conversion of wet biomass and other waste byproducts into biofuel and fine chemicals in hydrothermal condition has gained extensive consideration.

This research work proposed novel biomass conversion processes for biomass and its derivatives utilizing catalytic hydrothermal reforming under subcritical conditions and experimentally showed process potential. For hydrothermal reforming process, the reaction environment is much different. Hot compressed liquid water behaves very special from normal water. The dielectric constant of water decreases as a result of the hydrogen bonds between water molecules becoming fewer and less persistent. This reduced dielectric constant enables hot compressed water to solvate small hydrophobic

organic molecules, allowing reactions to occur. The ionic product of water is relatively high in subcritical range. The high levels of H^+ and OH^- mean that many acid or base catalyzed reactions are accelerated. Despite the high temperature, the compressibility of subcritical water is rather low. Therefore, this relatively high density combined with the high dissociation constant of subcritical water, favors ionic reactions, as a result hydrolysis and degradation of biomass derivatives is enhanced. Consequently, the main essence of hydrothermal reforming of biomass is to benefit from the special properties of super-, near- and subcritical water as solvent, as catalyst and its presence as reactant, hence biomass and its derivatives can be directly converted to desired product, along with high solubility of the intermediates in water medium suppresses of unwanted tar and coke formation. Hydrothermal processing offers a number of potential advantages. Feedstock derived from biomass can be hydrothermally transformed to produce a range of gasified or liquefied fuel products such as methane, hydrogen, biofuel, chemicals that are usable at commercial scale.

In the Chapter 2, 3 and 4 described catalytic hydrothermal reforming of biomass and its derivatives for the production of liquid fuel and fuel gas. The feedstocks were water-solubles obtained from the pyrolysis of biomass, inedible vegetable oil and alkaline solutions of lignin, respectively. Otherwise, these feedstocks usually referred as byproducts or wastes from various industrial process and low grade biomass which utilization restricted due to undesirable properties. However those feedstocks converted fuel gas and liquid fuel as a result of employment of catalytic hydrothermal reforming. The pressurized product gases had high heating values due to relatively low CO_2 thanks to dissolution of most of CO_2, which produced at high amounts from high oxygen content of biomass, in water. Particularly, organic compounds contained in water solubles from pyrolysis and alkaline solution of lignin, were nearly completely gasified to combustible fuel gas rich in methane and hydrogen. As a result remained water solutions were cleaned from organics pollution, which meant treatment of waste streams. The liquid fuel that obtained from inedible vegetable oil was consisted of hydrocarbons mostly long-chain alkanes, which can be used directly or treated more suitable fuels. Alternatively, CHTR of biomass has potential to produce various value-added chemicals from low-value waste byproducts from numerous industries by using

catalysts and additives. This was demonstrated via experimentally with the production of phenolic compounds by CHTR of lignin dissolved in alkaline solution.

In hydrothermal process inorganic compounds that cause severe corrosion problems are included in the aqueous product. It can facilitate recovery and recycling of inorganic chemicals in their ionic form, for affordable use as fertilizers. Thus inorganic compounds such as alkali salts, which are applied for dissolution of water-insoluble organic compounds as well as lignin, in the liquid product are able to serve over again by recycling or can be combined with different types of feeds in the proper way.

This novel biomass conversion process of biomass-derivatives is supposed to be applicable in many chemical and power generation processes that generate exhaust liquids contain organics since properties of the feedstock used in this study is relatively severe as a reaction condition. The most important disadvantage of hydrothermal reforming might be energy for heating up water. But the calculation of energy efficiency is expected to be desirable as the reforming system because heat can be recovered by the exhaust hot water and by combustion of a part of product fuel gases.

For the better understanding of the catalytic hydrothermal reforming of biomass in subcritical condition and for the further research and development of the process, following points are required to be focused on for future fundamental studies:

1) When hydrothermal process is performed at low temperature, especially in subcritical condition or when more complex feedstock is treated, hydrothermal reforming is often carried out in the presence of additives or catalysts to enhance efficiency and performance of process. However, catalyst deactivation regularly arises from three main issues: the presence of chemical poisons in the feedstock, a reduction in the number of exposed metal atoms in the catalyst itself, and support issues. For the first issue, sulfur is commonly known catalyst poison. Sulfur irreversibly binds to the surface of some metals making the active sites unavailable to perform the desired chemistry. For the second one, loss of catalyst surface area due to crystallite growth or sintering causes catalyst deactivation. The third key issue is support degradation. It affects the effective surface area and pore structure of the catalyst. Finally future studies need to explore on more development work of catalyst to identify superior catalysts, supports and active

materials that resist deactivation and withstand better in hydrothermal process for extended period.

2) The most significant drawback for the industrial application is expected high investment costs needed for reforming system design and specialized materials to withstand, because hydrothermal reforming process is operated under high pressure, high temperature with a flow of viscous and acidic liquids or often corrosive environments of hydrothermal media.

3) Then again, several engineering challenges remain for hydrothermal processing. These include unknown or largely uncharacterized reaction pathways and kinetics, inadequate solid management issue that lead to precipitation of inorganic materials and can result in fouling and plugging problems.

As a final point, this process can expand the usability of low rank fuels, and impact on the environment in terms of clean fuel resources and treatment of waste streams, is significantly very high.

ACKNOWLEDGMENTS

The present study was carried out at the Interdisciplinary Graduate School of Engineering Sciences in Kyushu University during the years 2010-2013. I would like to express my deepest appreciation to all those who provided me the possibility to complete this study.

First of all, I would like to express my sincere gratitude to my supervisor Prof. Jun-ichiro Hayashi for his generous help and invaluable assistance, support and guidance throughout this research and also my daily life in Japan. His energy and knowledge, suggestions and advices contributed tremendously to our studies. I wish to give my warmest thanks to Associate Prof. Koyo Norinaga for his kind support and valuable recommendations as well for introducing me Kyushu University.

I would like to express my deepest gratitude to Ass. Prof. Shinji Kudo, without whose knowledge and assistance, this study would not have been successful. To work with him has been a great opportunity for me, I am grateful for his persistent help, fruitful discussion and for many things I have learned and gained from him.

Special thanks are extended to Prof. Hisahiro Einaga and Jin Miyawaki, the members of the doctoral thesis examination committee, for their constructive discussions and comments. I am also thankful to Prof. B.Enkhsaruul of National University of Mongolia, for her encouragement and recommending me to study in Japan. Moreover, I would like to thank to Prof. Andrea Kruse and her co-workers in Karlsruhe Institute of Technology of Germany, for kind cooperation and friendly relationship.

Besides, I would like to thank the authority of Kyushu University for providing us with financial means, good environment and facilities to complete our study. I would like to acknowledge the Mitsubishi Corporation for financial support that was essential for my study in Japan. Furthermore, I would like to take this opportunity to thank to the Global-Centre of Excellence (G-COE) program in “Novel Carbon Resource Sciences” of Kyushu University, for great opportunities, which helped to broaden our experiences.

I wish to record my gratitude with much appreciation to all my graduate friends, our laboratory members, all my colleagues at Kyushu University for their valuable assistance, friendly relationship and kind cooperation. Wish you all the best.

Finally, I dedicate my dissertation to my beloved families and I would like to express my love and heartfelt gratitude to my parents, my husband, my children and my brothers; for their endless love and blessing, support and patience through the period of my studies. Wish you all the best and I love you.